THE ROLE OF LIPID PHOSPHATE PHOSPHATASES AND THEIR PUTATIVE RECEPTORS IN GERM CELL MIGRATION AND SURVIVAL IN *DROSOPHILA MELANOGASTER*

Camilla Burnett

A thesis submitted to University College London
at the University of London for the degree
of Doctor of Philosophy

December 2004

MRC Laboratory for Molecular Cell Biology
University College London
Gower Street
London
WC1E 6BT

ProQuest LLC
789 East Eisenhower Parkway
P.O. Box 1346
Ann Arbor, MI 48106-1346

Dedicated to my mother and father

ABSTRACT

During development, a variety of cell types undertake a guided migration to their target location and, consequently, display motile, proliferative and invasive behaviours. Failure in guided migration can result in severe developmental errors, including the formation of metastatic cancers or, in the case of germ cells, congenital defects. Primordial germ cells (PGCs) are the germ line stem cell progenitors that produce the gametes and pass the genetic material from generation to generation. In *Drosophila melanogaster*, as in many other organisms, the PGCs are set-aside at the beginning of embryogenesis as a distinct sub-set of cells that are easily detectable by immunochemical means. As such, they provide a good system in which to study the control of cell migration during development. Furthermore, since they are subject to various cell death and cell survival signals during their journey, they provide an opportunity to study the regulation of stem cell survival *in vivo*.

wunen and *wunen-2* encode lipid phosphate phosphatases (LPPs) and regulate *Drosophila* PGC survival and migration. LPP-like activity has been detected in all cell and tissue types so far studied, but remarkably little is known of their biological functions, and their physiological substrates remain elusive. The first aim of this work was to investigate differences in substrate recognition between *Drosophila* Wunen and the mammalian LPP isoforms, both *in vitro*, by means of biochemical assays and *in vivo*, by examining the ability of the mammalian isoforms to recognise the same physiological substrate as Wunen in *Drosophila* embryos. It also investigates hetero- and homo-oligomerisation of the fly and mammalian LPPs as a possible mechanism of action.

In order to fully understand these proteins, it is necessary to identify and characterise their receptors. This work identifies a G protein-coupled receptor involved in *Drosophila* PGC migration and survival, and investigates its possible relationship to Wunen.

ACKNOWLEDGEMENTS

A great many thanks must go to Ken Howard, my supervisor, for his advice and encouragement throughout this work, alongside his enormous support and understanding over the last three years. I also owe a large debt of gratitude to Penny Makridou for so much hard work and assistance in the lab.

A big thank-you goes to Adrian Harwood, Jonny Ryves and the rest of the Harwood lab, for helping me out with a multitude of problems, and special thanks to Emma Dalton, for providing so much help, not to mention entertainment, over the years.

There are many people at the LMCB who have helped me enormously before, after and during this work, all of whom I am immensely grateful to. A special mention should go to all of the core staff as well as to Nathalie Franc and her lab for stocks, reagents and advice.

I must also thank Martin Raff, who alongside Ken encouraged me to undertake this project, and without whose wise words it never would have been, as well as Linda Partridge, for her support and guidance.

Thanks must go to the *Drosophila* community at large, who have willingly and readily donated a variety of fly stocks and reagents over the years.

Finally, a huge thank-you to my family, and to Leon, for their unfailing belief.

Contents

List of Figures

List of Tables

LIST OF ABBREVIATIONS

BDGP	Berkeley Drosophila Genome Project
cDNA	Complementary DNA
C1P	Ceramide-1-phosphate
CPO	Chloroperoxidase
DAG	Diacylglycerol
DGPP	Diacylglycerol pyrophosphate
EDG	Endothelial differentiation gene
EGFR	Epidermal growth factor receptor
EMS	Ethyl methane sulphonate
FGF	Fibroblast growth factor
GFP	green fluorescent protein
GPCR	G protein-coupled receptor
GGTT1	Geranygeranyl transferase type 1
HMGCoA	3-hydroxy-3-methylglutaryl coenzyme A
HMGCoAr	3-hydroxy-3-methylglutaryl coenzyme A reductase
HRP	Horse-radish peroxidase
ISH	*in situ* hybridisation
JAK	Janus kinase
LPA	Lysophosphatidic acid
LPP	Lipid phosphate phosphatase
MAG	Monoacylglycerol
M3	Myc (trimeric)
NEM	*N*-ethylmaleimide
PA	Phosphatidic acid
PAP	Phosphatidic acid phosphatase
PBS	Phosphate buffered saline
PCR	Polymerase chain reaction
PDGF	Platelet-derived growth factor
PDGFR	Platelet-derived growth factor receptor

PFA	Para formaldehyde
PGCs	Primordial germ cells
PLA	Phospholipase A
PRG-1	Plasticity-related gene-1
PT	PBS/Tween X-100
PVF1	PDGF/VEGF factor 1
PVR	PDGF/VEGF receptor
RTK	Receptor tyrosine kinase
s.d.	Standard deviation
S1P	Sphingosine-1-phosphate
STAT	Signal transducer and activator of transcription
TL	Total Lysate
UAS	Upstream Activating Sequence
VEGF	Vascular-endothelial growth factor
VEGFR	Vascular-endothelial growth factor receptor

WUNEN

In Chinese mythology, Wunen was a marshal in Heaven, sent down to earth as punishment for bad behaviour. There he took the form of a pig, and was adopted by a monk, who sent him on a pilgrimage to retrieve some Buddhist teachings. Rather than fulfilling his mission, however, Wunen kept wandering off to search for food, and chase women. In failing to reach his destination or practise good behaviour, he had lost his way, both spiritually and physically.

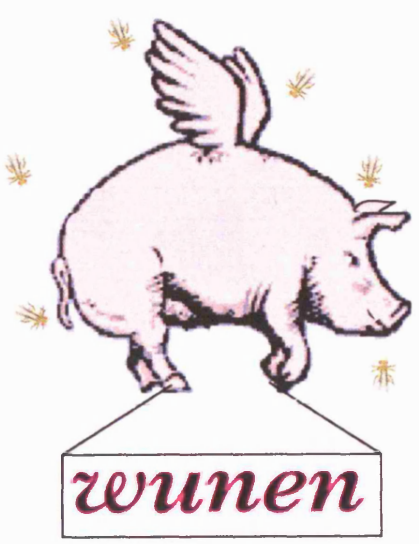

1) INTRODUCTION

1.1) Migratory cell types in *Drosophila*

The ability of cells to initiate and undertake guided migrations, sometimes over long distances, is an essential prerequisite of both foetal and adult development, from gastrulation up to organogenesis, and from instigation of the inflammatory response, to wound healing. Since cell migration is instrumental to so many processes, failure in its regulation can result in a wide range of pathologies, such as defects in brain development, foetal malformations, or tumourigenesis. The range of cell types that are capable of displaying motile behaviour is diverse, yet it is becoming increasingly apparent that many of the signalling pathways involved in the regulation of cell motility/migration are highly conserved, both from cell type to type, and between organisms.

There are a number of cell types that display motility during the development of *Drosophila melanogaster*, and research has revealed some of the signalling pathways responsible for their directed movement.

1.1a) *Border cells*

The *Drosophila* egg chamber consists of 15 nurse cells, which supply RNA and protein to the single oocyte, all surrounded by a monolayer of somatic follicular epithelial cells. The border cells arise as a group of 6 to 10 cells from the anterior follicular epithelium. During oogenesis, the border cell cluster migrates between the nurse cells towards the oocyte, located at the posterior end of the chamber. Upon arrival at the oocyte, they reorient and migrate dorsally, coming to lie over the oocyte nucleus. Their primary function upon arrival is to create the pore in the micropyle for sperm entry during fertilisation (Montell, 2003; Rorth, 2002).

A number of genes have been characterised that regulate border cell migration. One of these, *slow border cells* (*slbo*), is a transcription factor, and homologue of vertebrate C/EBP (CCAAT enhancer binding protein). Loss of *slbo* results in defects in border cell migration, and a number of downstream targets of *slbo* have subsequently been identified and shown to be required for correct migration of the border cell cluster (Montell, 2003).

The JAK/STAT signalling cascade is instrumental in a number of different developmental processes, and has been conserved from flies to vertebrates. Activation of the JAK/STAT cascade can be from an array of different ligands, including cytokines and growth factors, and can result in growth, differentiation and

migration. The ligands bind their specific membrane-bound receptor, which associates with a cytoplasmic tyrosine kinase of the Janus family (JAK). Upon receptor dimerisation, the JAK phosphorylates one of its tyrosine residues, resulting in the recruitment of cytoplasmic STAT (signal transducer and activator of transcription). STAT, having also been phosphorylated by JAK, dimerises, translocates to the nucleus, and induces gene transcription (Hombria and Brown, 2002). In *Drosophila*, there is one known STAT (Stat92E) (Hou et al., 1996; Yan et al., 1996), one JAK (Hopscotch) (Binari and Perrimon, 1994) and one ligand (Unpaired) (Harrison et al., 1998). In 2001, Domeless was identified as the receptor for the JAK/STAT pathway (Brown et al., 2001). A gain-of-function screen for genes interacting with *slbo* identified Stat92E, and so revealed the importance of the JAK/STAT pathway in border cell migration. Whilst Unpaired is required in the polar cells to induce border cell migration, it was demonstrated that hopscotch and Stat92E are required within the border cells themselves (Beccari et al., 2002).

Whilst components of the JAK/STAT pathway induce border cell migration, PVR/EGFR and PVF1 regulate guidance to the oocyte. PVF1 (PDGF/VEGF factor 1) is a *Drosophila* homologue of mammalian platelet-derived/vascular-endothelial growth factors, identified in a gain-of-function screen, alongside its receptor, PVR (Duchek et al., 2001). Both PVR and EGFR (epidermal growth factor receptor) are expressed in border cells, where they perceive the guidance signals, PVF1 and Gurken, produced by the oocyte. EGFR appears to be largely redundant for this purpose, with border cells able to utilise either receptor to successfully locate the oocyte. EGFR is, however, specifically required for the second, dorsal phase of border cell migration, in response to Gurken (Duchek and Rorth, 2001; Duchek et al., 2001). In vertebrates, PDGF and its receptors are essential for a number of critical developmental processes, and loss of either PDGFR results in embryonic lethality. In mice, a wide range of cell types, including oligodendrocytes and lung alveolar smooth muscle cells, are dependent on PDGFα signals for correct development (for review see (Tallquist and Kazlauskas, 2004)).

1.1b) *Hemocytes*

As with vertebrate blood cells, hemocytes in *Drosophila* undergo a characteristic migration beginning at stage 8. Hemocytes first arise 2 hours post-gastrulation, and are detected as a discrete population of cells in the procephalic mesoderm. As gastrulation proceeds they divide into two clusters, migrating anteriorly and posteriorly. From stages 13 to 14 they migrate towards the centre of the embryo, whereupon they spread out and disperse evenly as single cells, although dense clusters remain in the head, fore- and hind-guts (Tepass et al., 1994). VEGFR is expressed in the precursors of the vertebrate vascular system, and both VEGFR and its ligands play critical roles in vasculogenesis and hematopoiesis. As with border cells, PVR and its ligands also appear to regulate hemocyte migration in *Drosophila*. It has been reported that hemocytes express PVR from stage 8 onwards, whilst cells lining the migratory route express the PVF ligands. Loss of PVR results in initiation of migration but a failure to disperse correctly at later stages, whilst ectopic expression of the ligand is sufficient to mis-direct hemocytes to inappropriate tissues (Cho et al., 2002).

1.1c) *Tracheal cells*

A receptor tyrosine kinase (RTK) and its growth factor ligand are also involved in the migration of tracheal tip cells during *Drosophila* embryogenesis. The branching respiratory network originates from 10 clusters of approximately 80 cells, known as the tracheal placodes, located on either side of the developing embryo. These placodes invaginate, and then branch 5 to 6 times, before fusion of the individual metameres. Branchless (Bnl) is an FGF-like (fibroblast growth factor-like) chemoattractant expressed in cells surrounding the placodes, and towards which the extending primary branches migrate. This signal is received by the FGF receptor, expressed by the tip cells, and encoded by *breathless* (*btl*) (Affolter and Shilo, 2000; Ribeiro et al., 2003; Uv et al., 2003). Alongside this system, it has also been shown that, as with border cells, JAK/STAT signalling is required for specification of a migratory cell fate in the tracheal cells (Ribeiro et al., 2003).

1.1d) *Primordial germ cells*

Although this is a far simplified overview of the main types of migratory cells in *Drosophila*, it serves to illustrate the overlap in signalling systems that are employed

to regulate, induce, or guide cells to their final destinations. But what of primordial germ cells (PGCs)? PGCs are the stem cell progenitors of the adult germ-line. In *Drosophila*, as in many organisms, the PGCs are set aside at the beginning of embryogenesis as a distinct sub-set of cells, both temporally and spatially removed from their target tissue the somatic gonad. In order to locate and coalesce with the gonad, it is necessary for this specialised group of cells to undertake an active and invasive migration through the developing embryo, a process that begins early on in embryogenesis.

1.2) *Drosophila* embryogenesis and PGC migration

Drosophila embryogenesis is divided into seventeen discreet stages determined by easily distinguishable morphological characteristics (Campus-Ortega, 1985). By the completion of oogenesis, the anterior-posterior and dorsal-ventral axes of the *Drosophila* egg have been established by the maternal signalling systems. Post-fertilisation the egg contains zygotic nuclei that undergo a rapid succession of divisions before migrating out to the periphery, coming to rest in a thin layer of cytoplasm surrounding the central yolk. At this stage, prior to cellularisation, the egg consists of a highly ordered cytoplasm with three levels of cytoskeletal organisation and the posteriorly located pole plasm (Foe and Alberts, 1983). Pole plasm is a specialised form of cytoplasm consisting of electron dense polar granules containing both RNA and protein. The pole plasm components are produced by the nurse cells during oogenesis, under the control of the maternal-effect genes. Any nuclei entering the pole plasm automatically follow a germline fate (Illmensee and Mahowald, 1974).

During stage 3, polar buds form around the nuclei at the posterior pole of the embryo, which divide once. The nuclei divide once more whilst the embryo remains as a syncytial blastoderm during stage 4, before pinching off to form 12 to 14 PGCs. Thus the PGCs are the first cells to form in the developing embryo, and are easily identified by immunostaining as a distinct cluster at the posterior pole (Fig.1, stage 4).

The embryo now undergoes cellularisation, just prior to the onset of gastrulation in stage 6. Towards the end of stage 5, the group of PGCs, now

numbering between 30 to 40, are carried dorsally by the movement of the underlying posterior midgut anlage (Fig.1, stage 8). As the posterior midgut invaginates, the PGCs are carried into the gut lumen, where they pack down towards its blind end before actively migrating out of the lumen across the single-celled gut epithelium (Fig.1, stage 9-10). Having exited at stage 10, the PGCs spread out over the basal side of the posterior midgut and re-orient themselves towards the overlying mesoderm. Having entered the lateral visceral mesoderm, the PGCs divide into two bilateral groups and continue their migration until they contact their target tissue, the somatic gonadal precursors in parasegments 10-12 (Martinez-Arias and Lawrence, 1985) (Fig.1, stage 12). These two cell types continue to remain associated with each other during germ band retraction. At around stage 13 they coalesce to form the two gonads (Fig.1, stage 13). Only 10 to 15 PGCs are found in each gonad by the end of embryogenesis, a significant reduction in overall number. A proportion, therefore, are 'lost' along the way, although as yet, the exact method of loss is not well understood (Bate, 1993; Campus-Ortega, 1985).

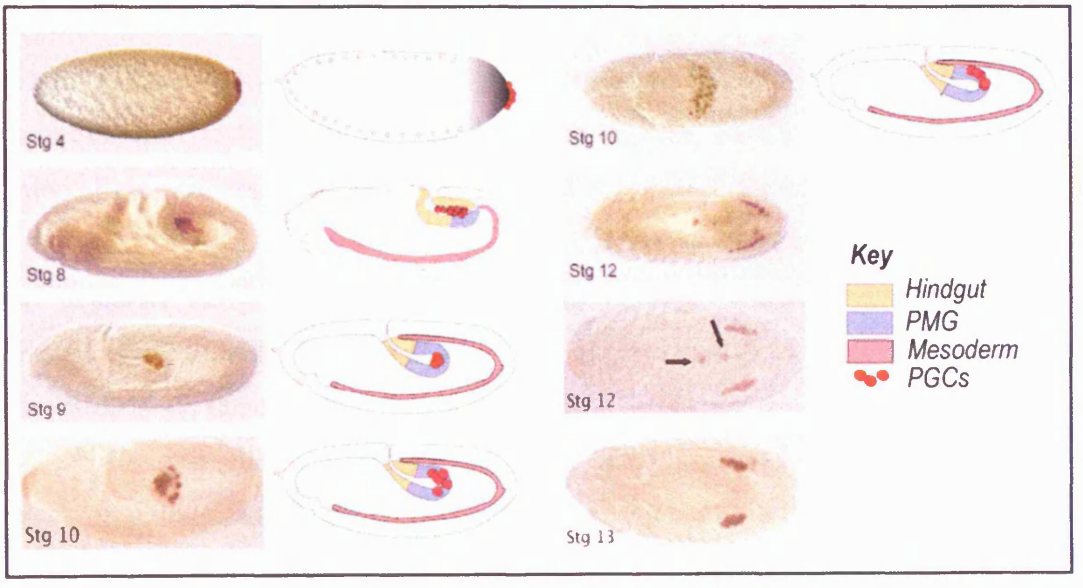

***Fig.1. Germ cell migration in* Drosophila.**

Embryos on the left of the figure are viewed laterally, whilst those on the right are viewed dorso-ventrally (except for the cartoon corresponding to stage 10, which is also oriented laterally). All are shown with their posterior to the right, with primordial germ cells (PGCs) stained for the germ cell-specific protein Vasa in brown. Cartoons to the right of photos are representative of the stage and indicate

mesoderm, posterior midgut (PMG), hindgut and PGCs according to the colour key. At stage 4, the graded area in the cartoon indicates the pole plasm, whilst the PGCs are located at the far posterior pole. This is the syncytial blastoderm stage, prior to cellularisation. Arrows in the stage 12 embryo indicate 'Lost' PGCs.

1.3) Factors regulating PGC migration

1.3a) *Structural changes during embryogenesis*

Work on the structural and morphological changes that occur during PGC migration led to a number of important insights in the mid 1990s. Using transplantation, microscopy and primary culture techniques, it was reported that the PGCs change shape from spherical to elongate at the beginning of gastrulation and extrude long pseudopodia into the surrounding environment. These shape changes are associated with rearrangements of their actin cytoskeleton. It was determined that the onset of migration through the polarised monolayer of the midgut epithelium is an active process that is PGC-specific and dependent on the developmental stage of the somatic tissue. It is associated with rearrangements of the adherens junctions between the posterior midgut cells, allowing the PGCs passage through the intercellular spaces. It was further reported that PGCs are capable of autonomous movement *in vitro*, and that they are able to orient correctly on the basal surface of the posterior midgut post exit in *snail twist* mutants, which as embryos lack the overlying mesoderm (Callaini et al., 1995; Jaglarz and Howard, 1994; Jaglarz and Howard, 1995; Leptin, 1991; Warrior, 1994).

Genetic studies demonstrated that PGC migration is independent of germ band retraction, and that initiation of migration can occur in the complete absence of endodermal tissue (Warrior, 1994). These analyses, however, did not unearth any of the signalling molecules involved in guiding the PGCs to their target tissue.

1.3b) **Drosophila** *genetics: screens and the power of the UAS/GAL4 system*

Over the years, numerous *Drosophila* genes have been identified and characterised, the majority through the use of large-scale genetic screens. These can employ a number of approaches and can uncover either zygotic or maternal-effect mutations. The original screens investigated loss-of-function phenotypes and typically

employed ethyl methane sulphonate (EMS) as a mutagen. EMS-mutagenesis was the basis of the Nobel prize winning screen by Christiane Nusslein-Volhard and Eric Wieschaus, which identified key genes involved in patterning the *Drosophila* embryo (Nusslein-Volhard and Wieschaus, 1980). X-ray irradiation, an alternative mutagen, has the advantage that it does not produce the mosaicism associated with mutagenesis of a single spermatid followed by segregation, that is often observed with EMS.

One method for uncovering genetic components of a pathway is to employ a screen for dominant enhancers or suppressors. This type of screen was utilised to elucidate the Sevenless RTK signalling pathway involved in the recruitment and specification of the R7 photoreceptor cell in fly ommatidia (for review see (Simon, 1994)).

For a proportion of genes, loss-of-function is lethal, making phenotypic analyses challenging. The use of clonal screens side steps this by specifically introducing targeted homozygous mutations to particular clones of cells, within a background of wild-type cells within a tissue. These clones can be induced via X-rays, or by employing the Flp-FRT technique developed by Golic and Lindquist (Golic and Lindquist, 1989; Xu and Rubin, 1993).

It is important when analysing the results of a zygotic screen to consider the possible role of maternal-effect genes. The maternal component of these genes is laid down during oogenesis, and this early contribution to the developing embryo may well mask the effects of a zygotic mutation. A saturation screen of the second chromosome identified a number of loci encoding maternal-effect genes. This screen isolated homozygous viable females that were phenotypically normal themselves, but which produced abnormal eggs. Out-crossing these females to wild-type males failed to rescue the observed phenotypes, confirming the role of maternal-effect genes. Phenotypic categories included complete failure of eggs to begin development, failure in syncytial blastoderm formation, failure in cellularisation, and failure to complete gastrulation (Schupbach and Wieschaus, 1989).

An alternative method is to screen for gain-of-function phenotypes, and this can be achieved by use of the multi-functional UAS/GAL4 system designed by Brand and Perrimon (Brand and Perrimon, 1993). GAL4 is a transcriptional activator, first identified in *Saccharomyces cerevisiae,* that regulates the transcription of the GAL1 and GAL10 genes by binding to a 17 base-pair stretch termed the

Upstream Activating Sequence (UAS). In 1993, Brand and Perrimon reported the development of the GAL4/UAS system in *Drosophila*, allowing for accurate temporal and spatial control of gene expression in a tissue-specific manner. The system works by cloning a gene of interest into a specially designed P-element vector that can be readily introduced into the *Drosophila* genome by standard microinjection/transformation techniques (Rubin and Spradling, 1982). The vector, termed pUAST, contains five tandemly arrayed and optimized UAS sequences upstream of the multiple cloning site, automatically placing control of the gene of interest cloned into this site under GAL4 regulation. There are many fly lines that express GAL4 in a variety of different tissues at varying times during development, and these are termed 'drivers', whilst flies containing an integrated UAS-geneX are termed 'responders'. One of the most valuable features of this system is that the driver and responder are maintained in separate lines. Only by crossing the two together is effective transcription of the gene initiated in the resulting F1 progeny. This means that genes that are otherwise toxic, lethal, or oncogenic can be kept quite happily in a dormant state as homozygous viable stocks until introduction of the GAL4 driver (Fig.2).

Various modifications and refinements of this system have since been developed (for a comprehensive review see (Duffy, 2002)). Addition of UAS target sequences to P-elements (transposable stretches of DNA that randomly insert in the 5' end of genes throughout the *Drosophila* genome) resulted in EP elements, whereby introduction of a GAL4 source results in the expression of endogenous genes and can be used alongside a reporter such as LacZ in genetic screens (Rorth, 1996).

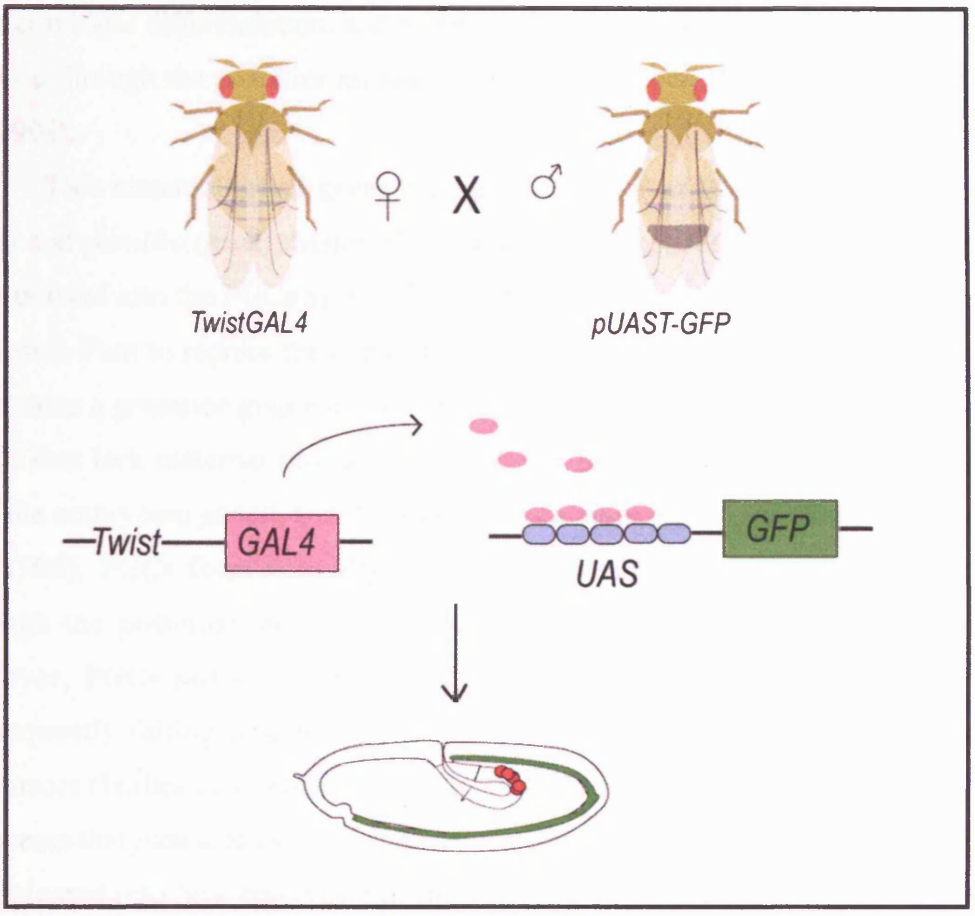

Fig.2. Schematic of the UAS/GAL4 system.

Flies containing a tissue-specific GAL4 driver are crossed to flies containing a UAS-geneX construct. In this example the driver is the mesoderm-specific twist-GAL4 and the responder is a GFP reporter. The result is F1 embryos with GFP expressed specifically in the mesoderm, shown here diagrammatically in a stage 10 embryo.

1.3c) *Genetic pathways*

Over the years a number of genes have been identified that regulate different stages of *Drosophila* PGC migration. These begin with genes expressed during oogenesis, the products of which regulate the expression of zygotic genes involved in PGC specification. Mutations in these maternal-effect genes can affect pole plasm formation (e.g. *oskar*, *vasa* or *tudor*) or, alternatively, anterior-posterior patterning (e.g. *gurken*) (Wylie, 1999). Disruption of these processes necessarily results in a failure to form PGCs. At around stage 9, *serpent* and *huckebein* are required for

correct midgut differentiation, and mutations in either results in a failure of PGCs to migrate through the posterior midgut surface (Jaglarz and Howard, 1994; Moore et al., 1998).

Two maternal-effect genes that specifically affect PGC migration are *nanos* (*nos*) and *pumilio* (*pum*). Maternal *nos* mRNA is localised to the pole plasm and incorporated into the PGCs as they form, whereupon the resultant Nos protein works alongside Pum to repress the translation of maternal *hunchback* (*hb*). Repression of *hb* creates a posterior gradient that results in abdominal specification. Transplanted PGCs that lack maternal *nos* do not migrate correctly, fail to become incorporated into the embryonic gonad, and demonstrate premature gene activation (Kobayashi et al., 1996). PGCs form normally in embryos lacking maternal Nos, and migrate through the posterior mid-gut wall as in wild-type. Having exited at stage 10, however, PGCs fail to disperse over the surface, and instead cluster together, subsequently failing to enter the mesoderm or connect with the somatic gonadal precursors (Forbes and Lehmann, 1998). As well as acting in concert to suppress *hb*, it appears that *pum* acts as a cofactor in the regulation of PGC migration. *pum-* PGCs transplanted into host embryos exit the posterior mid-gut normally, but also fail to associate with the embryonic gonad, and again, gene expression is initiated prematurely. It is postulated that this premature gene activation may 'trick' the PGCs into 'believing' that they have already completed their migration, so arresting them at too early a stage (Asaoka-Taguchi et al., 1999).

Interestingly, embryos from *nos* homozygous mothers showed a reduction in PGC number starting at stages 9-10 (Asaoka-Taguchi et al., 1999). This PGC loss was suppressed in combination with Df(3L)H99, a deletion that removes *reaper*, *head involution defective* and *grim*, all essential components for apoptosis. When transplanted into host embryos, these PGCs were incorporated into a range of somatic tissues. Here, they assumed the morphology of these tissues, expressed somatic tissue-specific markers and lost expression of the PGC-specific marker Vasa (Hayashi et al., 2004). Thus prevention of apoptosis in these PGCs allows them to differentiate into somatic cells. Furthermore, a proportion of these *nos-* PGCs resumed the ability to migrate correctly to the gonads, leaving the authors to conclude that whilst Nos is not essential for PGC migration, it is required to suppress apoptosis. This suppression subsequently allows correct migration to the embryonic

gonads. It also appears to suppress the pathway leading to a somatic cell fate, a novel and interesting role.

Researchers recently investigated interactions between the receptor tyrosine kinase Torso, STAT92E, and Ras during embryogenesis. They noted that mutations in each of these resulted in fewer PGCs at cellularisation, whereas double mutants in STAT92E and Ras had a much more dramatic reduction in number. They concluded that co-activation of STAT92E and Ras by Torso is required for PGC proliferation. Furthermore, embryos deficient in maternal STAT92E demonstrated PGC migration defects – rather than associating with the overlying dorsal mesoderm post-exit from the midgut at stage 11, PGCs were found still associated with the midgut itself. Paternal rescue resulted in the formation of a single, over-populated gonad, indicating a possible failure of the PGCs to separate correctly into two bilateral groups. Loss of both maternal and zygotic STAT92E resulted in a failure to form any gonads, with PGCs scattering randomly throughout the embryo. Conversely, increased activation of STAT92E by over-expression of Hopscotch resulted in increased motility, with PGCs showing early invasiveness into the interior of the embryo at stages 4-5, and premature exit through the midgut. Increased levels of STAT92E gave supernumerary PGCs, with any that failed to migrate correctly to the gonads also failing to be eliminated, the usual course for 'lost' PGCs in wild-type embryos (Li et al., 2003). Embryos deficient in Ras displayed similar defects in PGC migration to those observed in STAT92E null embryos. Loss of Torso resulted in PGCs that were completely immotile. Interestingly ectopic expression of Unpaired was sufficient to perturb migration, with PGCs ending up in ectopic locations. The authors conclude that somatic tissues secrete ligands that activate the STAT92E and/or Ras signalling pathways, providing migratory cues for the PGCs (Li et al., 2003).

An exhaustive screen of the third chromosome by EMS mutagenesis identified yet more genes, including *zinc finger homeodomain-1* (*zfh-1*), *heartless* (*htl*) and *fear of intimacy* (*foi*). In *zfh-1* or *htl* mutants, PGCs exit the posterior midgut but fail to migrate into the overlying mesoderm, instead remaining on the midgut basal surface. Mutations in *foi* result in an aberration in PGC and gonadal mesoderm coalescence, with the somatic gonadal precursors failing to associate tightly with one another (Moore et al., 1998). All three of these mutations, however, alongside many others found in this screen, affect the development of the gonadal

mesoderm, which consequently results in perturbed PGC migration, rather than disrupting the intrinsic migratory properties of PGCs themselves.

One gene also identified by this screen (although first cloned in 1988 (Gertler et al., 1988)), that does affect PGC migration and not mesodermal development, was *columbus*. *columbus* encodes a *Drosophila* homologue of 3-hydroxy-3-methylglutaryl coenzyme A reductase (*hmgcr*). In *hmgcr* mutants, a proportion of PGCs remain associated with the endoderm and fail to enter the mesoderm. Those that do successfully make it to the mesoderm then scatter, failing to associate with their target tissue the gonadal mesoderm. In fact, HMGCoAr is expressed in the gonadal mesoderm, and by using a number of gonadal mesoderm-specific markers, it was determined that the development of this tissue is unaffected in these mutants. Use of the UAS/GAL4 system (Brand and Perrimon, 1993) demonstrated that ectopic expression of HMGCoAr in alternative tissues was sufficient to attract PGCs to those tissues (Van Doren et al., 1998). Thus it is postulated that HMGCoAr influences PGC migration by mediating a somatic signal that behaves as an attractive guidance cue.

A second gene identified by the EMS mutagenesis screen was *hedgehog* (*hh*). *hh* encodes a secreted signalling protein and is required for patterning during early embryogenesis in animals. In flies, Hh has a number of both short and long range signalling roles, including regulation of patterning and formation of the somatic gonadal mesoderm (Ingham and McMahon, 2001). Consequently, mutations in *hh* also result in perturbed PGC migration as one would expect from disruption of these processes (Moore et al., 1998). In 2001, however, it was reported that mis-expression of Hh using a number of different GAL4 drivers attracted PGCs to ectopic locations, a phenotype strikingly similar to that observed for HMGCoAr. Using a lacZ reporter construct, alongside antibodies to the mesoderm marker Clift, researchers were able to determine that Hh is expressed in the somatic gonadal precursor cells. Furthermore, generating germline clones in four genes in the Hh pathway (*smoothened*, *patched*, *protein kinase A* and *fused*) also resulted in aberrant PGC migration (Deshpande et al., 2001). Whilst these data may indicate that Hh is acting to modify a secondary signalling molecule that regulates PGC migration, it is also possible that Hh itself acts as an attractive somatic signal influencing PGC migration directly.

In mammals, HMGCoAr catalyses the conversion of HMGCoA to mevalonate, a precursor of, among other things, isoprenoids and cholesterol. Hh is first synthesised as a precursor protein, before undergoing autoproteolysis by its C-terminal domain into two smaller peptides. Addition of cholesterol to the C-terminus of the N-terminal peptide results in an active signalling molecule (Nusse, 2003). This requirement for a cholesterol modification, alongside its PGC migration phenotype and expression data, raised the possibility that Hh could be acting downstream in the *hmgcr* pathway. This has since been ruled out by a computational analysis of the *Drosophila* genome, which revealed that flies lack the majority of enzymes involved in the synthesis of cholesterol (Santos and Lehmann, 2004b). Further investigation of the *Drosophila* homologues discovered by this analysis revealed that three genes downstream of *hmgcr*, namely *fpps*, encoding farnesyl-diphosphate synthase, *quemao* (*qm*), encoding geranylgeranyl-diphosphate synthase, and geranylgeranyl transferase type 1 (GGTT1) are all necessary for successful PGC migration (Fig.3). The first two genes, *fpp* and *qm*, are both required for the synthesis of isoprenoids: whilst a mutation in either gene results in a weak PGC migration defect, similar to that seen in *hmgcr* mutants, mutations in both genes results in a strong PGC migration defect. Furthermore, these mutations enhance the phenotype seen in the *hmgcr* mutant. This indicates that these genes cooperate to synthesise downstream GGTT1 and that it is GGTT1 itself, or, more specifically, the geranylgeranylation of proteins, that plays a significant role in guiding PGC migration. This is further substantiated by the fact that mutations in the β sub-unit of GGTT1 have the same phenotype in flies as does pharmacological blocking of GGTT1 or its precursors in zebrafish, indicating an evolutionarily conserved signalling pathway (Thorpe et al., 2004).

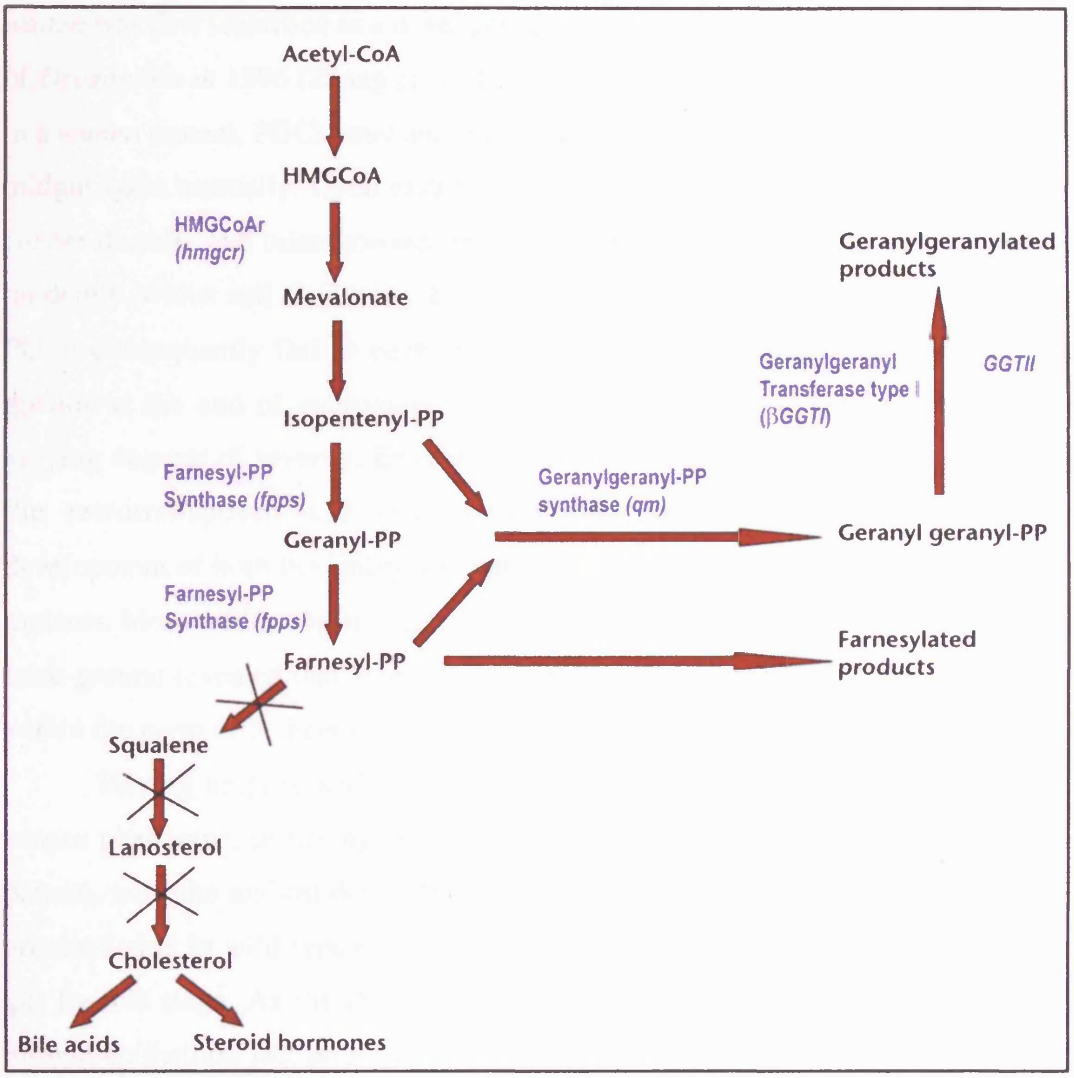

Fig.3. Biosynthesis of cholesterol and isoprenoids. *For simplification, only those enzymes and products implicated in* Drosophila *PGC migration are shown. Crosses indicate where* Drosophila *homologues are lacking in the cholesterol pathway. (Adapted from Thorpe et al., 2004 and Santos and Lehmann, 2004).*

1.3d) *Wunen and Wunen-2*

To date, two distinct pathways have been discovered that control *Drosophila* PGC migration through somatic signals, and both appear to act via some level of lipid modification. The first, as touched upon above, involves HMGCoA reductase and the geranylgeranylation of target proteins. The second involves Wunen (Wun) and its closely related counterpart Wunen-2 (Wun-2).

wunen was first identified as a novel genetic locus at 45D on the second chromosome of *Drosophila* in 1996 (Zhang et al., 1996). It was shown by deficiency analysis that in a *wunen* mutant, PGCs enter and pack down towards the distal end of the posterior midgut quite normally. Upon exiting the gut at stage 10, however, the PGCs fail to cluster dorsally and orient towards the overlying mesoderm - instead they spread out randomly, whilst still displaying the physical characteristics of motility. A number of PGCs consequently fail to contact the somatic gonad and are found outside the gonads at the end of embryogenesis (Fig. 4). This is a variable phenotype with varying degrees of severity. Examination of *forkhead* expression and expression of the retrotransposon 412 confirmed normal molecular and morphological development of both the embryonic gut primordium and the somatic gonad in these mutants. Mosaic flies containing wild-type germ cells in either a *wunen* or wild-type back-ground revealed that Wunen function is required in the somatic tissue and not within the germ cells themselves (Zhang et al., 1996).

Having mapped and subsequently cloned the transcript responsible for the *wunen* phenotype, *in situ* hybridisation (ISH) revealed a dynamic RNA expression pattern, with the highest detectable levels in the hindgut primordium, where PGCs are not found in wild-type embryos, having packed down into the distal end of the gut by this stage. As the PGCs move up towards the apical side of the posterior midgut epithelium just prior to exit, Wunen expression increases on the lower side, *i.e.* in the region of the gut that the PGCs are actively migrating *away* from. Moreover, ectopic expression of Wunen in the overlying mesoderm using a fly strain containing the UAS-Wun^{c18} construct crossed to flies carrying the twist-GAL4 driver (Greig and Akam, 1993) prevents PGCs from entering this normally attractive tissue and the majority are left outside the gonad (Zhang et al., 1997) (Fig. 4).

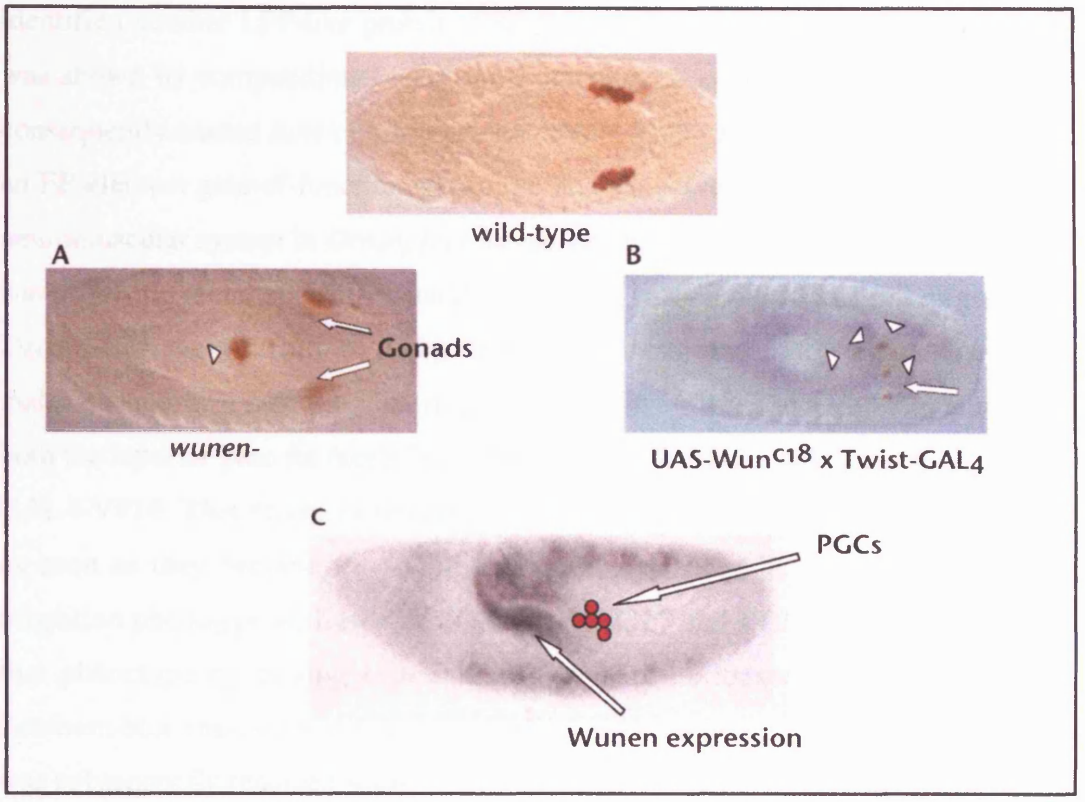

Fig.4. Wunen expression and phenotypes.

Embryos in A and B are viewed dorso-ventrally with the posterior on the right and are stage 13. The embryo in C is viewed laterally at stage 10. Germ cells are stained with a monoclonal anti-Vasa antibody and are visualised in brown. ***A)*** *In Wunen loss-of-function mutants, a number of PGCs fail to contact the somatic gonad and are left ectopic to the gonads at the end of embryogenesis. The arrowhead indicates these, whilst arrows indicate the gonads.* ***B)*** *Ectopic expression of Wunen in the mesoderm (stained blue) results in perturbation of PGC migration and PGC loss. Only one PGC has successfully located the gonad, as indicated by the arrow. Just four other PGCs remain but have failed to reach the gonad, as indicated by the arrowheads.* **C)** *Wunen expression pattern in a stage 10 embryo by ISH. High levels of expression are indicated in the hindgut and region of the posterior midgut that the PGCs avoid as they exit. The PGCs are shown diagrammatically in red exiting the midgut.*

Analysis of the *wunen* sequence revealed homology to the mammalian lipid phosphate phosphatases (LPPs). In 1998 a large-scale screen for genes expressed during *Drosophila* embryogenesis encoding secreted or transmembrane proteins

identified another LPP-like protein, CK02248 (Kopczynski et al., 1998). CK02248 was shown by computational analyses to encode a homologue of *wunen*, and was consequently named *tunen* (A.M.Hayden, 2000). This gene was further identified in an EP-element gain-of-function screen for genes involved in the development of the neuromuscular system in *Drosophila* larvae, again as a novel gene with homology to *wunen* (Kraut et al., 2001). A similar screen for genes involved in PGC migration in *Drosophila* again identified this gene (Starz-Gaiano et al., 2001). For this screen, males containing a randomly inserted EP element were crossed to females containing both the reporter gene fat facets-lacZ (faf-lacZ) and the germ-cell specific driver nos-GAL4-VP16. This drives expression of each random gene specifically in the PGCs as soon as they become transcriptionally active at stage 9. Having determined a migration phenotype with two EP elements, EP2217 and EP2650, and re-confirmed that phenotype by driving expression of each in the mesoderm, plasmid rescue, Southern blot analyses and sequencing revealed *tunen* as the gene responsible and it was subsequently renamed *wunen-2* (Starz-Gaiano et al., 2001) (Fig.5).

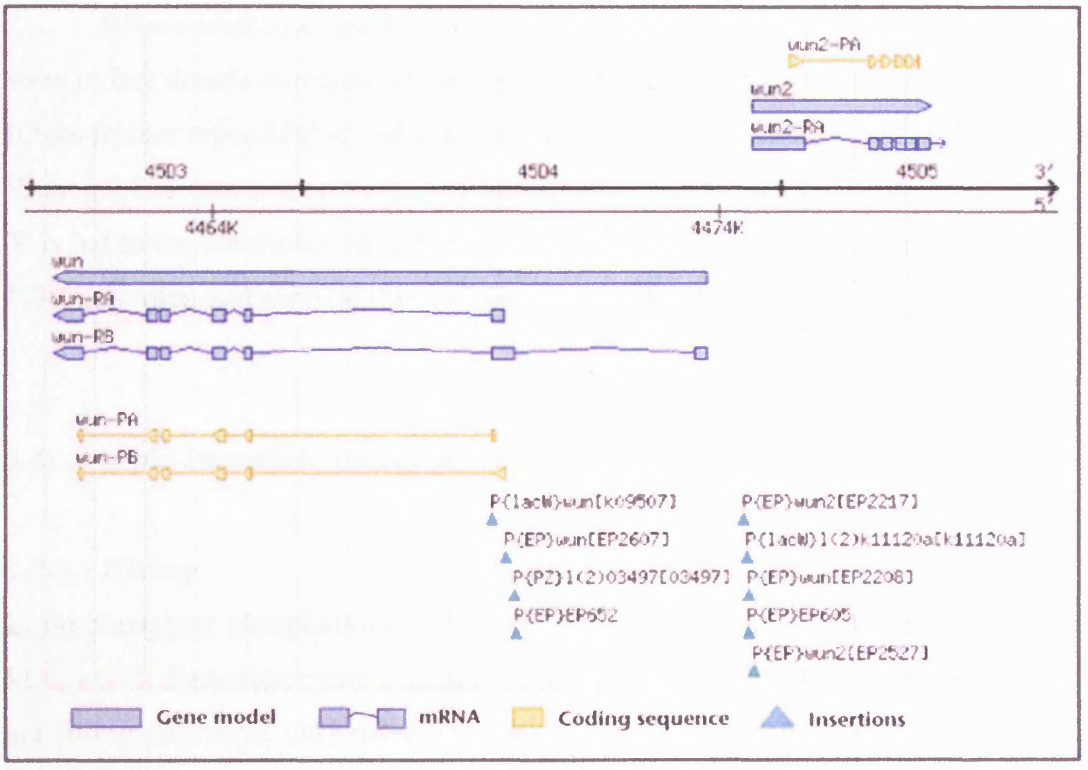

Fig.5. The* wun *and* wun-*2 genomic region, indicating introns and translated regions (Adapted from FlyBase (2003).)

wunen-2 is transcribed 5Kb away from *wunen*, in the opposite direction and ISH confirmed that *wunen-2* has the same mRNA expression profile as *wunen*, with dynamic expression in the epidermis, lateral neuroblasts and the anterior midgut, but with strongest expression in the hindgut and lower side of the posterior midgut. Just like Wunen, ectopic expression of Wunen-2 in the mesoderm repels PGCs and prevents them from entering this tissue. Interestingly, close analyses of these Wunen-2 embryos revealed a second, later phenotype. Starting at stage 11, embryos over-expressing Wunen-2 in the mesoderm showed a dramatic reduction in PGC number – in many embryos between only two to four PGCs were left by the end of embryogenesis. The same result was further confirmed for Wunen, as seen in Fig.4B. Development of the mesoderm in these embryos was unaffected, but the same reduction in number was observed when Wunen-2 was ectopically expressed in either the nervous system or the trachea. Thus not only are Wunen and its counterpart Wunen-2 involved in regulating PGC migration, they also appear to play a pivotal role in PGC survival.

RNase protection and ISH data indicated that the original mutations in *wunen* were in fact double mutations removing both Wunen and Wunen-2 somatic function. It was further reported that insertions EP2607 and EP2527 removed both Wunen and Wunen-2 function respectively, with neither demonstrating a PGC migration defect. This led to the conclusion that Wunen and Wunen-2 function redundantly to control PGC migration and survival (Starz-Gaiano et al., 2001).

1.4) Lipid Phosphate Phosphatases (LPPs):

1.4a) *History*

Lipid phosphate phosphatases (LPPs) are integral membrane proteins of around 35 kDa, which dephosphorylate a number of bioactive lipid phosphates involved in lipid signalling pathways. Originally, phosphatidic acid phosphatase (PAP) activity was identified as important for the production of the second messenger diacylglycerol (DAG) from phosphatidic acid (PA), a precursor of triacylglycerols, phosphatidylcholine and phosphatidylethanolamine. The PAP-1 enzyme is located in the cytosol where it provides a reservoir of activity and it is activated by

translocation to the endoplasmic reticulum. A second distinct PAP-like enzyme was first identified and characterised from rat liver preparations by Brindley *et al* in 1991. By developing specific assays, they were able to demonstrate that this second PAP, which they named PAP-2, localised to the plasma membrane and showed a high affinity for PA as a substrate. Unlike PAP-1, PAP-2 proved to be insensitive to *N*-ethylmaleimide (NEM) inhibition and was Mg^{2+} independent (Jamal et al., 1991).

The PAP-2 enzymes were renamed lipid phosphate phosphatases (LPPs) following the discovery that they are capable of dephosphorylating a range of phospholipid substrates, alongside PA.

The first successfully cloned mouse LPP-1 cDNA (Kai et al., 1996) was quickly followed by identification of a second isoform, rat Dri42 (LPP-3), and then human LPP-1 and LPP-3 (Barila et al., 1996; Kai et al., 1996; Kai et al., 1997). The third isoform, LPP-2, was also identified in humans (Hooks et al., 1998; Roberts et al., 1998). Having established the existence of three isoforms, splice variants were reported for the human protein (hLPP-1α) and identified in rat lung by RT-PCR (LPP-1a, b and c) (Leung et al., 1998; Nanjundan and Possmayer, 2001a). More recently, Plasticity-related gene-1 (PRG-1), a novel member of the LPP family, has been identified in rat hippocampus (Brauer et al., 2003).

Besides the mammalian and *Drosophila* LPP isoforms, LPP homologues have been identified in *Saccharomyces cerevisiae* and *Arabidopsis thaliana* (Pierrugues et al., 2001; Toke et al., 1998).

1.4b) *LPP structure*

By using the *Escherichia coli* gene *pgpB* in the National Center for Biotechnology Information (NCBI) BLAST search program, Stukey and Carman identified a novel sequence motif present in twenty-three established or predicted LPP proteins (Stukey and Carman, 1997). From this, they proposed a novel phosphatase superfamily based on amino-acid sequence homology, and including fungal haloperoxidases, mammalian G6Pase, rat Dri42 and Wunen. The reported phosphatase sequence motif consists of three highly conserved domains, all between 4 to 11 amino-acids in length, and each including 3 or 4 absolutely conserved residues. The order of the domains in each protein is invariant (Fig.6).

Fig.6. The three conserved domains that characterize the phosphatase superfamily *(as proposed by Stukey and Carman, 1997). Amino-acids shown to be essential for catalytic activity are highlighted in orange.*

Further analyses using a statistically based search and multiple sequence alignment program (PROBE) (Neuwald, 1997) indicated that these membrane-associated proteins share conserved structural elements and may share a similar catalytic mechanism to related soluble globular enzymes. The family includes vanadium chloroperoxidase (CPO) of *Curvularia inaequalis*. This is an important family member, as its structure is already known. Comparisons with CPO led to the development of models for structure, and mechanisms of hydrolysis, for other family members, specifically in this case, the LPPs.

Hydropathy analysis indicates that the LPPs are membrane-spanning proteins. Studies into the topology of Dri42 using truncated proteins fused to a reporter confirmed this, and demonstrated that not only are both the N- and C-termini cytosolic, but that the 6 hydrophobic segments are inserted into the membrane by alternating halt/transfer and insertion signals (Barila et al., 1996). In 1999, Jasinska *et al.* demonstrated that LPP activity is only detected in the membrane fraction of rat2 fibroblasts stably expressing mLPP-1. Using a C-terminal tagged GFP-fusion protein, confocal microscopy, and immunostaining, they were also able to show that the C-terminus of mLPP-1 is cytosolic (Jasinska et al., 1999). As a follow up to this work they used site-directed mutagenesis to demonstrate that seven of the amino-acids within the three conserved domains are absolutely required for catalytic

activity and, therefore, that these domains constitute the active site. Taken together, these results confirm that the active site, composed of the three domains, is located on the outer surface of the plasma membrane. The mammalian LPPs contain a conserved N-glycosylation site. It was further established that this site resides between domains 1 and 2 and is not required for catalysis. This further supports the location of the active site as extracellular (Zhang et al., 2000b) (Fig.7).

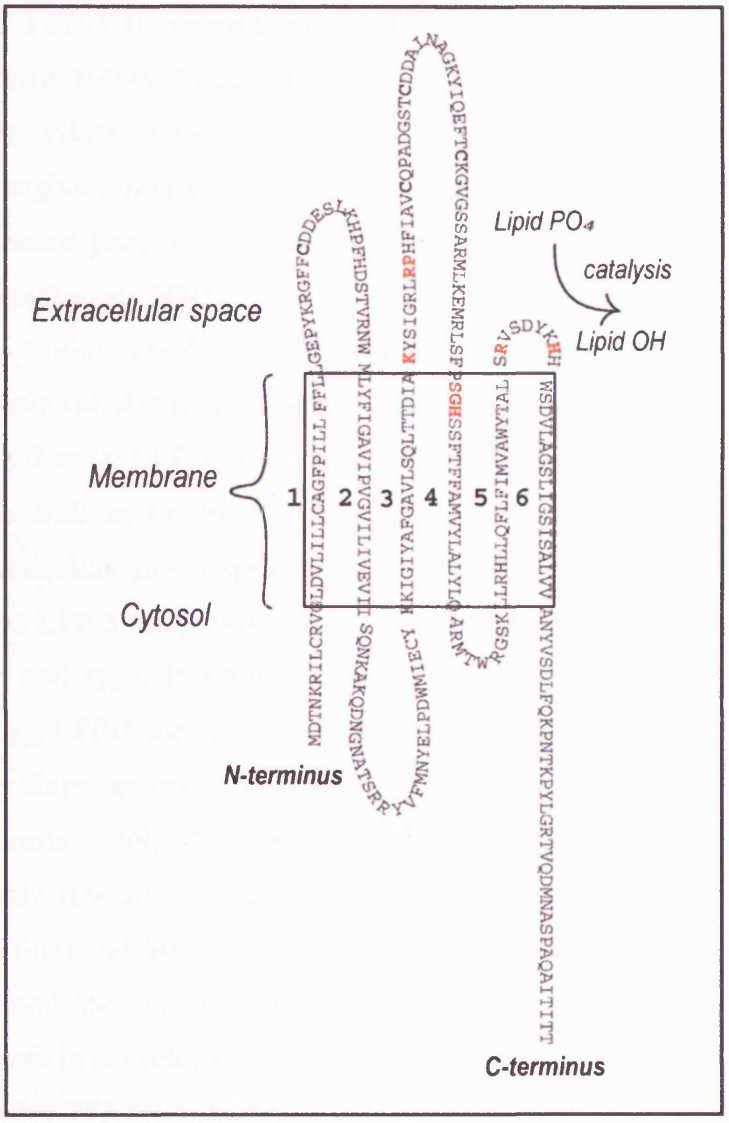

Fig.7. Proposed topology of the Wunen protein.

The diagram demonstrates the putative membrane topology of the Wunen protein and its transmembrane domains, and acts as a representation of other members of the LPP family. The completely conserved residues required for catalytic activity are shown in red.

1.4c) *LPP localisation*

Purification of the LPPs has proved challenging, leaving antibodies to these proteins hard to come by. Nevertheless, LPP-like activity has been detected in all cell and tissue types so far studied, in a range of different organisms, including yeasts and plants. Despite previous problems, Andrew Morris' group did obtain an antibody to an N-terminal peptide sequence specific to LPP-3. They used this to examine the expression of LPP-3 in various mouse tissues, finding it to be differentially expressed in brain, kidney, liver, heart, spleen, lung and skeletal muscle (Sciorra and Morris, 1999). Whilst whole mount ISH indicates that LPP-1 and LPP-2 are expressed throughout mouse embryogenesis, LPP-3 displays a tissue-specific and dynamic expression pattern, coinciding with its role during embryonic development (Escalante-Alcalde et al., 2003).

To begin to elucidate the physiological function of the LPPs, it is necessary to characterise their cellular localisations. Work on LPP-1 and LPP-2 is a little less comprehensive than for LPP-3, but indicates that both proteins localise to the plasma membrane, as well as to ill-defined intracellular compartments (possibly the endoplasmic reticulum and Golgi apparatus) (Alderton et al., 2001; Jasinska et al., 1999). Work on LPP-3 has proved more exhaustive and indicates that localisation is dependent on cell type. If stably expressed in human embryonic kidney cells (HEK293 cells), LPP-3 localises predominantly to the plasma membrane, as has been found by three separate groups (Alderton et al., 2001; Ishikawa et al., 2000; Sciorra and Morris, 1999). If expressed in COS7 cells, however, LPP-3 localises to the endoplasmic reticulum, as does rat Dri42 in both FRIC B cells (foetal rat intestinal cell line) and MDCK cells (Madin-Darby canine kidney) (Barila et al., 1996; Sciorra and Morris, 1999). It has also been reported that 10-15% of LPP-3 activity is present in caveolin-enriched, detergent-resistant membrane microdomains (DRMs) in Swiss 3T3 cells (Sciorra and Morris, 1999). This localisation is LPP-3 specific, is not detected for LPP-1 and is further substantiated by findings that LPP-3 activity is highly enriched in similar domains from rat lung tissue, isolated rat type II cells and mouse lung epithelial cell lines (MLE12 and MLE15) (Nanjundan and Possmayer, 2001b).

More recently, Jia *et al.* reported that LPP-1 and LPP-3 in MDCK cells localise

to distinct sub-domains of the plasma membrane. They determined that both contain sorting signals (a six residue N-terminal sequence in LPP-1 and a dityrosine motif in the second cytoplasmic loop of LPP-3) which result in LPP-1 localising to the apical side of the plasma membrane, and LPP-3 localising to the baso-lateral sub-domain (Jia et al., 2003).

1.4d) *LPP substrates*

The three LPP isoforms can de-phosphorylate a variety of phospholipids, namely phosphatidic acid (PA), lysophosphatidic acid (LPA), sphingosine-1-phosphate (S1P), ceramide-1-phosphate (C1P) and diacylglycerol pyrophosphate (DGPP). The primary source of LPA and S1P production in vertebrates is activated blood platelets. Here, PA is converted to LPA through the action of Phospholipase A2 (PLA2) (Fig.8). S1P is generated by the action of sphingosine kinase (Fig.9). Both products are released into the extracellular environment where they become active signalling components of serum.

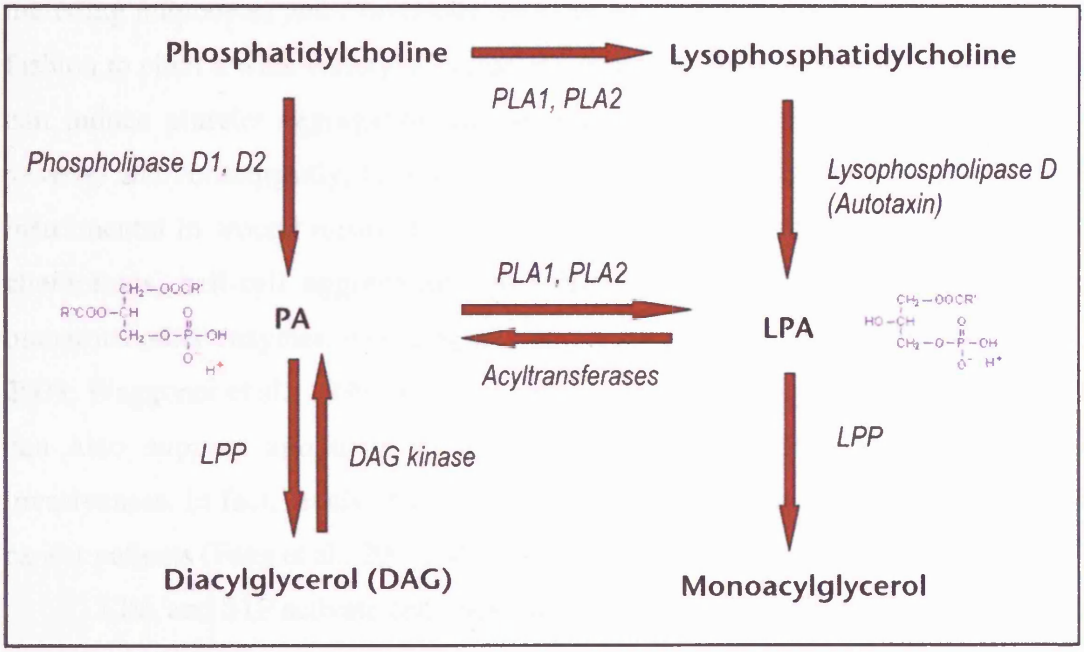

Fig.8. The action of LPPs on PA and LPA *(adapted from Brindley (Brindley, 2004)).*

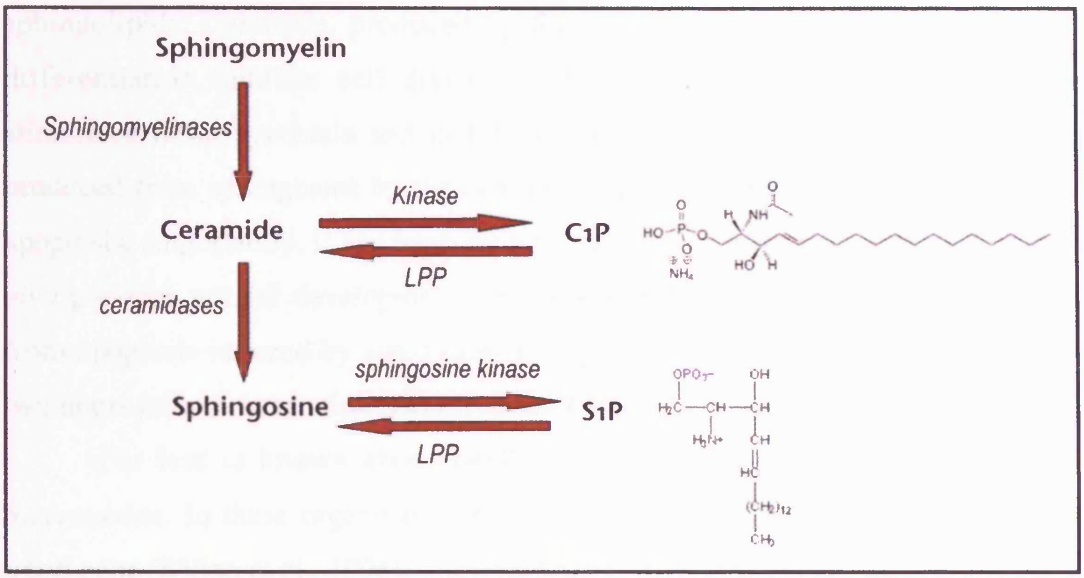

Fig.9. The action of LPPs on S1P and C1P *(adapted from Waggoner et al (Waggoner et al., 1999)).*

In fact both LPA and S1P are released from a number of different cell types, including adipocytes and fibroblasts, and can act in either a paracrine or autocrine fashion to elicit a wide variety of biological or pathological responses. LPA and S1P can induce platelet aggregation and angiogenesis (the formation of new blood vessels) and consequently, following their release from activated platelets, may be instrumental in wound repair. They are also known to stimulate cell proliferation, chemotaxis, cell-cell aggregation, growth-cone collapse and the activation of numerous other enzymes, including phospholipase D (Moolenaar, 1999; Pyne et al., 2004; Waggoner et al., 1999). LPA can prevent apoptosis in certain cell types, but it can also support apoptosis in others; furthermore, LPA promotes tumour invasiveness. In fact, levels of LPA are specifically raised in the ascites of ovarian cancer patients (Fang et al., 2000; Mills et al., 2002).

LPA and S1P activate cell responses through their specific G protein-coupled receptors (GPCRs). There are at least seven members of these endothelial differentiation gene (Edg) receptors - Edg2, 4, and 7 are selective for LPA, whilst Edg1, 3 and 5 are selective for S1P. Multiple receptors can be expressed at any one time in any particular cell type, and can initiate a wide range of signalling pathways.

The conversion of sphingomyelin to the precursor ceramide by sphingomyelinases is the first step in the generation of a number of bioactive

sphingolipids. Ceramide, produced by the action of LPPs on C1P, induces cell differentiation, inhibits cell division and induces apoptosis. Conversely C1P stimulates DNA synthesis and cell proliferation (Waggoner et al., 1999). S1P, produced from sphingosine by the actions of sphingosine kinase, can also prevent apoptosis. Importantly, it has been shown that treating mouse oocytes with S1P *ex vivo* prevents normal developmental apoptosis, and, furthermore, protects oocytes from apoptosis induced by anti-cancer therapies. An *in vivo* administration of S1P two hours prior to irradiation also prevents oocyte loss in mice (Morita et al., 2000).

Far less is known about DGPP, a novel lipid discovered in *E.coli* and *S.cerevisiae*. In these organisms, DGPP phosphatase (in *E.coli* the product of the *pgpB* gene (Dillon et al., 1996)) converts DGPP to PA, then dephosphorylates PA to produce DAG. LPP isolated from rat liver has been shown to catalyse the same reaction *in vitro*, as has mLPP-1, and rLPP-1 from membrane preparations of rat2 fibroblasts presented with DGPP in triton micelle assays (Dillon et al., 1997; Jasinska et al., 1999).

The ability to modulate these bioactive substrates *in vitro* implies that the LPP family of enzymes may have important roles in regulating the levels of these potent signalling molecules *in vivo*. This regulation may involve the attenuation of their activities by dephosphorylation to a biologically inactive form, or transformation of their activities through conversion to an alternative bioactive form.

1.4e) *Physiological functions of LPPs*

Despite the enormous amount of research that has been carried out on the LPPs, remarkably little is known of their actual functions *in vivo*, and their true physiological substrates remain frustratingly elusive. Data are certainly available on the differential expression patterns of the separate LPP isoforms, but this does not tell us what function they are actually performing. Knowledge of where the LPPs are expressed *in vivo*, however, in conjunction with *in vitro* data and the phenotypic results of ectopic expression and knockouts in different organisms, should eventually prove illuminating.

One of the first genes to be characterised, rat Dri42, may function in intestinal epithelial differentiation during development. Dri42, expressed in liver, kidney and lung epithelia, was first discovered during a search for genes up-regulated during development and differentiation. The mature villus epithelium

consists of three distinct cell types – absorptive enterocytes, goblet cells and enteroendocrine cells. Dri42 mRNA is expressed along the entire villus epithelium in both horizontal and vertical axes. Furthermore, Dri42 has been localised by ISH to developing and mature rat brain and spinal cord (Barila et al., 1994; Barila et al., 1996; Suzuki et al., 1999).

Northern analyses have shown the human splice variant hLPP-1α to be down-regulated in tumour tissue, with the most dramatic changes seen in colon tumours. What specific role LPP-1 has in this case is still not known, but it has been proposed that it may present a gene therapy target in the future (Leung et al., 1998).

The AtLPP genes in *A.thaliana* encode homologues to the mammalian LPPs. Whilst AtLPP2 is expressed ubiquitously throughout the plant, AtLPP1 is selectively expressed in the leaves and roots. Subjecting the plant to a number of external stimuli, including oxidative stress, ionising and gamma radiation and G-protein activation, resulted in a rapid and transient rise in the levels of AtLPP1 expression, but no increase in AtLPP2, indicating either redundancy or distinct functions for each of these genes. Since PA and DGPP also accumulated in response to stress in these plants, it is speculated that in *A.thaliana* the function of at least one LPP gene may be to attenuate the potent signalling properties of these molecules (Pierrugues et al., 2001).

The use of gene targeting in embryonic stem cells allowed Zhang *et al.* to delete transmembrane domains 2 and 3, as well as domain 1, of mouse LPP-2. They interbred the resultant viable, fertile, heterozygous adults to produce homozygous null progeny. The lack of an LPP-2 transcript was confirmed by Northern analyses. Not only were the null offspring born at the expected ratio, they were also perfectly viable and fertile adults, with no obvious phenotypic defects. Thorough histopathological analyses revealed no abnormalities in any of the major organ systems. The authors were left to conclude that in mice at least, LPP-2 is non-essential during embryonic development and possibly redundant to the LPP-1 and LPP-3 isoforms (Zhang et al., 2000a).

In a striking contrast to these findings, mice null for LPP-3 displayed distinct and dramatic developmental defects. Using targeted mutagenesis, Escalante-Alcalde *et al.* deleted parts of the fourth, fifth and sixth transmembrane domains as well as the second internal and third external loop of LPP-3 in mice embryos. Analyses of

embryoid bodies (cell structures derived from embryonic stem cells that have differentiated into the three germ layers - ectoderm, endoderm and mesoderm) confirmed the lack of intact protein, and the absence of phosphatase activity. Heterozygous mice were viable and fertile, but when interbred failed to produce any homozygous null offspring, indicating that LPP-3 is a vital gene for completion of embryogenesis in the mouse. PCR analysis of embryos seven to ten days post gestation indicated the expected ratio of wild-type to heterozygotes to homozygotes, demonstrating that the lethality of the null mutation occurs prior to embryonic day ten. Observation of homozygous null embryos prior to their death revealed a number of gross abnormalities. Besides a developmental retardation of twelve to twenty-four hours, endothelial cells failed to organise into a capillary network, resulting in limited formation of yolk-sac vasculature. This was coupled with incorrect development of the allantois (the precursor to the umbilical cord), resulting in a failure to form a chorio-allantoic placenta. The chorio-allantoic placenta separates the foetal and maternal circulatory systems and is essential for provision of nutrients to, and removal of waste from, the developing embryo (Escalante-Alcalde et al., 2003).

Thirty percent of LPP-3 null embryos revealed further abnormalities, including anterior truncation and shortening of the anterior-posterior axes, as well as duplication of axial structures. In *Xenopus laevis*, correct establishment of the dorsoventral axis is dependent on the Wnt/β-catenin signalling pathway. When Wnt is absent from cells, β-catenin is phosphorylated by glycogen synthase kinase 3 (GSK3) and targeted for ubiquitination and degradation in proteosomes. When Wnt is active, however, GSK3 is prevented from phosphorylating β-catenin through activation of Dishevelled, resulting in β-catenin stabilisation. β-catenin is then free to accumulate in the nucleus, where it interacts with members of the T-cell factor (TCF) and Lymphoid enhancer factor (LEF) transcription factors, to activate the expression of Wnt target genes. Stabilisation of β-catenin on the dorsal side of developing *X.laevis* embryos is critical for dorsoventral organisation (Weaver and Kimelman, 2004).

Increased expression of β-catenin in mouse embryos resulted in axis duplication. Evidence from Escalante-Alcalde *et al.* indicates a novel and previously unrealised role for LPP-3 in the regulation of β-catenin signalling during

embryogenesis. They showed that not only does ectopic expression of LPP-3 in HEK293 cells inhibit TCF-activated transcription mediated by endogenous β-catenin, but that levels of endogenous β-catenin activity are raised in LPP-3 null embryonic stem cells, along with the expression of the Wnt target gene *brachyury*. Expression of mouse LPP-3 by introduction of mRNA into 2 dorsal blastomeres of a 4-cell stage *X.laevis* embryo resulted in a ventralising affect similar to that seen from injection of Wnt agonists. Furthermore, they observed the same inhibition of TCF/β-catenin-dependent transcription in HEK293 cells when they over-expressed LPP-3 constructs in which a key catalytic site had been mutated or ablated, removing phosphatase activity (Escalante-Alcalde et al., 2003).

The conclusion from this work is that mouse LPP-3 is not only critical for early vascularisation and formation of the chorio-allantoic placenta, but may also act as an antagonist to the Wnt/β-catenin signalling pathway. Significantly, this latter role appears to be independent of its phosphatase activity.

A further role in angiogenesis has been suggested for hLPP-3 by findings that this protein contains an RGD domain in the second extracellular loop. RGD domains interact with integrins – receptor proteins that mediate cell binding and response to the extracellular matrix. hLPP-3 was identified in a screen for genes influencing capillary morphogenesis, and was subsequently named VCIP (VEGF and type 1 collagen inducible protein) (Humtsoe et al., 2003) before sequence analysis identified it as identical to the previously characterised hLPP-3 (Kai et al., 1997). Expression of VCIP in a cultured monolayer of endothelial cells was induced by addition of the cytokines VEGF, FGF and PMA. Expression of VCIP in HEK293 cells promoted cell-cell interactions and the formation of aggregates, whereas expression of VCIP carrying a mutation in the RGD domain, or expression of the vector alone, had no effect. Interestingly, levels of apoptosis in the cells expressing the mutated RGD domain were increased, leading authors to speculate that this mutation may somehow alter the phosphatase activity of the enzyme, increasing its dephosphorylation of lipid phosphates to apoptosis-promoting factors such as sphingosine and ceramide (Humtsoe et al., 2003). It was shown through the use of a variety of techniques including solid-phase ligand binding assays, that VCIP specifically recognises the integrins $\alpha_v\beta_3$ and $\alpha_5\beta_1$, and that VCIP is preferentially expressed in inflamed and angiogenic tissues, co-localised to areas of $\alpha_v\beta_3$ (Humtsoe

et al., 2003). Significantly, hLPP-1 and hLPP-2 do not possess this RGD domain, indicating a specific and novel role of the LPP-3 isoform in humans. Interestingly, despite its role in vasculogenesis and capillary formation, mLPP-3 also lacks this domain, perhaps pointing towards a conserved function through a divergent mechanism. It is pertinent to note that both Wunen and Wunen-2 also lack this RGD domain.

Ubiquitous over-expression of LPP-1 in mice using an actin-promoter also resulted in multiple developmental defects, in a transgene copy-number (*i.e.* dose) dependent manner. Although no defects were observed in development of the major organs, pups were born with decreased birth weight and a decrease in body hair due to an overall reduction in the density of hair bulbs. Litter sizes from these animals were smaller than average and although ovaries and uteruses from affected females showed no gross abnormalities, testes were atrophic with disrupted spermatogenesis. Interestingly, circulating LPA plasma levels were unaffected in these mice (Yue et al., 2004).

PRG-1, recently identified in lesioned rat hippocampus, putatively encodes another member of the LPP family. Biological findings with PRG-1 are also novel and exciting, and may prove particularly relevant in the ongoing search for the physiological substrates of the LPPs, especially Wunen. PRG-1 is primarily expressed in the central nervous system (with minor expression in the testis) and appears to be vertebrate-specific. ISH indicates that it is expressed in the developing hippocampus in neurones. During development, axonal outgrowth proceeds through a phospholipid-rich extra-cellular environment. In this environment LPA acts as a repellent, inducing neurite retraction and cell rounding. Whilst post-natal entorhinal axons expressing PRG-1 are resistant to LPA-induced collapse, those from embryonic day 16 with no PRG-1 expression show no such resistance (Brauer et al., 2003).

Exposure to LPA also induced growth cone collapse in the neuronal cell line N1E-115. Introduction of PRG-1 expression into these cells made them resistant to LPA-induced growth cone collapse, and extra-cellular LPA degradation increased five-fold. Mutation of one conserved and essential residue required for phosphatase activity in LPPs (His252 to Lysine) did not protect against growth cone collapse in these cells and resulted in a loss of observed phosphatase activity, suggesting that the

phosphatase activity is required for the protective effects of PRG-1 (Brauer et al., 2003).

Doubts have been raised, however, as to the validity of these findings within the context of the LPP 'field', since three key residues, absolutely conserved between other members of the family and essential for phosphatase activity, show non-conserved substitutions in the PRG-1 protein (Fig. 6). Discrepancies appear to exist between data generated in the original study (Brauer et al., 2003) and subsequent data generated using radiolabelled phospholipid substrates in both N1E-115 and HEK293 cells, leaving others to conclude that PRG-1 activity is not in fact directly attributable to an LPP activity (McDermott et al., 2004). As noted by the original researchers and cited in their response to this criticism, however, data published from the work presented here clearly demonstrates that the different LPP isoforms present very different bioactivities when assayed within an actual *in vivo* system (Brauer et al., 2004; Burnett and Howard, 2003). Whilst still contested at the present time, it remains to be determined as to whether PRG-1 is truly a novel member of the LPP family. If it proves to be so, then it would appear that LPP proteins might regulate axonal outgrowth in mammalian systems.

Similar to the role of LPP in mouse axis specification, *Drosophila* Wunen has been implicated in the development of left/right asymmetry during embryogenesis (Ligoxygakis et al., 2001). Combined with its function in germ cell migration and survival, therefore, Wunen appears to be important for a number of developmental processes and provides a good opportunity to study these enzymes in greater detail.

1.5) Aims of the investigation

As interest in the physiological significance of the LPPs increases, it becomes increasingly important to identify their endogenous substrates and to characterise their exact roles *in vivo*. Given the remarkable bioactivity of the known lipid substrates for these enzymes and the specificity of some of their receptors, it seems curious that the separate isoforms should present such broad range activity in biochemical assays. Much of the work on substrate specificity to date, however, has used triton micelle assays or cell culture techniques, rather than directly testing for substrate preference *in vivo* using model organisms.

The aim of the present work was to explore potential specificities in substrate recognition between the different LPP isoforms both biochemically *in vitro*, and biologically *in vivo*, by examining their ability to recognise an endogenous substrate within a physiological environment. A further aim was to investigate the ability of the LPPs to form and function as oligomeric complexes, and the requirement or otherwise of these complexes for both biological and biochemical activity either *in vitro* or *in vivo*.

As Wunen influences PGC migration and survival, there must be receptors present on the surface of PGCs that can recognise and interpret this signal. This work also set out to identify and characterise such a receptor(s), and investigate any role it may itself play in PGC guidance and survival during *Drosophila* embryogenesis.

2) CHAPTER ONE

Substrate Specificities of the LPP Isoforms

2.1) Introduction

The structure of the LPPs has yet to be solved and consequently much of the information regarding mechanisms of catalysis and interactions within the active site has been gleaned from structural knowledge of chloroperoxidase (CPO). CPO is a member of the phosphatase superfamily proposed by Stukey and Carman (Stukey and Carman, 1997) and found in the fungus *Curvularia inaequalis*. In the presence of hydrogen peroxide, CPO converts chloride to hypochlorous acid. It is believed to use this to oxidize plant walls, enabling its subsequent entry into the plant. The crystal structure of CPO was solved in 1996 and has facilitated models projecting the catalytic mechanism of the LPPs (Hemrika et al., 1997; Messerschmidt and Wever, 1996; Neuwald, 1997). CPO contains a vanadate ion bound to its active site through interactions with a number of residues that are highly conserved throughout the superfamily. It is believed that this ion is bound in a similar manner to the phosphate group in the LPPs. Indeed, vanadium displays phosphatase activity, but also acts as an inhibitor to a range of phosphate-metabolizing enzymes. Likewise, the peroxidase activity of CPO is inhibited by the presence of phosphate (Stankiewicz et al., 1995).

The seven residues highlighted in orange in Fig.6 are predicted to interact directly with the vanadate ion in CPO via Hydrogen-bonds. The corresponding residues in mouse LPP-1 and Wunen are shown in Table 1. By individually mutating each of these residues, immnopurifying GFP-tagged versions of each protein and investigating their subsequent ability to dephosphorylate ^{32}P-LPA, Zhang *et al* were able to demonstrate that, true to the proposed model, each of these residues is essential for catalytic activity in mouse LPP-1 (Zhang et al., 2000b), and together compose a three dimensional extra-cellular catalytic site. Mutation of H274 and H326 in Wunen-2 also eliminated its biological activity on PGCs when over-expressed in the mesoderm (Starz-Gaiano et al., 2001).

CPO	*Mouse LPP-1*	*Wunen*	*Wunen-2*
K353	K120	K132	K214
R360	R127	R139	R221
P361	P128	P141	P222
S402	S169	S190	S272
H404	H171	H192	H274
R490	R217	R238	R320
H496	H223	H244	H326

Table 1. Conserved amino-acids. *The seven amino-acids believed to constitute the active site within the three conserved LPP phosphatase domains. All seven were shown to be essential for catalytic activity in the mouse (Zhang et al., 2000b).*

Past work has demonstrated that all three of the LPP isoforms are capable of dephosphorylating five known phospholipid substrates, namely PA, LPA, S1P, C1P and DGPP, with varying degrees of specificity (Dillon et al., 1997; Furneisen and Carman, 2000; Jasinska et al., 1999; Kai et al., 1997; Roberts et al., 1998; Waggoner et al., 1996). Interestingly, considerable discrepancies exist between published results on relative substrate preference. For example, Kai *et al* reported that whilst LPA was hydrolyzed more efficiently than C1P, LPP-1 showed no activity whatsoever on S1P. Conversely, Roberts *et al* reported that four substrates were hydrolyzed in order of preference: LPA>PA>S1P>C1P, whereas Jasinska *et al.* observed similar levels of efficiency for all four. Conflicting data also exists for LPP-3, with Kai *et al.* recording activity on S1P at eight times the rate of activity on LPA and C1P, whilst Roberts *et al.*, seemingly in complete contradiction, reported that LPA and PA were hydrolyzed more efficiently than C1P, which in turn was hydrolyzed more efficiently than S1P. Variation in substrate specificity between groups investigating the enzymological properties of *S.cerevisiae* may prove illuminating here. In initial studies, LPP-1 was shown to have higher activity on LPA than DGPP (Toke et al., 1998). Subsequent experiments, however, proved the reverse to be true, and a change in buffer pH was cited as the reason (Furneisen and Carman, 2000).

Most, if not all, of the work on substrate specificity has been carried out in triton micelle assays, under biochemical conditions. The discrepancy between the published results is of concern since it indicates that assay conditions, and the methods of substrate presentation and enzyme purification, are potentially critical to efficiency of hydrolysis of individual phospholipids. Although shown to be active on these five substrates, there has been no indication as to whether these enzymes are capable of recognizing any of these substrates *in vivo*. This leaves the question of what the true physiological substrate(s) of any of the LPP isoforms is, completely unanswered.

Considering the potent bioactivity of the apparent lipid substrates and the specificity of their receptors, it seems curious that the LPPs should present such broad-range activities in biochemical assays. To date, it is unknown whether the fly LPP, Wunen, can dephosphorylate any of the mammalian lipid phosphate substrates *in vitro*. The first aim of this work was to examine differences in substrate recognition or specificity between *Drosophila* Wunen and the mammalian isoforms, both biochemically on a range of known substrates, and biologically, by investigating their abilities to dephosphorylate the PGC-specific guidance molecule that functions as a substrate for Wunen.

2.2) Results

2.21) Sequence analyses and cloning of the LPPs

2.21a) *Sequence analyses of Wunen and the mammalian LPPs*

wunen and *wunen-2* have a remarkably similar messenger RNA pattern and over-expression phenotype, indicating a high degree of conservation between the two genes. A phylogenetic tree, as calculated by ClustalW, clearly indicates that both Wunen and Wunen-2 are most homologous to the human LPP-3 isoform (Fig.10).

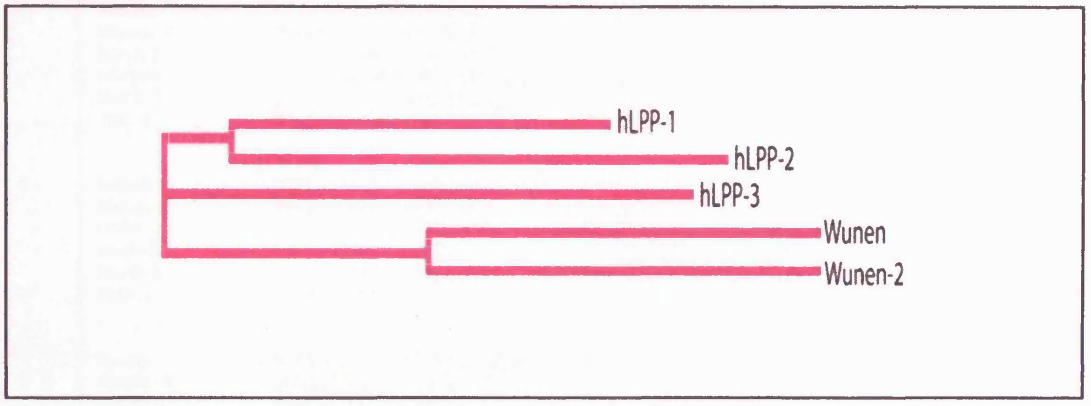

Fig.10. Phylogenetic Tree. *A phylogenetic tree as calculated by ClustalW (http://www.ebi.ac.uk/clustalw/) indicates that Wunen and Wunen-2 bear greatest homology to hLPP-3.*

A ClustalW alignment was employed to investigate the relationship between the *Drosophila* LPPs and the three mammalian isoforms. The results indicate a high degree of homology, with an almost complete conservation of the three main phosphatase domains. In between the transmembrane domains are regions that are less well conserved, with the C-termini demonstrating considerable heterogeneity (Fig.11).

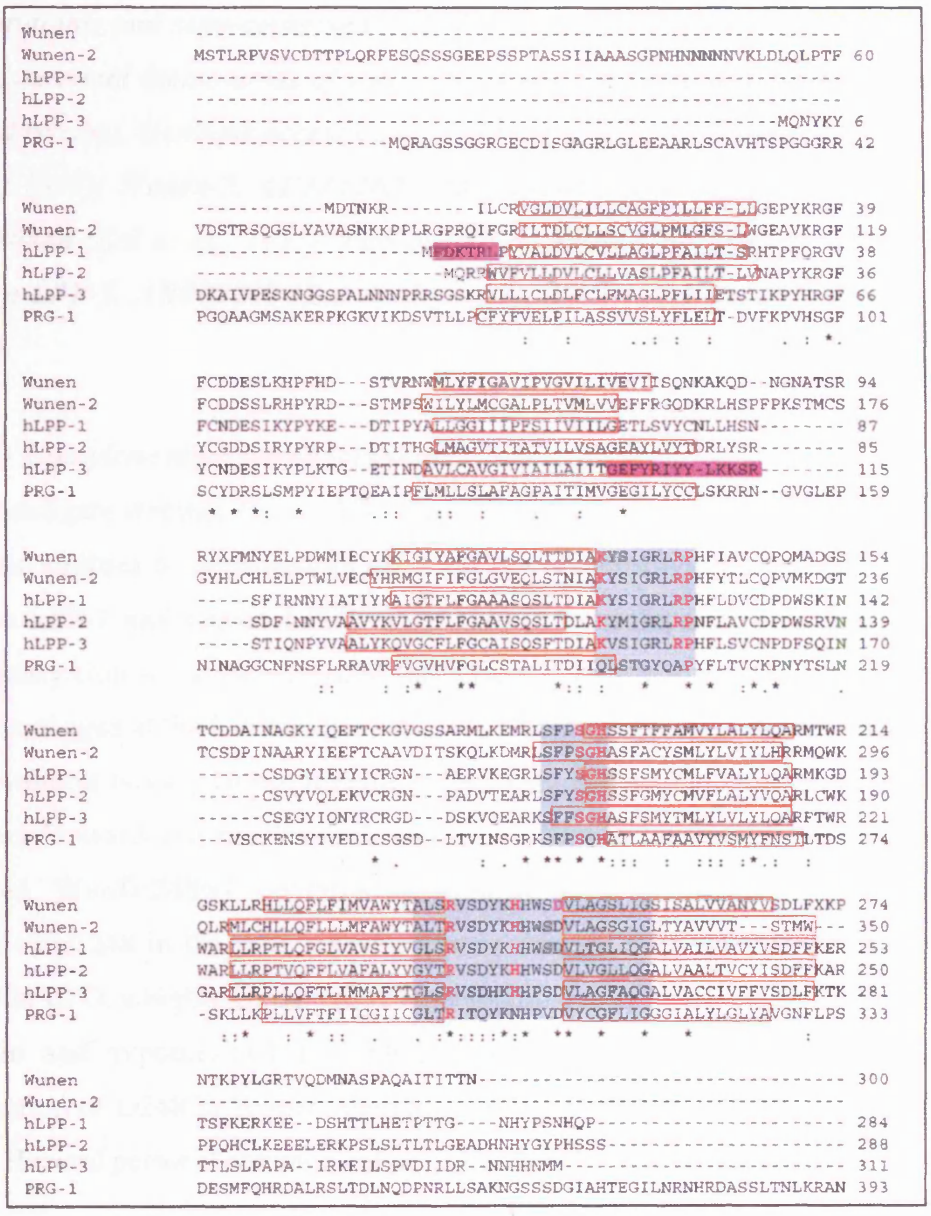

Fig.11. Sequence alignment of Wunen and Wunen-2 with the mammalian LPP isoforms and PRG-1, calculated using ClustalW. *The six transmembrane domains are indicated by ORANGE boxes, as predicted by TMPred (http://www.ch.embnet.org/software/TMPRED_form.html; (Hofmann, 1993). The three conserved catalytic domains are shaded in PALE BLUE, with those residues absolutely required for catalytic activity shown in RED. N-glycosylation sites are highlighted in GREEN. The N-terminal apical sorting signal in LPP-1, and the dityrosine motif targeting LPP-3 to the basolateral subdomain are shaded in PURPLE. The D:248>T mutation is shown in MAUVE. Asterisks indicate amino-acids that are identical between all six sequences, colons indicate conserved*

substitutions, and semi-conserved substitutions are shown by a dot. ***N.B.*** *The last 370 C-terminal amino-acids of PRG-1 have not been included in the diagram for spatial reasons. GenBank accession numbers are as follows: Wunen,* ***U73822*** *(Zhang et al., 1997); Wunen-2,* ***AF331162*** *(Starz-Gaiano et al., 2001); human LPP-1,* ***AB000888*** *(Kai et al., 1997); human LPP-2,* ***AF047760*** *(Roberts et al., 1998); human LPP-3,* ***AB000889*** *(Kai et al., 1997); PRG-1,* ***AF541281*** *(Brauer et al., 2003).*

2.21b) Complementary DNAs (cDNAs)

To investigate whether *Drosophila* Wunen and the mammalian LPP isoforms differ in their abilities to dephosphorylate a variety of phospholipid substrates *in vitro*, mouse LPP-1 and human LPP-3 were chosen for comparison, as they had been previously cloned and characterized (Kai et al., 1996; Kai et al., 1997) and, alongside Wunen, tagged at the C-terminus with green fluorescent protein (GFP). Each of these was available already cloned into the transformation vector pUAST (work performed by Ken Howard and previous lab members). WunD:248>TGFP was chosen as a control. WunD:248>T contains an aspartic acid to threonine conversion at amino-acid 248 in the sixth transmembrane domain (Fig.11). This corresponds to D500 in CPO, a highly conserved residue reported to be required for catalysis in this protein and hypothesized as contributing to the active site (Neuwald, 1997). Disruption of D248 in Wunen, therefore, was proposed to result in a catalytic null (Ken Howard personal communication), although this had never been proven.

2.21c) *Transfection of S2 cells and analyses of protein size*

Before comparing biochemical activities, it was necessary to confirm that each of the GFP-tagged constructs encoded a protein of the correct predicted size, and was capable of transcribing the GFP marker. This was done by individually transfecting each construct into *Drosophila* Schneider cells (S2 cells) alongside the ubiquitous driver Actin5C-GAL4 (a kind gift from Tom Kornberg). After twenty-four to forty-eight hours, expression of the GFP protein was clearly visible under the fluorescent microscope. These cells were maintained at 25°C for a further two days until expression appeared optimal. They were then spun down and washed in PBS (phosphate buffered saline) before lysis in a buffer containing protease inhibitors. Aliquots were analyzed by standard Western blotting procedures, and visualised with

a mouse monoclonal antibody to GFP (Roche), followed by a horse-radish peroxidase (HRP)-conjugated anti-mouse secondary antibody (Jackson ImmunoResearch Laboratories). The results clearly indicated proteins of the correct predicted size in each case, demonstrating that each protein was successfully synthesized in these cells (Fig. 12).

Fig.12. Confirmation of protein size. *Blots were probed with a monoclonal antibody to GFP.*

2.22) Biochemical analyses of LPP substrate preference

2.22a) *Immunocapture of GFP-tagged proteins*

To test biochemical activities, each construct was once again transfected into S2 cells alongside Actin5C-GAL4, and the cells were allowed to express the relevant protein for three to four days. When protein expression was observed to be at least 30% of total cell number, cells were spun down, washed, and lysed in buffer. Individual cell extracts were then incubated for two hours at room temperature with Fusion Aid GFP resin. This resin utilizes an affinity-purified antibody to GFP coupled through a stable hydrophilic spacer arm to cross-linked 4% agarose beads, enabling it to specifically recognize and capture the GFP epitope (Vector Laboratories). Untransfected S2 cells were used as a control. After incubation, the resin was washed extensively for several hours to ensure removal of any extraneous unbound protein. An aliquot of the final wash was kept for Western analyses. In order to confirm that

each protein was expressed, a sample of total cell lysate prior to incubation was run on the gel, alongside a sample of the final wash (to confirm that no unbound protein was present), and a sample of each resin to confirm that each protein had been immunocaptured.

2.22b) ***Inorganic phosphate release assay***

In order to avoid the use of radiolabelled lipid substrates, both time-consuming and hazardous, the Molecular Probes PiPer® phosphate release assay (Cambridge Bioscience) was adapted for this research (Fig.13).

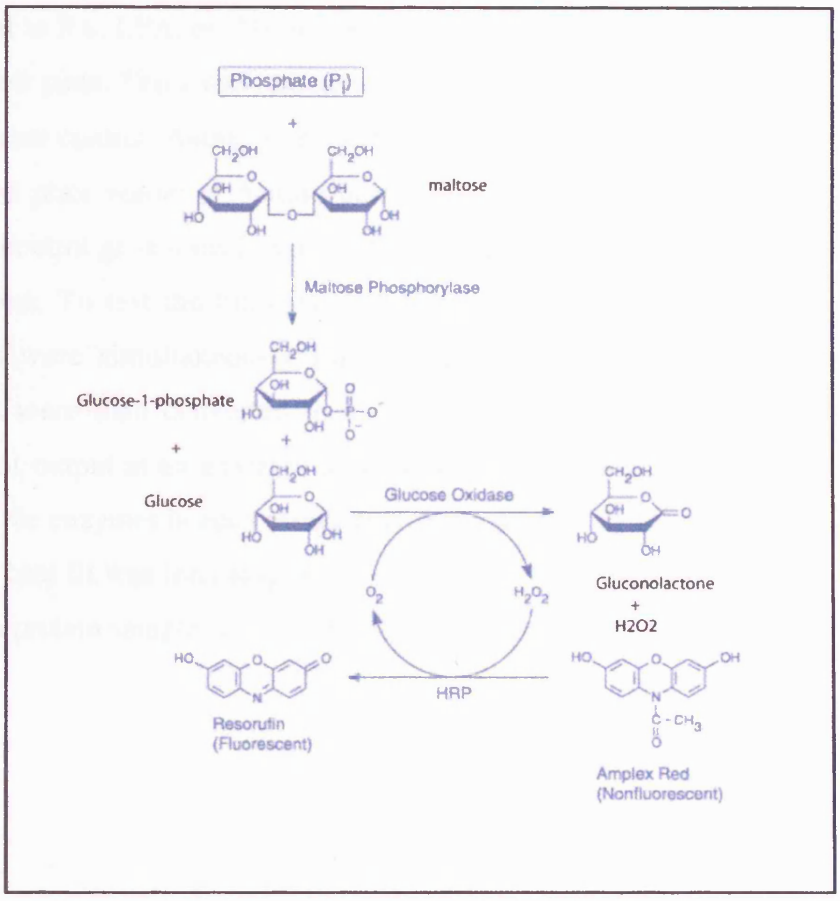

Fig.13. The PiPer ® phosphate release assay.

In the presence of inorganic phosphate, maltose phosphorylase converts maltose to glucose-1-phosphate and glucose. Gluconolactone and hydrogen peroxide (H2O2) are then formed by the action of glucose oxidase. Using horseradish peroxidase as a catalyst, the H2O2 reacts with the Amplex™ Red reagent to produce the fluorescent product resorufin. The increase in detectable fluorescence/absorbance is therefore

proportional to the amount of phosphate present. Figure adapted from http://www.probes.com (Molecular Probes).

In keeping with previously published results, the following substrates were chosen for the experiment – PA, LPA, C1P, and S1P. PA was used at a final concentration of 70μM, LPA and C1P were used at a final concentration of 500μM. Despite numerous attempts, employing various methods, S1P gave no discernable results with any of the constructs. Since mLPP-1 has shown previous activity on S1P, the conclusion must be that S1P failed to solubilize under these conditions.

For the assay, 50μl of resin containing the relevant immunocaptured protein was added to PA, LPA, or C1P in suspension, and pipetted into three separate wells in a 96-well plate. Three wells contained bare resin with no immunocaptured protein as a substrate control. Assays were performed at 37°C and fluorescent output read in a standard plate-reader at 5 time points during the assay period (Fig.14). Each substrate control gave a small but constant value, which was subtracted from each of the samples. To test the linearity of the detection system, a series of phosphate standards were simultaneously run in triplicate in each assay. The phosphate standards were then converted to nanomoles (nMoles) of phosphate relative to flourescent output at an arbitrary time point that appeared to fall within the linear range for the enzymes in each assay. This data was used to produce a standard curve. A line of best fit was then employed to calculate the amount of phosphate released from each protein sample at the same time point (Fig.15).

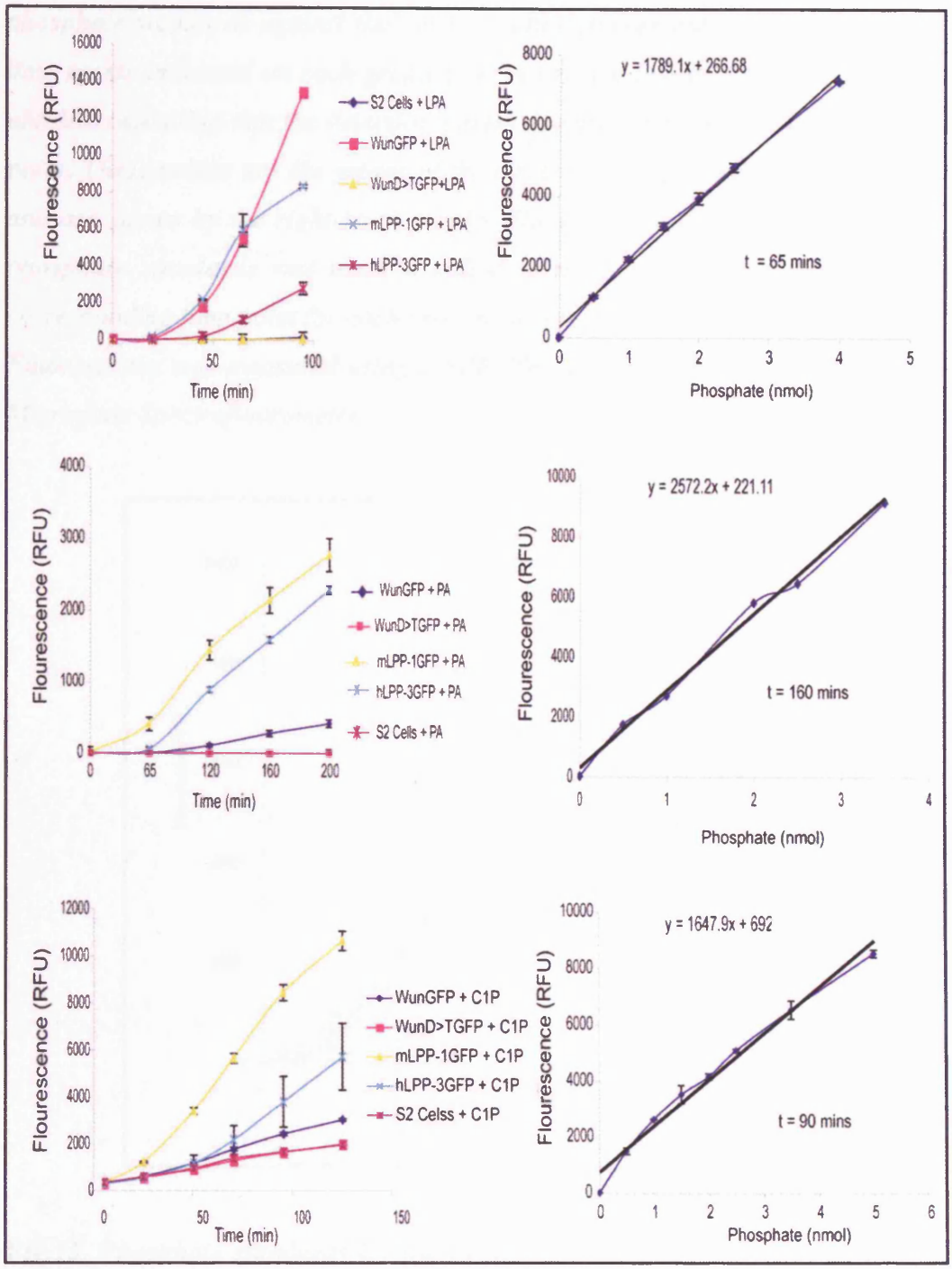

Fig.14. PiPer® Phosphate release assay results. *Each left-hand graph shows the mean fluorescent readout from the triplicate experiments for each protein over time with each of the three substrates, +/- standard deviation (s.d). The sequential action of the enzymes involved in the detection system following exposure to phosphate in solution accounts for the 20-minute lag period seen at the start of the assay. Running phosphate standards alone produces the same lag period (Fig.15). Plotting*

phosphate standards against the corresponding fluorescent readout at the chosen time points indicated on each graph gives a straight line in the presence of 4 to 6 nMoles, indicating that the detection system displays first order kinetics at this time point. These values are the means of the three samples for each standard, +/- s.d. and are shown by the right-hand graphs. The equation of the line for each set of phosphate standards was used to calculate nMoles phosphate released at the corresponding time point for each protein sample. RFU, relative fluorescence units. Fluorescence was measured using a SPECTRAmax™ GEMINI XS Dual Scanning Microplate Spectrafluorometer.

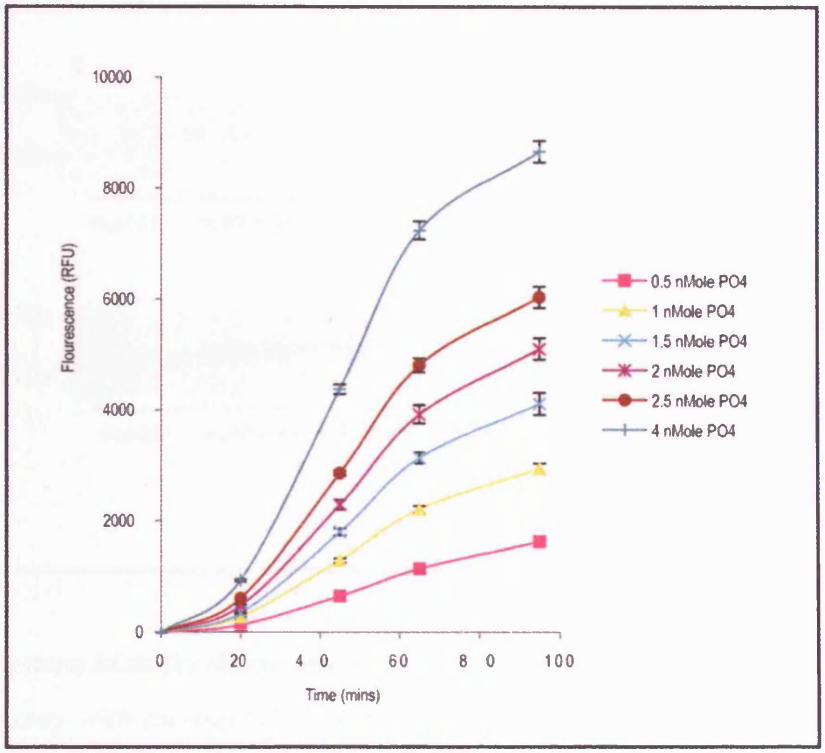

Fig.15. Phosphate standards for the LPA assay. *Each of the phosphate standards shows a 20-minute lag period at the beginning of the assay, due to the sequential action of the enzymes involved. Each value is the mean of the three readouts for each standard at each time point, +/- s.d.*

Immediately following an assay, samples were removed from each well, added to an equal volume of loading buffer and boiled briefly before loading onto an agarose gel for electrophoresis followed by Western analysis. Following development of each

blot, densitometry analyses were performed using BioRad Quantity One software. This enabled the direct comparison of relative protein amounts between samples on the same blot. These density readings were then used to calculate the nMoles of phosphate released per unit density (Fig. 16 and Tables 2-5).

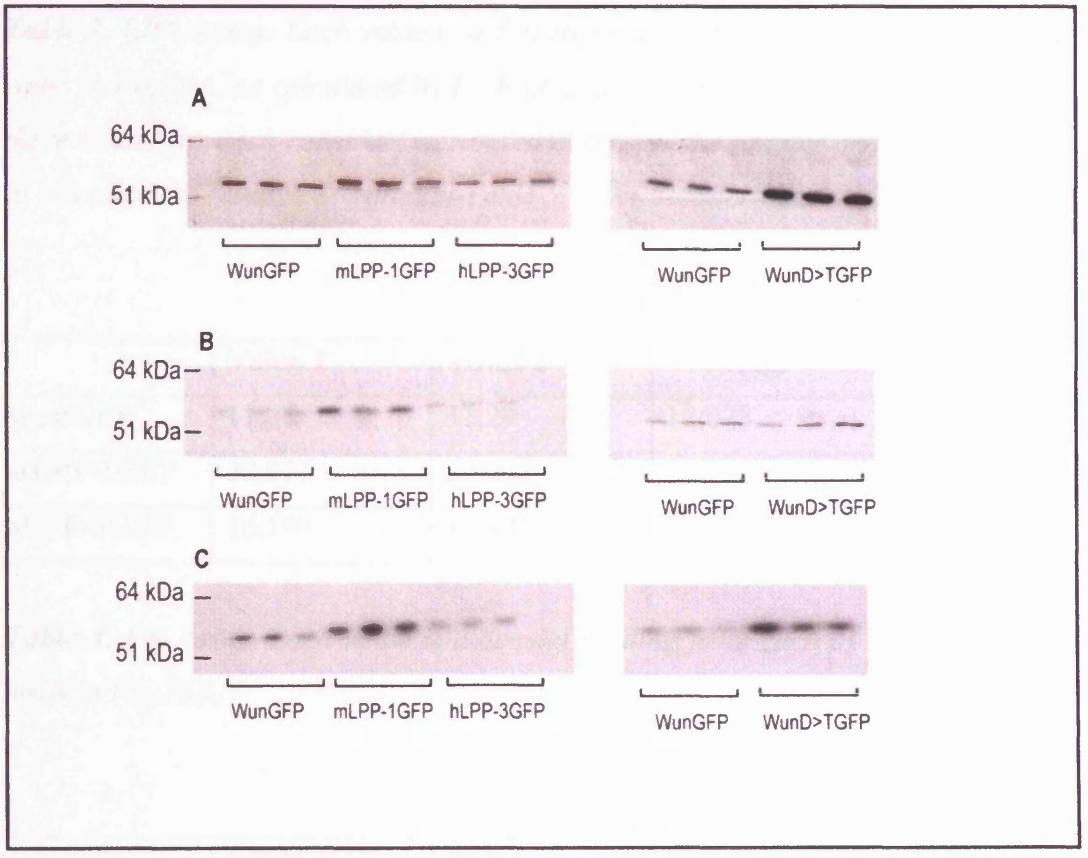

Fig.16. Western blots for densitometry. *All three wells for each protein were blotted for each assay with an anti-GFP antibody, and analysed by BioRad Quantity One software. The WunD:248>TGFP samples were blotted separately next to a repeat sample of WunGFP due to insufficient wells in each gel. As WunD:248>TGFP is a catalytic null, the blots primarily demonstrate that the protein is present at sufficiently high levels in each experiment.* ***A)*** *Results for the LPA assay.* ***B)*** *Results for the PA assay.* ***C)*** *Results for the C1P assay.*

	Value 1	Value 2	Value 3	s.d.
WunGFP	40.664	35.392	32.933	3.950
mLPP-1GFP	43.438	41.389	34.038	4.943
hLPP-3GFP	26.305	29.229	28.671	1.552

Table 2. LPA Assay. *Each value is a density reading from each of the three sample wells in Fig.16A, as calculated by BioRad Quantity One software. The means of the three values for each construct were used alongside the nMoles phosphate released to calculate the relative activities in Table 5. s.d = standard deviation.*

	Value 1	Value 2	Value 3	s.d.
WunGFP	11.25	11.29	12.028	0.439
mLPP-1GFP	30.971	27.096	36.12	4.527
hLPP-3GFP	16.197	13.301	12.354	2.002

Table 3. PA Assay. *Each value is a density reading from each of the three sample wells in Fig.16B.*

	Value 1	Value 2	Value 3	s.d.
WunGFP	26.046	25.039	18.178	4.281
mLPP-1GFP	35.631	61.362	44.345	13.087
hLPP-3GFP	19.691	18.874	16.595	1.605

Table 4. C1P Assay. *Each value is a density reading from each of the three sample wells in Fig.16C.*

Construct	*nMoles PO4 released (mean +/- s.d.)*	*nMoles PO4 released per unit density (mean +/- s.d.)*	*Relative activity*
LPA			
WunGFP	2.819 +/- 0.180	0.079 +/- 0.012	1.00
mLPP-1GFP	3.056 +/- 0.496	0.079 +/- 0.024	1.00
hLPP-3GFP	0.359 +/- 0.109	0.013 +/- 0.004	0.16
WunD:248>TGFP	~0.000 +/- 0.156	0.000 +/- 0.002	0.00
Untransfected S2	~0.000 +/- 0.017	N/A	0.00
PA			
WunGFP	0.021 +/- 0.016	0.002+/-0.001	1.00
mLPP-1GFP	0.745+/-0.070	0.024+/-0.003	12.00
hLPP-3GFP	0.530+/-0.018	0.038+/-0.005	19.00
WunD:248>TGFP	~0.000+/-0.029	0.000+/- 0.002	0.00
Untransfected S2	~0.000+/-0.015	N/A	0.00
C1P			
WunGFP	0.098 +/- 0.045	0.004+/-0.001	1.00
mLPP-1GFP	3.754 +/- 0.207	0.083+/-0.020	20.75
hLPP-3GFP	0.933 +/- 0.662	0.049+/-0.034	12.25
WunD:248>TGFP	~0.000 +/- 0.026	0.000+/-0.003	0.00
Untransfected S2	~0.000 +/- 0.049	N/A	0.00

***Table 5.* Relative activities of the LPPs.** *Each immunocaptured enzyme was incubated in triplicate with LPA, PA or C1P in the PiPer® phosphate release assay, and the nMoles phosphate released for each individual sample calculated from a standard curve. The means of the three readings for each enzyme is presented, +/- s.d.. Less than 11% of total substrate was broken down in any of the experiments. The density for each individual sample on a Western blot was calculated using Bio-Rad Quantity One, and used to calculate nMoles PO4 released per unit density.*

The putative catalytic null, WunD:248>TGFP, had absolutely no activity in this assay on any of the three substrates presented to it, despite the presence of significant levels of protein as determined by Western analysis. This shows for the first time that this amino-acid is indeed critical for catalysis of phospholipid substrates under these conditions. Whilst mLPP-1 and Wunen displayed similar levels of activity on LPA, hLPP-3 was considerably less active. hLPP-3 showed approximately 1.6 times more activity on PA, however, than mLPP-1, whilst mLPP-1 appeared approximately 1.7 times more active on C1P than hLPP-3. In comparison, Wunen displayed negligible activity on C1P or PA.

2.23) Biological analyses of LPP substrate preference

2.23a) *Phenotypic consequences of ectopic expression in the mesoderm*

The next step was to explore potential differences in substrate choice when faced with a physiological substrate *in vivo*, by examining the ability of each LPP to recognise the same germ cell specific guidance and survival factor as *Drosophila* Wunen. In order to do this, transformant flies were generated for each construct using standard microinjection techniques (Rubin and Spradling, 1982). Four to ten day old males carrying a homozygous viable insert on an autosome were crossed *en masse* to homozygous viable twist-GAL4 virgins (homozygous viable on the X chromosome), to drive expression of each protein specifically in the mesoderm. Flies were maintained at 25°C and embryos from over-night lays collected on apple-juice plates. These were dechorionated and fixed prior to immunostaining with a primary antibody to GFP to visualize protein expression in the mesoderm, and a primary antibody to Vasa, to visualize the PGCs (Fig.17).

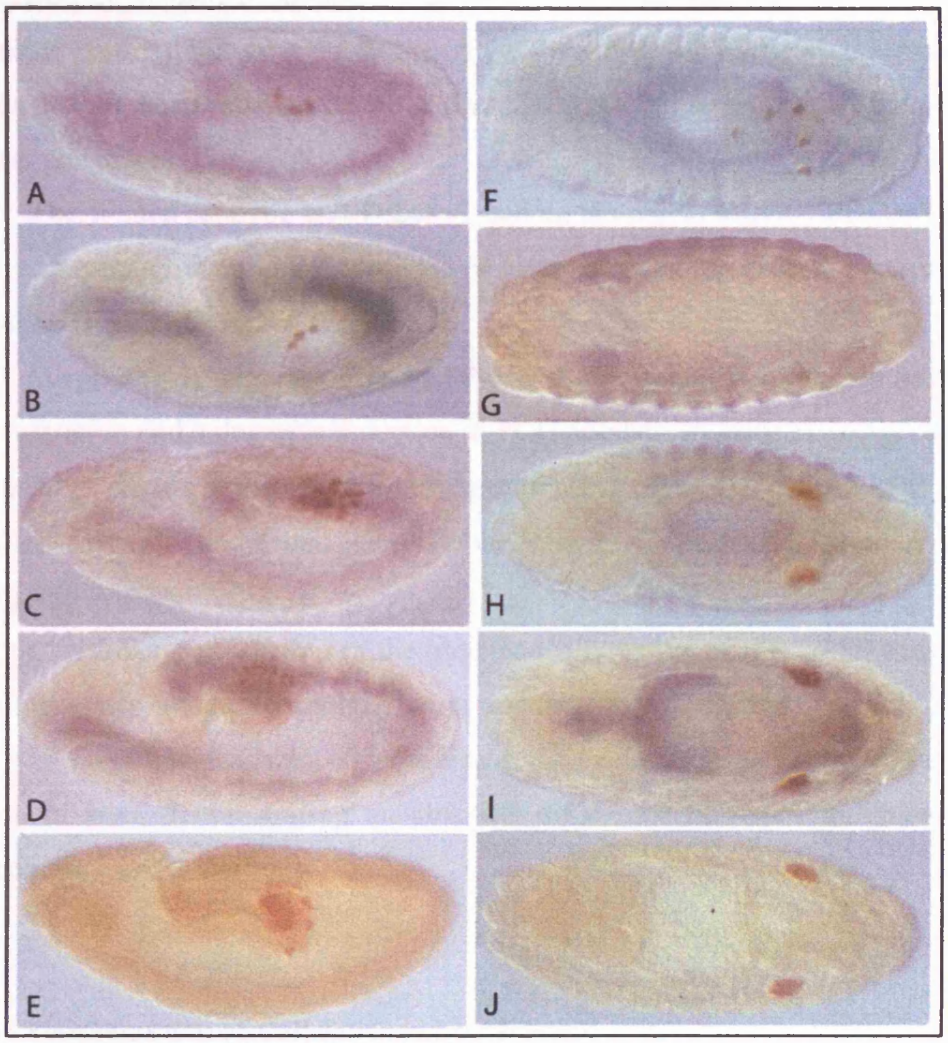

Fig.17. Ectopic expression in the mesoderm. *Embryos were immunostained with anti-Vasa antibody to visualize the PGCs in brown, and anti-GFP to visualize protein expression in blue. Embryos in figures A-E are viewed laterally with the posterior pole to the right, embryos in F-J are viewed dorso-ventrally. Expression of WunGFP (A) or hLPP-3GFP (B) at stage 10 results in an early loss of PGCs compared to ectopic expression of WunD:248>TGFP (C) or mLPP-1GFP (D). These can be compared to a wild-type embryo (E) with a full complement of PGCs at the same stage. By the end of embryogenesis, those expressing WunGFP (F) or hLPP-3GFP (G) show a dramatic loss of PGCs, whilst those that remain demonstrate migration defects. Embryos expressing WunD:248>TGFP (H) or mLPP-1GFP (I), however, show no apparent perturbation or loss, and have formed two clear gonads, as seen in a wild-type embryo at the same stage (J). Wild-type embryos do not express GFP and consequently show no blue staining.*

Expression of WunGFP disrupted PGC migration and reduced PGC number, as previously reported for untagged Wunen. PGCs are observed in tissues other than the gonads, having been repelled from the mesoderm, so failing to contact the somatic gonadal precursors (Fig. 17 A, F).

The Wunen catalytic null D:248>T had no biological activity. PGC migration occurred normally even in the presence of high levels of the mutant protein in the mesoderm (Fig. 17 C, H).

Surprisingly, expression of hLPP-3GFP also resulted in highly perturbed PGC migration and a dramatic reduction in PGC number. In some embryos only one or two PGCs remain at the end of embryogenesis (Fig. 17 B, G). Human LPP-3 may, therefore, recognise and dephosphorylate the same PGC specific substrate in flies as *Drosophila* Wunen.

Conversely, expression of the biochemically active mLPP-1GFP showed no phenotype, with no aberrant migration or apparent PGC loss (Fig. 17 D, I). Mouse LPP-1 is therefore incapable of recognizing the same germ cell specific factor as Wunen *in vivo*, demonstrating an absolute difference in functional bioactivity between the 1 and 3 isoforms.

2.24) Confirmation of Cell-Surface Localisation

2.24a) *Confocal microscopy*

The LPPs have been shown to possess ecto-enzymatic activity, and structural and enzymatic analyses indicate that, as transmembrane proteins, they should be localised to the plasma membrane. Although it is not know if the germ cell migration phenotype is caused by an extracellular activity of Wunen or hLPP-3, it was necessary to exclude the possibility that mLPP-1GFP was simply failing to traffic correctly to the cell-surface, thus potentially precluding its access to a substrate. Embryos expressing the GFP-fusion proteins in their mesoderms were examined by confocal microscopy. All of the proteins were readily detected on the mesodermal cell surface (Fig. 18). Proteins were not observed localising to intracellular membrane structures when transiently expressed in embryonic mesoderm by this method.

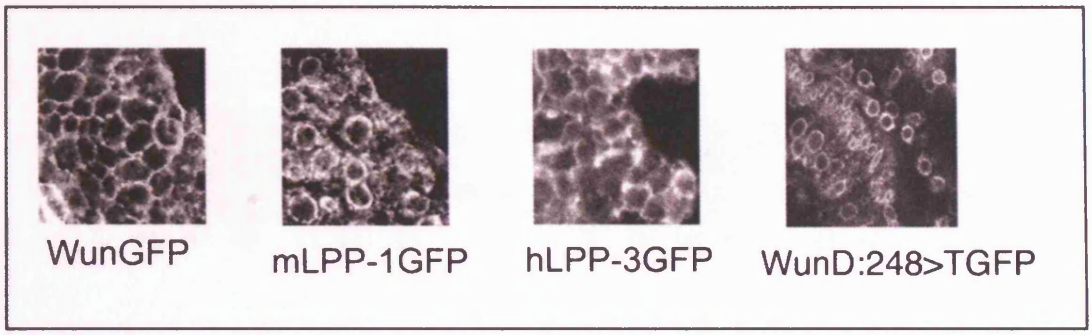

Fig.18. Confocal microscopy. *Confocal microscopy showing WunGFP, mLPP1-GFP, hLPP-3GFP and WunD:248>TGFP at the surface of mesodermal cells in* Drosophila *embryos. Protein expression is driven by twist-GAL4.*

2.24b) ***Cell-surface biotinylation***

The presence of each protein at the cell surface was confirmed by biotinylation of stable cell lines expressing either hLPP-3GFP or mLPP-1GFP. These cells were co-transfected with a pUAST-hygro construct that confers hygromycin resistance. Addition of hygromycin to the media allows for selection of those cells stably expressing both hygromycin resistance and up to four other constructs, one of which necessarily is Actin5C-GAL4. In these cell lines up to eighty percent of the total population express the protein of interest (Makridou et al., 2003). The intact cells were incubated with NHS-biotin. N-Hydroxysuccinimide (NHS)-activated biotin reacts with primary amino groups (-NH2) by nucleophilic attack. This interaction results in the formation of an amide bond and the release of the NHS. NHS-biotin is cell impermeable and can only bind to those proteins present on the surface of intact cells. After incubation the reaction was quenched by the addition of ammonium chloride and the cells were washed extensively to remove any unbound biotinylated product prior to lysis. Lysates were spun at 13,000 rpm and the resulting cytosolic supernatent run over a monomeric biotin binding avidin column. Samples of each wash followed by each eluate were analyzed by Western blot (Fig.19).

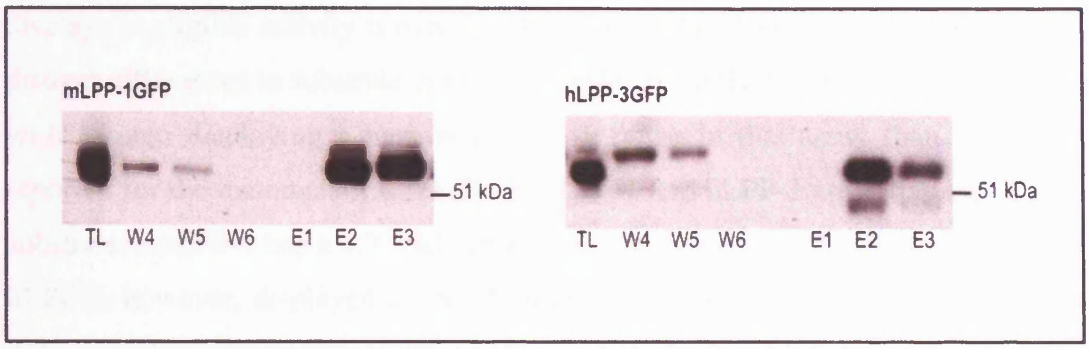

Fig.19. Biotinylation of cell surface proteins. *Biotinylation of mLPP-1GFP and hLPP-3GFP at the surface of S2 cells detected with a monoclonal anti-GFP antibody.* ***TL*** *= total lysate (cytosolic supernatent) prior to capture on the column;* ***W*** *= washes – protein that is not biotinylated and has not bound to the column.* ***E*** *= elutions – cell-surface protein that is biotinylated and has bound to the column.*

These results confirmed that both the biologically active hLPP-3GFP, and the biologically inactive mLPP-1GFP, were both present at the cell-surface at roughly equal proportions.

2.3) Summary

It has previously been shown that point mutations in the conserved catalytic domain of Wunen-2 remove biological activity *in vivo* (Starz-Gaiano et al., 2001). The results presented here are the first time that loss of phosphatase activity as confirmed in a biochemical assay, however, has been shown to also remove biological function, and indicates that converting a single aspartic acid to threonine at residue 248 is sufficient to remove catalytic activity both *in vitro* and *in vivo* in Wunen. Importantly, this tells us that the affect of Wunen (and likely human LPP-3) on PGC migration and survival can be directly attributed to its phosphatase activity.

Although these are not detailed kinetic analyses, this work demonstrates that the fly LPP Wunen, and mammalian LPP-1 and 3, differ in relative activities on PA, LPA and C1P in the PiPer® phosphate release assay. This is the first time that a *Drosophila* LPP has been shown to be active on any of these phospholipid substrates. Whilst Wunen can dephosphorylate LPA with similar efficiency to mLPP-1, it

displays negligible activity towards both PA and C1P. This indicates that there are distinct differences in substrate preference between the fly and mammalian enzymes, with Wunen displaying a narrower activity range in this assay than previously reported for the mammalian LPPs. Both mLPP-1 and hLPP-3 are active on all three substrates. mLPP-1 has a 1.7 fold higher activity on C1P than hLPP-3 in this assay. hLPP-3, however, displayed a 1.6 fold higher activity to mLPP-1 on PA. Previous data on activity for each isoform on these substrates has tended to vary somewhat (Kai *et al.*, 1997; Roberts *et al.*, 1998). The inconsistencies that have been observed for the same isoform on the same substrates may be due to the particular assay conditions or method of enzyme preparation. This could account for the variation in relative activities between Wunen and hLPP-3 *in vitro*, despite their close homology. Alternatively, there may be fundamental differences between the fly and mammalian isoforms that will only be uncovered with a more detailed analysis of their structures.

Perhaps more importantly, this work also shows that hLPP-3 is highly active when ectopically expressed in *Drosophila* embryos, as assayed by the disruption of PGC migration and survival, resulting in a phenotype similar to ectopic expression of Wunen or Wunen-2. That hLPP-3 shows the same phenotype in a bioassay as the *Drosophila* LPPs, may point towards a signalling pathway regulating germ cell migration and survival that has been conserved from flies to man. Conversely, though active in the biochemical assay, mLPP-1 is completely inactive *in vivo*, and has no apparent affect on PGC migration or survival. This demonstrates an absolute difference in functional bioactivity between the mammalian LPP isoforms. That the LPP isoforms present different functional outputs when assayed *in vivo*, holds a number of implications. It may be that the LPP-1 isoform simply cannot recognize or catalyze the dephosphorylation of the specific factor seen by Wunen and LPP-3. This would then demonstrate specificity in substrate choice between the isoforms, and may indicate that the germ cell specific factor is *not* PA, LPA or C1P, on which mLPP-1 is active *in vitro*, particularly since Wunen displays negligible activity towards PA and C1P in the same assay. Alternatively, there may be specific components of the pathway that are required for selection and recognition of the factor. It is possible that as yet unidentified conformational or structural differences in mLPP-1 preclude its association with these factors, thus inhibiting its enzymatic function in this system. Thus, LPA *could* potentially be the factor, and the unnatural presentation and high concentration of LPA in the biochemical assay may over-ride

the specific selection mechanisms used to regulate activity *in vivo*, allowing mLPP-1 access to this otherwise inaccessible substrate. Primary sequence analyses have not identified any immediate candidates for residues conferring such a difference, although it has been speculated that the regions of heterogeneity present between these proteins could be responsible for regulation of activity or substrate specificity (Neuwald, 1997). Indeed, the contributions of the N- and C-termini to the biological and biochemical properties of the LPPs have yet to be reported in any detail.

This work has now been published:

Burnett, C. and Howard, K. (2003). Fly and mammalian lipid phosphate phosphatase isoforms differ in activity both in vitro and in vivo. *EMBO Rep* **4**, 793-9.

3) CHAPTER TWO

Oligomerisation of the LPPs as a Mechanism of Action

3.1) Introduction

Oligomerisation of protein sub-units occurs frequently within biological systems and is particularly common with transmembrane receptors. GPCRs, a large and diverse family of seven transmembrane receptors, are now known to form both homo-and hetero-oligomeric receptor complexes. Work to determine this employed a variety of techniques including the use of chimeric receptor sub-units, point mutations, cross-linking and co-immunoprecipitation of differentially tagged proteins. More recently the use of bioluminescence or fluorescence resonance energy transfer (BRET and FRET) has confirmed the presence of receptor dimers in intact living cells (for review see (Bouvier, 2001).

p53 is a good example of an oligomeric multifunctional cellular protein, perhaps best known for its role in the suppression of tumourigenesis. p53 is activated in response to cellular stress and can regulate or arrest the cell-cycle, as well as induce apoptosis, in an affected cell. In fact mutations in p53 have been characterised in fifty percent of known cancers. The protein consists of a central DNA-binding domain, an N-terminal transactivation domain and C-terminal localisation and oligomerisation signals. Rather than a single unit, the active form of p53 consists of a tetramer made up of two dimers. A *Drosophila* homologue of p53, dmp53, demonstrates the same oligomerisation activities as those reported for human p53 (Chan et al., 2004; Hofseth et al., 2004; Sutcliffe and Brehm, 2004).

It is now known that the molecular weight of the LPPs falls at around 35 kDa. The first attempts to purify LPP activity from membranes, however, indicated a much larger molecular mass. Indeed, SDS polyacrylamide gel electrophoresis of extracts from porcine thymus indicated an 83 kDa band that was shown convincingly to account for the observed enzymatic activity (Kanoh et al., 1992). It wasn't until a few years later that this proved inaccurate, as the enzyme was re-purified and the enzymatic activity shown to be attributable to a much smaller protein of 31-35 kDa (Kai et al., 1996; Siess and Hofstetter, 1996). The original work using porcine membrane-extracts, however, had clearly demonstrated that the native enzyme possessed a molecular weight of 150 kDa. Purification of LPP activity from rat liver membranes and analysis of its Stokes' radius and sedimentation coefficient also indicated a molecular mass of 186 kDa. These results led both groups to postulate that although enzymatic function can be observed for the smaller species *in vitro*, the

native protein may exist as homo-oligomers and may even form hexameric complexes.

This is a theory that had endured but had yet to be proven. The second aim of this work was to investigate this theory in more detail, to determine by use of biochemical techniques whether or not the LPPs oligomerise and if so, how specific these interactions are. If it proved to be the case that LPPs can form complexes, the next aim was to determine whether these complexes are required for activity either biochemically, or biologically.

3.2) Results

3.21) Transfection of S2 cells and analyses of protein size

In order to examine the ability of the LPPs to oligomerise through the use of a variety of biochemical techniques, it was necessary to utilise differentially tagged versions of each protein. Full length Wunen, WunD:248>T and mLPP-1 were available with a C-terminal trimeric myc tag repeat (M3) (Fig.20).

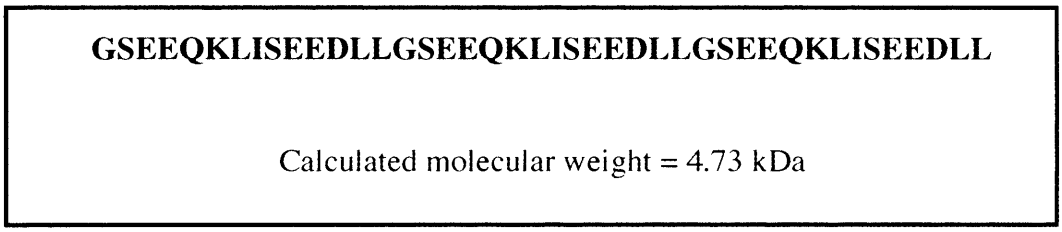

Fig.20. The sequence of the trimeric myc tag repeat.

In addition, GFP and M3 tagged versions of WunD2 were available. WunD2 is a truncation of the last thirty-five C-terminal amino-acids of Wunen (Fig.21). Each of these tagged constructs had been previously cloned into the pUAST vector by other lab members, and were available completely sequenced by overlapping comfort reads through their coding regions.

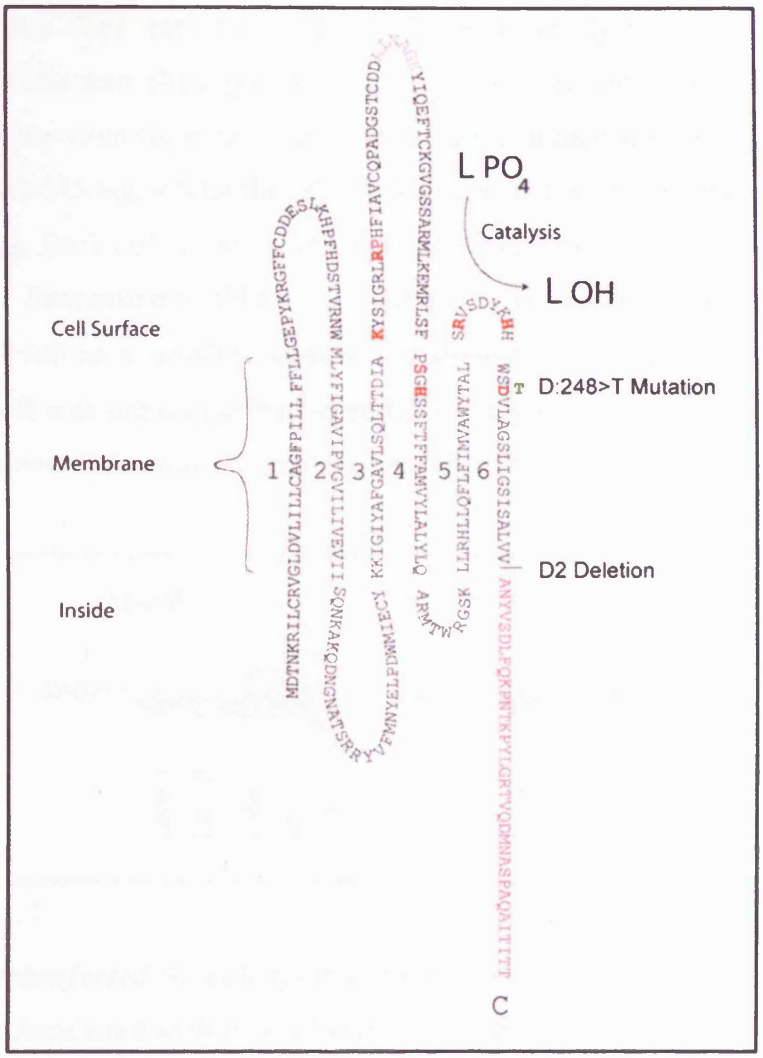

Fig.21. The D2 truncation. *Schematic diagram of full-length Wunen with the last thirty-five C-terminal amino-acids that are absent in D2 highlighted in PINK. Conserved residues required for catalysis are in RED, whilst the D:248>T mutation present only in full-length Wunen is indicated in GREEN.*

3.22) Co-transfections

3.22a) *Confirmation of protein expression in S2 cells*

To determine if the LPPs can interact and form complexes it was first necessary to confirm that S2 cells would transcribe both proteins simultaneously, and that the myc tagged pUAST constructs transcribe proteins of the correct predicted size. S2 cells were transfected with combinations of the differentially tagged constructs and left to

express for two days until the GFP marker was clearly visible by fluorescent microscopy. Cells were then spun down and lysates analysed by Western blot. Two identical gels were run for each sample – one was then incubated with a monoclonal antibody to the M3 tag, whilst the other was incubated with a monoclonal antibody to the GFP tag. Each cell lysate clearly showed expression of both tagged proteins in each case. Smoothened-GFP (SmoGFP) was co-transfected alongside WunD:248>TM3 as a possible control transmembrane protein for use in future experiments. It was not transcribed at sufficient amounts to be detectable by these techniques, however, so was not used further (Fig.22).

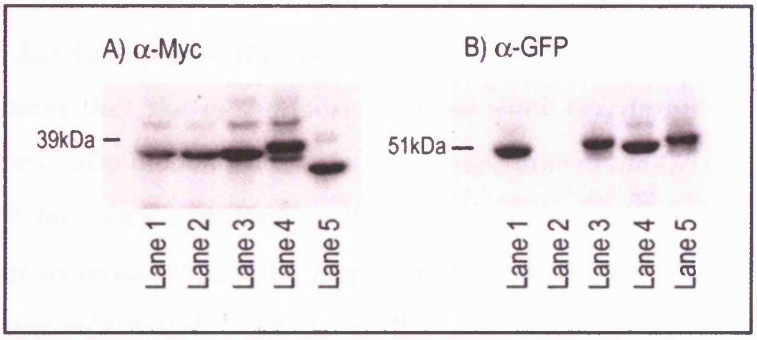

Fig.22. Co-transfected S2 cell lysates. A) *Incubated with monoclonal anti-myc antibody.* ***B)*** *Incubated with monoclonal anti-GFP antibody. This is a five second exposure following ECL detection. Lane 1 = WunD:248>TM3 + WunGFP; lane 2 = WunD248>TM3 + SmoGFP; lane 3 = WunM3 + hLPP-3GFP; lane 4 = WunGFP + mLPP-1GFP; lane 5 = WunD2M3 + hLPP-3GFP.*

3.22b) ***Immunoprecipitation assays: formation of homo-oligomers***

To investigate whether LPPs are able to interact and form homo-oligomeric complexes, S2 cells were co-transfected with either WunM3 plus WunGFP plus Actin5C-GAL4, or with mLPP-1M3 plus mLPP-3GFP plus Actin5C-GAL4. After two days cells were spun down, washed and resuspended in 0.1% triton X-100 lysis buffer. Aliquots were then incubated for two hours with 50µl of Anti-c-Myc Agarose Affinity Gel (Sigma). After incubation the supernatant was removed (termed the 'load') before extensive washing. Samples of the load, the final wash and the resin were then boiled and loaded onto two separate gels for analysis with either a monoclonal anti-myc antibody or a monoclonal anti-GFP antibody (Fig. 23).

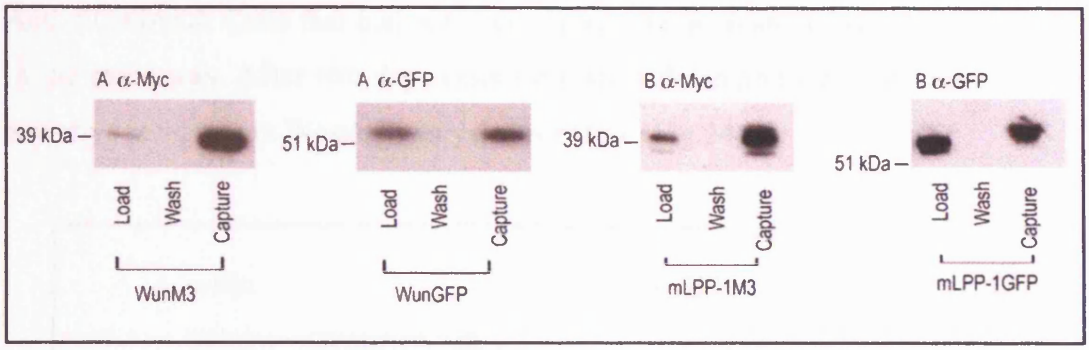

Fig.23. Immunoprecipitation assays: formation of homo-oligomers. A) *WunM3 plus WunGFP. There is only a weak band visible in the WunM3 load, as the majority of the protein has been captured by the resin, as seen by the strong band in the third lane. This shows that the anti-myc resin does work to capture the M3 tagged proteins. There is also a band present in the capture lane of the GFP blot, indicating that WunGFP has been captured on the resin. As the resin is myc specific, the WunGFP must be associating with, and brought down by, the WunM3 protein.* ***B)*** *mLPP1-M3 plus mLPP-1GFP. Again mLPP-1GFP is clearly detected by the anti-GFP antibody and thus must be captured and immunoprecipitated alongside mLPP-1M3, indicating an interaction. As controls, the last two lanes contained either untransfected S2 cells or a sample of resin that has not been incubated with any protein. Both lanes are blank when detected with either anti-myc or anti-GFP antibodies, indicating that the bands seen in the load and capture lanes are totally specific to the transfected and tagged proteins (lanes not shown).*

In all these cases there is no band visible in the 'wash' lane indicating that there is no extraneous unbound protein present – the bands in the 'capture' lanes correspond only to that protein immunocaptured on the resin.

These results indicate that under these conditions full length Wunen and mLPP-1 can form homo-oligomeric complexes. Unfortunately, despite attempts to create such a construct by lab members, a myc tagged version of hLPP-3 was not available.

3.22c) ***Immunoprecipitation assays: formation of hetero-oligomers***

Could LPPs form hetero-oligomeric complexes between isomeric forms, or between species? To investigate this S2 cells were transfected with either WunM3 plus

hLPP-3GFP plus Actin5C-GAL4, or WunGFP plus mLPP-1M3 plus Actin5C-GAL4. Cells that had not been transfected with any construct were treated in the same way. After two days cells were spun down and incubated with 50µl of anti-myc resin before Western analysis, as before (Fig.24).

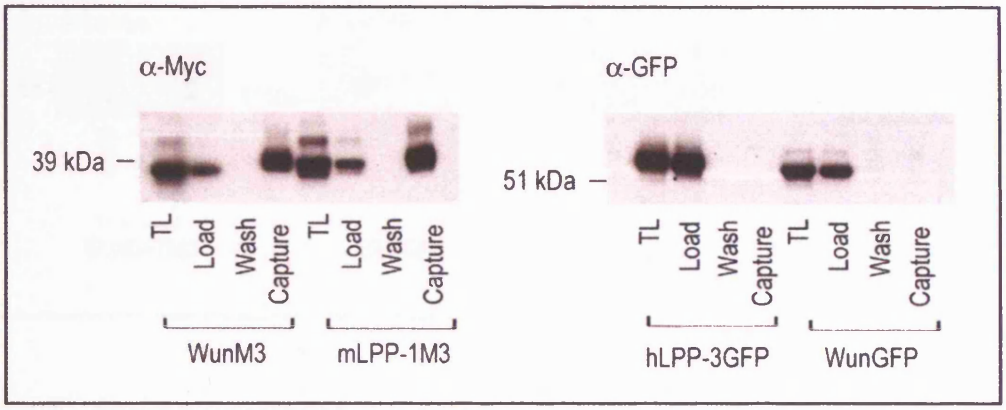

Fig.24. Immunoprecipitation assays: formation of hetero-oligomers. *In these blots, TL refers to Total Lysate – an aliquot of cell lysate prior to incubation on the resin. In the left-hand blot (anti-myc antibody) both mLPP-3M3 and WunM3 are present in the capture lanes, so have been immunoprecipitated on the resin. In the right-hand blot (anti-GFP antibody) although WunGFP and mLPP-1GFP are present in the total lysate and load, neither has been co-captured on the resin indicating that they are not immunoprecipitated alongside their myc tagged counter-part.*

These results indicate that whilst LPPs can form homo-oligomers, they do not form hetero-oligomeric complexes, pointing towards a specific self-interaction. These results also show that the immunocapture of GFP in Fig.22 is due to a true interaction between protein monomers and not due to an artefact of the procedure.

3.22d) *Immunoprecipitation assays: prevention of oligomerisation*

Results reported here indicate that the LPPs can form specific interactions between full-length monomers of the same protein. In the case of tetrameric p53, only one fully functional, non-mutated sub-unit is required for transcriptional activity of the complex, although a single monomer that lacks the C-terminal tetramerisation domain is inactive (Chan et al., 2004). Does oligomerisation of the LPPs depend on the presence of an intact catalytic site in each monomer, or the C-terminus? In order

to determine this, S2 cells were transfected with either WunD:248>TM3 plus WunGFP plus Actin5C-GAL4, or WunD2M3 plus WunGFP plus Actin5C-GAL4. Cell lysates were incubated with anti-myc resin and analysed as before (Fig.25).

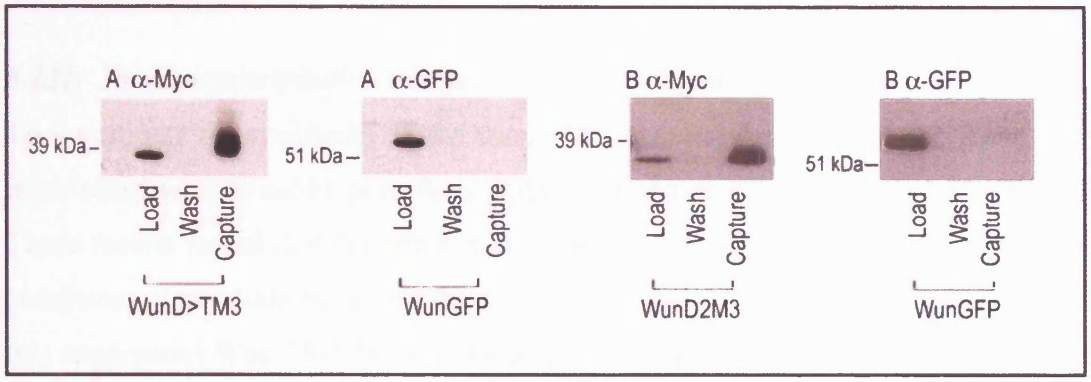

Fig.25. Immunoprecipitation assays: prevention of oligomerisation. A) *WunD:248>TM3 is clearly immunocaptured as seen on the left-hand anti-myc blot. WunGFP, however, is* not *co-precipitated as seen by the total absence of signal in the capture lane of the right-hand blot.* ***B)*** *The WunD2M3 is captured but does not bring down WunGFP as seen by the presence of WunD2M3 in the capture lane of the left-hand blot and the absence of WunGFP in the capture lane of the right-hand blot.*

These results demonstrate that mutation of one amino-acid essential for catalytic activity in one monomer is enough to prevent oligomerisation between otherwise identical protein sub-units. Since truncation of the last thirty-five C-terminal amino-acids also prevents this association, these residues must also be critical in the formation of homo-oligomers. These results further confirm the specificity of the observed interactions, and again indicate that they are genuine associations and not artefacts.

3.22e) *Immunoprecipitation assays: repeat with NEM*

The homo-oligomerisation of Wunen with itself, the catalytic null and the truncation was repeated with the addition of 2 mM *N*-ethylmaleimide (NEM) to the lysis buffer. NEM is an effective reducing agent, used here to remove any bonds that may have formed through oxidation, leading to artefactual oligomers. S2 cells were transfected with WunGFP plus Actin5C-GAL4 plus either WunM3, WunD:248>TM3 or

WunD2M3. The results confirmed the results obtained without addition of NEM to the lysis buffer, that full-length monomers of Wunen can form interactions that are abolished by mutation of the catalytic site in one monomer, or truncation of the C-terminus.

3.22f) ***Immunoprecipitation assays: Wunen and Wunen-2***

To investigate the specificity of the homo-oligomerisation in more detail, cells were transfected with WunM3 plus Wun-2GFP (Fig.26) or Wun-2M3 plus Wun-2GFP. These results reveal that Wunen and Wunen-2 do not form associations under these conditions, again indicating that the associations that do form are highly specific. In this experiment Wun-2M3 failed to immunoprecipitate on the resin. This may be due to a structural or conformational incompatibility. The experiment was repeated using a Wun-2myc construct donated by the Lehmann lab and tagged at the C-terminus with a single myc sequence. This construct failed to be expressed in S2 cells at high enough levels to detect on these Western blots.

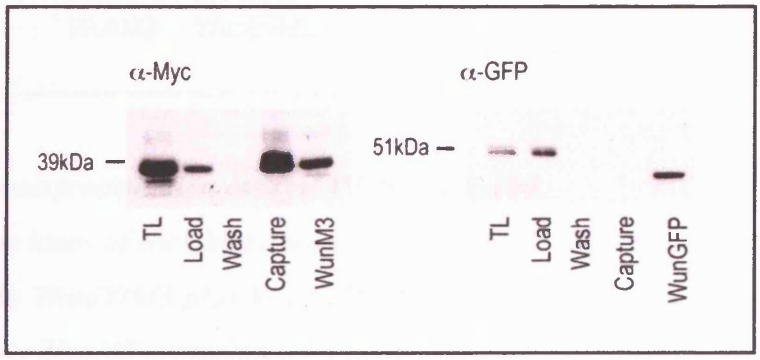

Fig.26. Immunoprecipitation assays: Wunen and Wunen-2. *WunM3 plus Wun-2GFP. The left-hand blot is probed with monoclonal anti-myc antibody, the right-hand blot is probed with monoclonal anti-GFP antibody. The last lane is an aliquot of an immunocapture of co-transfected WunM3 plus WunGFP, run as a control.*

This confirms that Wunen and Wunen-2 fail to form associations. Despite several attempts using different constructs, Wun-2M3 failed to be expressed at adequate levels. Thus the question of whether Wunen-2 can homo-oligomerise is left

unanswered, although evidence from Wunen and mLPP-1 would suggest that it probably does.

3.22g) ***Immunoprecipitation assays: 1% triton X-100***

The co-transfections of WunM3 plus WunGFP, and WunD2M3 plus WunGFP, were repeated, but the S2 cells expressing the proteins were lysed into buffer containing 1% triton X-100 (as opposed to 0.1% as previously) before immunocapture on the resin and Western analyses as before (Fig.27).

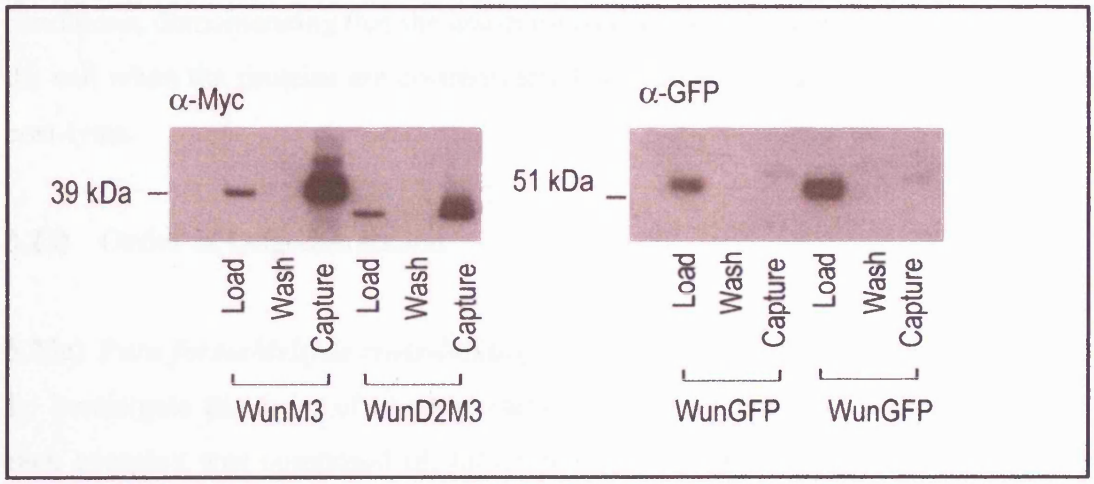

Fig.27. Immunoprecipitation assays: 1% triton X-100.

The first three lanes of each blot correspond to WunM3 plus WunGFP, the last three correspond to WunD2M3 plus WunGFP. Addition of 1% triton X-100 to the lysis buffer prevents WunM3 immunoprecipitating WunGFP.

This shows that in the presence of increased detergent concentration the association between Wunen monomers is disrupted – WunGFP is no longer immunocaptured alongside WunM3. This further confirms that the resin does not recognise the GFP epitope, and that previously observed immunocaptured GFP must be due to that protein's association with its myc tagged counterpart.

3.22h) ***Immunoprecipitation assays: post-transfection***

S2 cells were singly transfected with either WunM3, WunGFP or WunD2M3 (plus the Actin5C-GAL4 driver) and lysed two days later in 0.1% triton X-100 buffer.

Aliquots of WunM3 and WunGFP, or WunD2M3 and WunGFP, were then mixed and incubated on ice for thirty minutes before immunocapture and Western analyses as before. A very weak band was detected for WunGFP, which may point towards an ability of these proteins to form associations post lysis. The experiment was repeated for WunM3 and WunGFP, this time with the addition of 1mM zinc chloride to half of the samples (zinc chloride can stabilize certain protein interactions under these conditions). Samples were mixed and incubated either on ice or at 25 °C for one hour before immunocapture and blotting.

No interaction between WunM3 and WunGFP was observed under these conditions, demonstrating that the associations that form do so within the confines of the cell when the proteins are co-transfected, and do not occur randomly in solution post-lysis.

3.23) Order of Oligomerisation

3.23a) *Para formaldehyde cross-linking*

To investigate the order of oligomerisation and to determine how many sub-units each complex was composed of, intact cells expressing each protein individually were incubated with 3% or 12% Para formaldehyde (PFA) for thirty or sixty minutes before the reaction was quenched by the addition of ammonium chloride. Cells were then washed and lysed in 0.1% triton X-100 buffer before samples were analysed. The cross-linking was repeated with WunD:248>TGFP, WunD2GFP, mLPP-1M3 and hLPP-3GFP in 3% PFA (Fig.28).

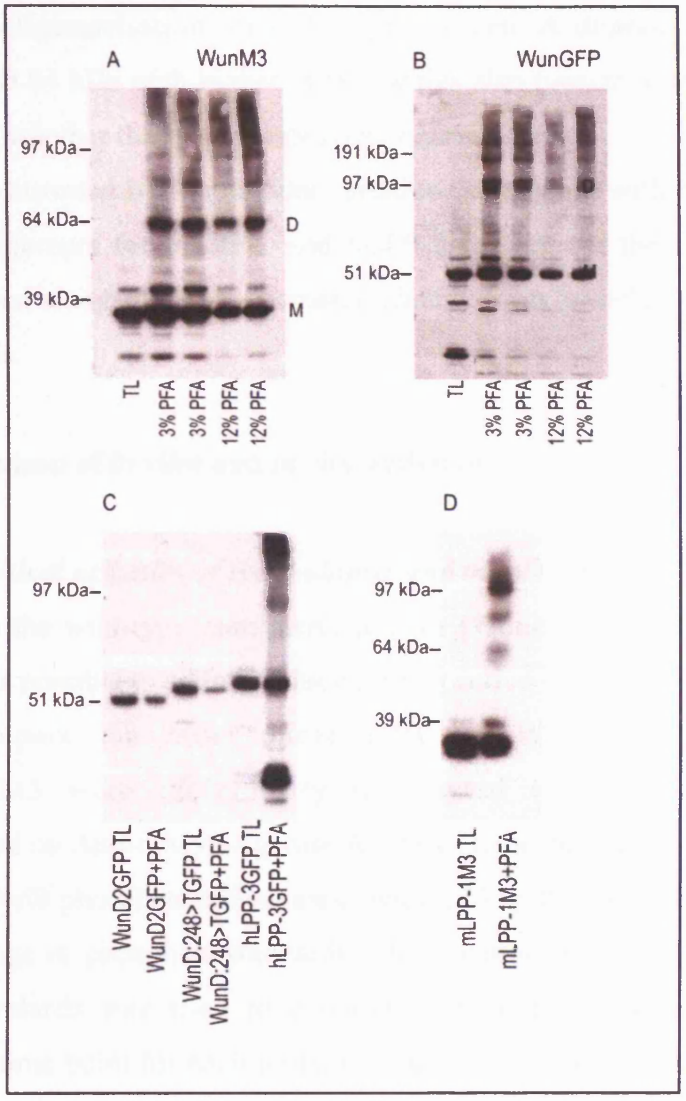

Fig.28. Para formaldehyde cross-linking

A) *WunM3 samples, probed with anti-myc antibody. The first lane is total lysate that has not been incubated with PFA. The second lane corresponds to 3% PFA for thirty minutes; lane three corresponds to 3% PFA for sixty minutes; lane four corresponds to 12% PFA for thirty minutes and lane five corresponds to 12% PFA for sixty minutes.* ***B)*** *WunGFP samples probed with anti-GFP antibody. The lanes correspond to the same treatments as for WunM3.* ***C)*** *Incubation of WunD2GFP, WunD:248>TGFP and hLPP-3GFP with and without PFA.* ***D)*** *Incubation of mLPP-1M3 with and without PFA.* ***M*** *= monomer;* ***D*** *= dimer. Bands that fall below the expected molecular weight for a protein most likely correspond to immunoreactive break-down products.*

This confirms oligomerisation for full-length Wunen. A dimeric form is clearly visible at around 64 kDa with higher order species also present. It is unclear at this point, however, whether these aggregates occur normally.

As demonstrated by immunoprecipitation, incubation with PFA reveals the presence of oligomers for mLPP-1 and hLPP-3 but not for the catalytic null or truncation. Again, alongside the monomer, a dimeric form is visible as well as higher order aggregates.

3.24) Comparison of *in vitro* and *in vivo* activities

3.24a) *Biochemical activities of the multimer and monomer*

With access to the wild-type multimeric protein (Wunen) and a monomeric form (WunD2) it was possible to address which form is active both *in vitro* and *in vivo*. In order to compare the biochemical activities WunM3, WunD2M3 and WunD:248>TM3 were individually transfected into S2 cells and then immunocaptured on Anti-c-Myc Agarose Affinity Gel as before. Aliquots were then fed into the PiPer® phosphate release assay with LPA as the substrate, and incubated alongside a range of phosphate standards. The equation of the line for each set of phosphate standards was used to calculate nMole phosphate released at the corresponding time point for each protein sample. Immediately following the assay all samples were Western blotted and analysed by densitometry to compare relative protein amounts and subsequently calculate relative activities, as before (Fig.29, Tables 6 and 7).

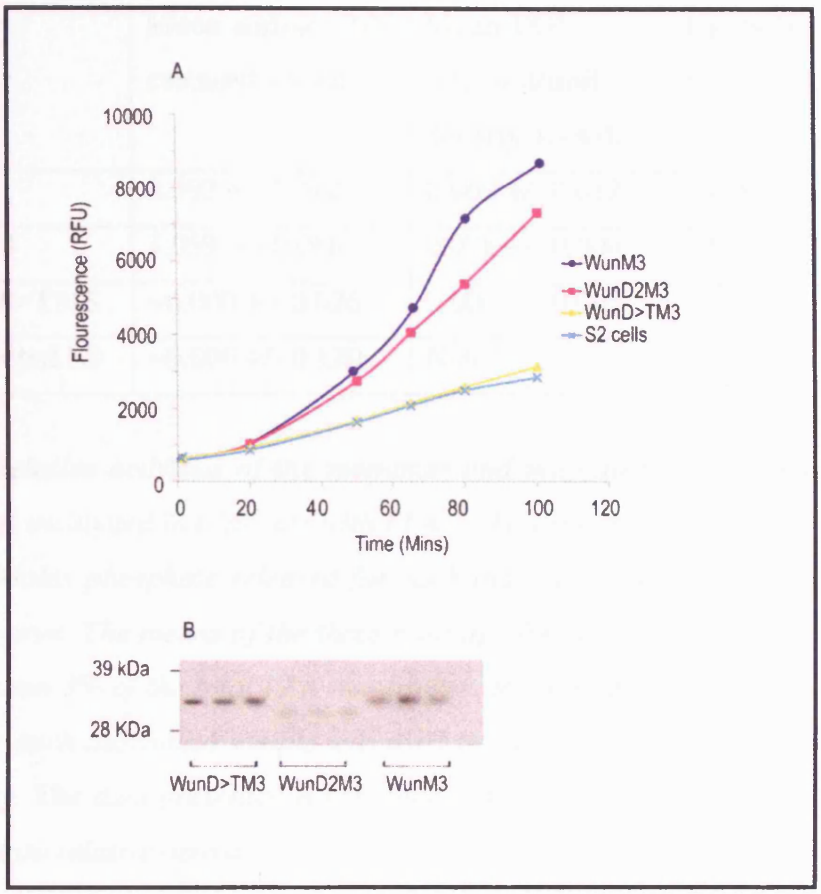

Fig.29. PiPer® phosphate release assay results. A) *The graph shows the mean fluorescent readout from triplicate experiments for each protein with LPA. RFU, relative fluorescence units. Fluorescence was measured using a SPECTRAmax™ GEMINI XS Dual Scanning Microplate Spectrafluorometer.*

B) *Western blot of all three protein samples for each construct.*

	Value 1	**Value 2**	**Value 3**	**s.d.**
WunM3	16.293	24.603	20.003	4.163
WunD2M3	13.762	13.163	13.522	0.301
WunD:248>TM3	22.817	21.507	22.434	0.673

Table 6. Densitometry. *Each value is a density reading from each of the three sample wells in Fig.29B, as calculated by BioRad Quantity One software.*

Construct	Mean nMole. PO^4 released +/- s.d.	Mean PO^4 released/unit density +/- s.d.	Relative activity
WunM3	1.392 +/- 0.340	0.069 +/- 0.012	1.00
WunD2M3	1.059 +/- 0.068	0.078 +/- 0.004	1.13
WunD:248>TM3	~0.000 +/- 0.026	0.000 +/- 0.001	0.00
Untransfected S2	~0.000 +/- 0.120	N/A	0.00

Table 7. Relative activities of the monomer and multimer. *Each immunocaptured enzyme was incubated in triplicate with LPA in the PiPer® phosphate release assay, and the nMoles phosphate released for each individual sample calculated from a standard curve. The means of the three readings for each enzyme is presented, +/- s.d.. Less than 3% of the total LPA was broken down in any of the experiments. The density for each individual sample was used to calculate nMoles PO4 released per unit density. The data presented is the mean of these values, +/- s.d.. This was then converted into relative activity.*

These results show that under these conditions, using immunopurified proteins, the monomeric version of Wunen, WunD2M3, is slightly more active than multimeric full-length Wunen. This indicates that dimerisation is *not* required for catalysis in this biochemical assay.

3.24b) *Biological activities of the multimer and monomer*

To examine the ability of the truncated, monomeric form to act on the PGC-specific survival factor in *Drosophila* embryos, transgenic flies were generated with WunD2GFP and WunD2M3, and crossed to the mesoderm driver twist-GAL4. Ectopic expression of WunD2GFP gave a similar phenotype to ectopic expression of full-length Wunen, with scattered germ cells, a failure to form functional gonads, and a marked reduction in germ cell number (Fig.30). This indicates that neither dimerisation nor the C-terminal thirty-five amino-acids are required for activity *in vivo*. Surprisingly, expression of WunD2M3, which has significant activity in the LPA assay, had no affect on PGC migration or survival (Fig.30). WunM3 was also mis-expressed *in vivo* and this too showed a total loss-of-function, despite high levels

of protein in the mesoderm and activity in the *in vitro* LPA assay (Fig. 30). This indicates that *in vivo*, this trimeric myc tag prevents the function of a previously active protein and cannot be relied on as a passive tag. These results also show that catalytic activity as assayed biochemically, is not a true reflection of activity as assayed *in vivo*.

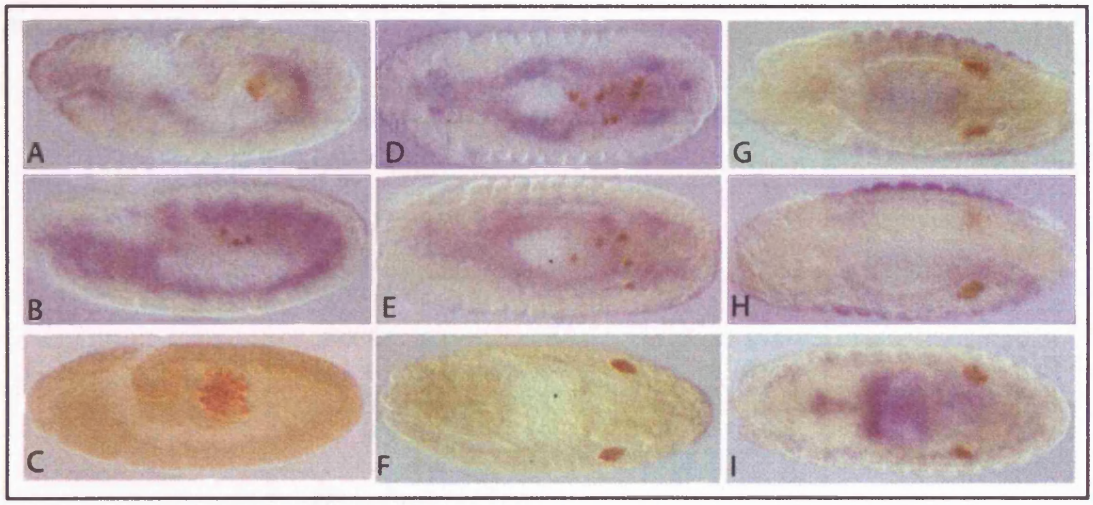

Fig.30. Ectopic expression in the mesoderm. *Embryos A-C are viewed laterally with the posterior pole to the right, embryos D-I are viewed dorso-ventrally. Expression of WunD2GFP* ***(A)*** *at stage 10 has a similar phenotype to WunGFP* ***(B)*** *with an early and dramatic loss of PGCs compared to wild-type* ***(C)****. By the end of embryogenesis, neither WunD2GFP* ***(D)*** *nor WunGFP* ***(E)*** *expressing embryos have formed gonads, as opposed to a wild-type embryo at the same stage* ***(F)****. Expression of WunD:248>TGFP* ***(G)****, WunD2M3* ***(H)*** *or WunM3* ***(I)*** *give no discernable phenotype with all embryos forming two distinct gonads. Wild-type embryos do not express GFP and consequently show no blue staining. Antibodies as before.*

3.25) Confirmation of Cell-Surface Localisation

3.25a) *Biotinylation of cell-surface proteins*

It was important to confirm that the M3 tag did not interfere with trafficking to the cell surface. This would then rule out the possibility that the M3 tag prevented WunM3 from reaching the cell surface precluding access to its substrate. Intact cells expressing either WunM3 or WunGFP were incubated with NHS-biotin, and lysates

run over a monomeric biotin-binding avidin column before Western blotting as before. As a control for the procedure, WunM3 was co-transfected with the cell-surface marker CD2 (Dunin-Borkowski and Brown, 1995) and blotted for the presence of CD2 and the internal protein tubulin. As the NHS-biotin biotinylates only those proteins on the cell-surface, CD2 should be present in the elutions, whereas tubulin should not be biotinylated and instead pass through the column in the washes (Fig. 31).

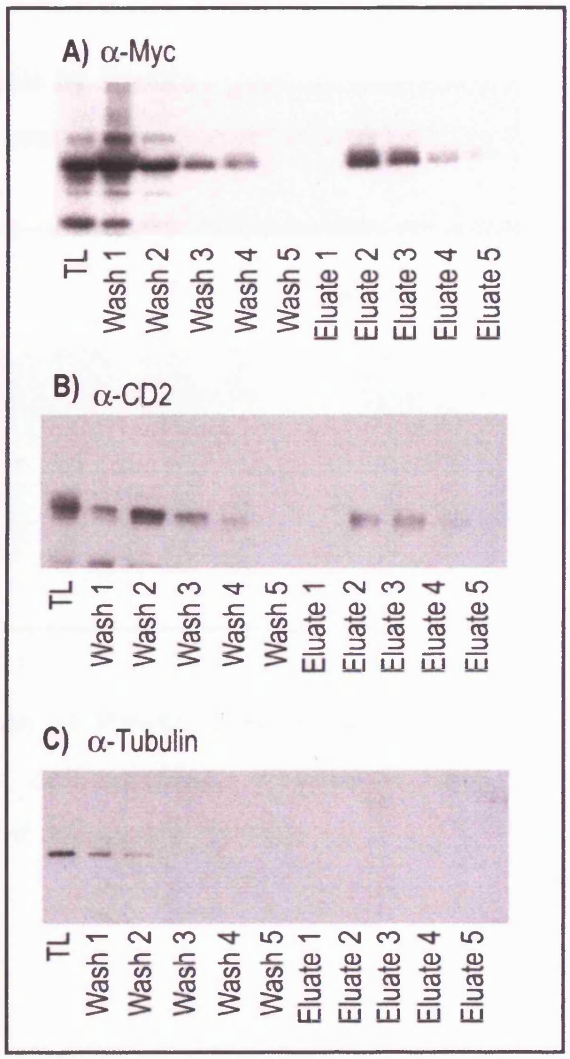

Fig.31. Biotinylation of cell-surface proteins. *S2 cells were co-transfected with WunM3 and CD2, and blotted for the presence of the M3 tag, CD2 and tubulin. TL = an aliquot of total cell lysate prior to column binding.* ***A)*** *WunM3 is detected in the elutions, demonstrating that it is biotinylated at the cell-surface. It is also detected in the washes. WunM3 is expressed at high levels in these cells and we*

would expect there to be a quantity of intracellular protein. Alternatively, the high level of WunM3 expression may have titrated out the biotin, leaving a percentage of WunM3 not biotinylated but still at the cell-surface. This protein would also pass out in the washes. ***B)*** *CD2, a cell-surface protein, is biotinylated, and so passes out in the elutions. Again, a proportion also passes out in the washes. This is probably intracellular protein that has yet to arrive at the cell-surface.* ***C)*** *Tubulin is an intracellular protein not found at the cell-surface. Consequently it is not biotinylated and is only detected in the washes.*

Densitometry analysis by Bio-Rad Quantity One Software indicated that similar percentages of each protein were present at the cell surface (Fig. 32).

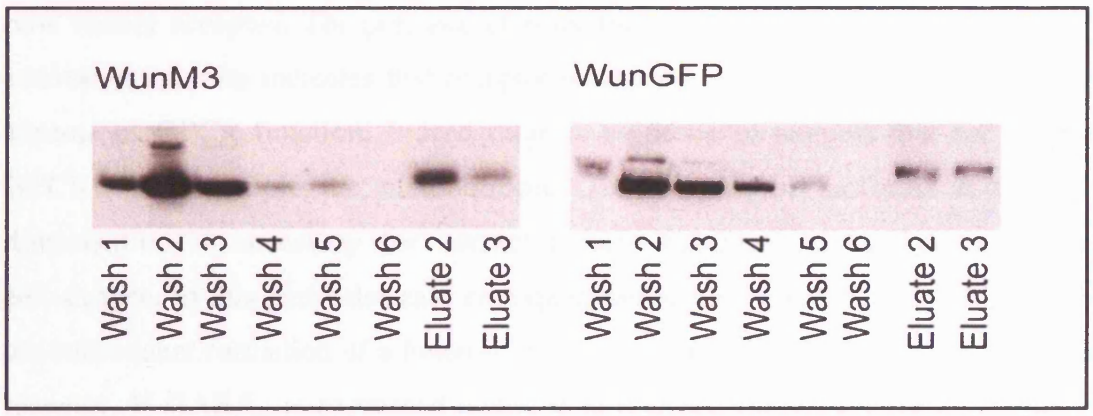

Fig.32. Biotinylation of WunM3 and WunGFP. *Biotinylation of WunM3 and WunGFP at the cell surface. Washes = non-biotinylated proteins; Eluates = biotinylated cell-surface proteins.*

3.3) Summary

The combination of these results demonstrate that the fly LPP Wunen dimerises, that a C-terminal truncation or mutation of a conserved catalytic residue prevents this association, and that dimerisation is not required for activity either *in vitro* or *in vivo*. They also show that whilst hLPP-3 and mLPP-1 can both homo-dimerise, none of the LPPs tested, including Wun-2, can form associations with Wunen.

This is the first time that an LPP has been shown to dimerise, although protein oligomerisation *per se* is not novel. Outer membrane phospholipase A (OMPLA) resides in an inactive, monomeric form in the outer membrane of gram-negative bacteria. Perturbation of the bacterial membrane activates the enzyme by reversible dimerisation (Dekker et al., 1997) forming functional active sites, substrate binding pockets and essential calcium binding sites (Snijder et al., 1999). Pre-incubation with increasing detergent results in dissociation into monomers and a 15-fold decrease in activity (Dekker et al., 1997). Wunen also forms dimers, which are dissociated by increasing detergent concentration, but the monomer remains active both *in vitro* and *in vivo*.

Dimerisation, or oligomerisation, is also believed to be an important feature of GPCR activation, with the existence of homo- and hetero-oligomeric complexes now widely accepted. The presence of constitutive homo-dimers in the absence of activating agonists indicates that receptor dimerisation may be important for other aspects of GPCR function. Indeed there is evidence to suggest that for certain GPCRs, for example the metabotropic GABA receptor isoforms A and B, dimerisation is necessary for correct protein folding and trafficking to the cell-surface. In this particular case co-expression of both $GABA_A$ and $GABA_B$ and the subsequent formation of a hetero-dimer is required for a functional cell-surface receptor. If $GABA_A$ is expressed alone, it is retained intracellularly and fails to transport to the cell surface. $GABA_B$, on the other hand, does reach the cell-surface but fails to function correctly (Bouvier, 2001).

Conversely, receptor-like protein tyrosine phosphatases (RPTPs) are also found as monomers or homo-dimers, but it is the monomeric version that is active. CD45, a transmembrane leukocyte-specific RPTP, was shown by chemical cross-linking and sucrose gradient ultracentrifugation to exist as monomers and homo-dimers, both of which associate with a 30 kDa phosphorylated protein (Takeda et al., 1992). Further work by the same group demonstrated that the associating protein, termed CD45-AP, exists in a complex with CD45 mediated through the single-span transmembrane domains. In CD45-AP-null cell lines, the proportion of CD45 dimers was significantly increased, indicating that CD45-AP inhibits dimerisation and results in increased activity of CD45. They further reported that this associating protein may play a further role in regulating access of CD45 to its substrate (Takeda et al., 2004). The inhibitory nature of the dimeric interaction lies in

a wedge-shaped element present on each monomer sub-unit that inserts into the active site of the corresponding monomer. Thus within the dimer, each active site is occupied by the opposing monomer's wedge. This wedge-mediated suppression of activity regulates biological activity of CD45 in cellular systems and is therefore believed to play a corresponding physiological role *in vivo*. It is proposed that ligand binding may stabilise the monomeric form (Jiang et al., 2000; Majeti et al., 1998)

Point mutations in the catalytic core of human arginase I, a metalloenzyme widely distributed from bacteria to mammals, breaks association between its monomers. L-arginine aminohydrolase (arginase) catalyzes the hydrolysis of L-arginine to L-ornithine and urea, so regulating their levels. Both of these amino-acids play vital roles in a range of metabolic processes. Arginase is found as trimers in eukaryotes, but hexamers in prokaryotes. As in Wunen, monomers retain wild-type activity in biochemical assays (Sabio et al., 2001). The mutated residue, involved in inter-monomer salt links, is believed to stabilise the multimeric structure since the monomer is less thermally stable and binds manganese with a reduced affinity. Although the absolute structure of the LPPs has yet to be determined, the superfamily is defined by three highly conserved domains proposed to form a 3-dimensional active site (Neuwald, 1997) (Stukey and Carman, 1997). It seems possible that the D:248>T mutation may also break oligomerisation due to structural changes in the catalytic core. The core may serve two separate functions – provision of an active site, and stabilisation of the quartenary structure. This may be substantiated in the future by the use of alternative point mutations in other catalytically important residues.

Truncation of the non-conserved C-terminal tail of avian sarcoma virus integrase (ASV IN) hampers multimerisation and results in loss of activity (Andrake and Skalka, 1995). Intergrase is required for the integration of retroviral DNA into a target genome and multimerisation is essential for catalytic function. In both ASV IN and arginase I it is proposed that the catalytic core *and* the C-terminus interact to form complexes. This could account for the loss of dimerisation seen in WunD2 and WunD:248>T. The loss of catalytic function would then be directly due to mutating a residue essential for catalytic activity.

It has recently been reported that the requirement of mLPP-3 in vasculogenesis in the mouse is independent of its phosphatase activity (Escalante-Alcalde et al., 2003). It has further been reported that hLPP-3 may be involved with

cell-cell interactions and the regulation of adhesion, possibly another phosphatase-independent role. It may be, therefore, that oligomerisation is required for an alternative function to PGC migration and survival, and possibly for the regulation of a phosphatase-independent role. Thus truncation of Wunen and prevention of oligomerisation may not interfere with its affects on PGCs, but may well inhibit or modify its activities elsewhere within *Drosophila.*

Although the Wunen monomer is active, it is not known whether the dimer is active or inactive. It may be that Wunen exists as both forms with dimerisation regulating activity or enzyme levels. Alternatively dimerisation may be required for wild-type function, protein folding or trafficking to the cell-surface, but driving expression of the monomeric protein at unnaturally high levels in the mesoderm may over-ride this, with a percentage of expressed protein reaching the cell-surface due to the unnaturally high levels present in the cell. That the M3 tag does not prevent catalysis on LPA, but absolutely prevents activity *in vivo* indicates caution should be applied in interpretation of biochemical data. Since the M3 tag does not prevent trafficking to the cell surface, it may instead introduce conformational or structural changes that prevent the enzyme from recognizing or associating with either the substrate, or an associating factor in the pathway.

This work has now been published:

Burnett, C., Makridou, P., Hewlett, L. and Howard, K. (2004). Lipid phosphate phosphatases dimerise, but this interaction is not required for in vivo activity. *BMC Biochem* **5**, 2.

4) CHAPTER THREE

Identification of a GPCR Involved in *Drosophila* PGC Migration

4.1) Introduction

Previous work has shown that the mammalian LPPs are capable of dephosphorylating a range of bioactive phospholipids, including LPA and S1P. The work presented here demonstrates for the first time that the fly LPP, Wunen, is also capable of dephosphorylating LPA *in vitro*. Both LPA and S1P function in a highly diverse range of pathways influencing such processes as cellular proliferation and differentiation, as well as cell survival and apoptosis. Perhaps more relevant to this work, however, are results implicating LPA, S1P and their receptors in the regulation of cell migration, tumour cell invasiveness and wound healing.

Cell migration and invasiveness are both key components of tumourigenesis. In the mid-1990s, researchers reported the isolation and identification of Ovarian Cancer Activating Factor (OCAF) from the ascites of ovarian cancer patients. Able to induce proliferation of ovarian cancer cells, OCAF was found to be composed of a variety of species of LPA (Xu et al., 1995b). In 1998, in a study of 165 women at the Cleveland Clinic Foundation, researchers confirmed that levels of LPA were significantly increased in the ascites of women suffering from either ovarian cancer or a range of other gynaecological malignancies. These results led to the suggestion that LPA may serve as a potent biomarker for early diagnosis of these diseases (Xu et al., 1998). LPA is known to induce ovarian cancer cell proliferation (Xu et al., 1995a), whilst it has also been shown to induce the chemotaxis and chemokinesis of four separate ovarian cancer cell lines (Bian et al., 2004).

Both LPA and S1P have been shown to increase the migration and proliferation of endothelial cells in the process of wound healing (Lee et al., 2000), whilst topical application of LPA increased the migration and subsequent infiltration of histiocyte macrophage cells to a full-thickness wound *in vivo*, resulting in an acceleration of wound repair (Balazs et al., 2001).

Olfactory ensheathing cells (OECs) demonstrate migratory behaviour throughout vertebrate adult life. OECs are a macroglia cell-type derived from the olfactory system that ensheath ingrowing olfactory nerve fibre. Interest in these cells stems from experiments demonstrating their ability to restore axonal re-growth and function, post-transplantation, in experimental models and the impact this may have in spinal cord injury research. Within the olfactory system of the adult rodent, neurons have an average life-span of thirty days, after which they degenerate and are

replaced from a stem cell population. These newly formed neurons extend axons that migrate to their destination in the olfactory bulb. Transplantation of cultured OECs into rat cortico-spinal tract lesions has resulted in induction of regeneration of the cut axons and the restoration of function by encouraging elongation along their original pathway, a process that is distinctly lacking in central nervous system injuries (Raisman, 2000; Raisman, 2003). Addition of LPA to OECs cultured on Transwell membranes increased their proliferation, but more significantly, enhanced their migration in a dose-dependent manner. This was associated with changes in cell morphology and actin re-organisation (Yan et al., 2003).

Another type of glial cell from the peripheral nervous system, Schwann cells, have been shown to respond to both LPA and S1P stimulation. In both primary rat cells and cells from the rat-derived SCL4.1/F7 line, S1P and LPA induced process retraction, cell spreading and the formation of lamellipodia. When assayed in a Boyden chamber, both LPA and S1P induced a significant increase in cell motility, with a gradient of S1P generating a directional chemotactic response (Barber et al., 2004).

LPA and S1P are similar molecules, both structurally and functionally. It should be of little surprise, then, that they bind and exert their affects through a single family of specific cell-surface receptors. So far five receptors have been identified that bind S1P, whilst three bind LPA. Originally termed the endothelial differentiation gene receptors (Edg), Edg1, 3, 5, 6 and 8 bind S1P, whilst Edg2, 4 and 7 bind LPA. They have now been renamed SIP_{1-5} and LPA_{1-3} (Takuwa et al., 2002).

The receptors for both LPA and S1P have also been implicated in influencing cell migration and invasiveness. In the study on epithelial wound healing, quantitative RT-PCR indicated a significant up-regulation of Edgs 1, 2 and 3 (Lee et al., 2000), whilst over-expression of Edg1 in HEK293 cells was shown to enhance chemotaxis, a result also observed in HUVEC (Human Umbilical Vein Endothelial Cells) and BAEC (Bovine Aortic Endothelial Cells) cell lines. Furthermore, cells were shown to migrate directionally in response to a gradient of S1P. The authors concluded from this study that the binding of S1P to the S1P-specific Edg1 receptor increases cell motility in vascular endothelial cells (Wang et al., 1999).

During zebra-fish development, myocardial precursor cells migrate towards the midline where they eventually fuse, forming the heart tube. A large-scale genetic screen revealed a novel mutation termed *miles-apart* (*mil*). In *mil* embryos the second wave of precursor migration is severely disrupted, a phenotype that is restricted to the myocardial precursor cells. Researchers discovered through the use of cell transplantations and genetic mosaics that, when introduced into a wild-type background, mutant cells could migrate normally. When the reverse was applied, however, wild-type cells failed to migrate correctly in a *mil* background. Further analysis revealed that *mil* encodes an Edg5 homologue, and expression of the protein in Jurkat T cells resulted in activation of S1P-associated signalling pathways upon exposure to S1P. Thus for cell migration to occur normally in this system, the S1P-specific Edg5 receptor is required not within the myocardial precursor cells themselves, but within the surrounding tissue (Kupperman et al., 2000).

In a similar vein, PGCs in *Drosophila* respond to extra-cellular signals regulated in some fashion by Wunen and Wunen-2, enzymes that we know can dephosphorylate LPA (their activity on S1P remains untested). It stands to reason, therefore, that in order to respond to these directional cues, PGCs should possess receptors on their surface that can interpret and respond to the appropriate and specific cues in their surrounding environment.

The Edg receptors are members of the GPCR superfamily, an extremely large family of proteins which is divided into three main sub-families: the rhodopsin and β2-adrenergic receptors (family A), the glucagon-like receptors (family B), and the metabotropic neurotransmitter-like receptors (family C). A degree of homology exists between members in the same family, but, overall, GPCRs make up a diverse and complex group, activating a wide variety of signal transduction pathways and binding an equally diverse range of ligands, including biogenic amines, lipids, peptides, nucleotides, ions and light. GPCRs share a common overall structure comprising seven transmembrane α-helical segments, which interact to form a three-dimensional barrel, with an extracellular N-terminal segment and an intracellular C-terminal tail.

GPCRs comprise a signal transduction unit consisting of the receptor linked to a trimeric G-protein (guanine nucleotide-binding regulatory protein) complex. Upon ligand binding to the GPCR, the G-protein is activated: the α sub-unit releases

GDP in exchange for GTP, and dissociates from the βγ part of the complex. Both the α and βγ units are then free to activate or inhibit an effector protein. Effectors include adenylyl cyclase and phospholipases C and D. Hydrolysis of GTP to GDP by an intrinsic GTPase activity of the α sub-unit terminates this process and returns the α sub-unit to the complex (Bouvier, 2001; Gether, 2000).

The third aim of this work was to search for sequences within the *Drosophila* genome that may encode putative PGC-specific receptors, and, having identified any, to test whether or not they do indeed function in the regulation of PGC migration.

4.2) Results

4.21) Computational Analyses

4.21a) *Identification of Gene 11*

Previous work in the Howard lab by Dan Marsden to identify sequences in the *Drosophila* genome with homology to the mammalian Edg receptors revealed Gene 11 (synonyms CG4322, EG:22E5.11) at 2C7-8 on the X chromosome. Gene 11 was identified in FlyBase as an orphan member of the rhodopsin-like superfamily, and sitting just 5' are two EP elements, EP(X)1529 and EP(X)1631. The full-length cDNA, RE26846, was ordered, cloned into the pUAST vector and sequenced, before injection into flies and recovery of transformants. Phenotypic analyses of this gene using ectopic expression and analysis of the insertions, revealed no significant perturbation in PGC migration and this work was not pursued any further.

4.21b) *Identification of Tre-1*

In 2002, Clark Coffman *et al* reported the results of an EMS mutagenesis screen of the X chromosome that identified a mutation affecting PGC migration and PGC programmed cell death, which they termed *scattershot* (*sctt*). In *sctt* embryos, PGCs enter the posterior mid-gut and traverse the epithelium normally, but then fail to reach the gonads and are left scattered throughout the posterior half of the embryo. Furthermore, these ectopic PGCs continue to express germ cell markers and are not eliminated as is usually seen for 'lost' (ectopic) PGCs during wild-type embryogenesis. *sctt* is a maternal-effect mutation and its product is required both maternally and zygotically. Paternal rescue results in wild-type numbers of PGCs locating and associating with the gonads, but does not restore the cell death phenotype – ectopic PGCs are not eliminated resulting in a significantly increased final overall number of PGCs (Coffman et al., 2002).

sctt maps to between 4C11 and 6D8 on the X chromosome. Computational analyses of this area revealed a number of genes, both annotated and putative. One gene, *Trehalose-1* (*tre-1, CG3171*), was identified as an orphan member of the rhodopsin-like superfamily, which maps to 5A11-5A12 (FlyBase, 2003).

The Genome Annotation Database of *Drosophila* (GadFly) identified RE07751 as a full-length cDNA for *tre-1*. A BLAST search using the *tre-1* sequence

revealed homology to CG4322, or Gene 11. As this had initially been identified through a search for Edg-like receptors, a ClustalW analysis was performed using sequences for *tre-1*, Gene 11 and Edgs1-8, and the results were used to construct a phylogenetic tree (Fig.33).

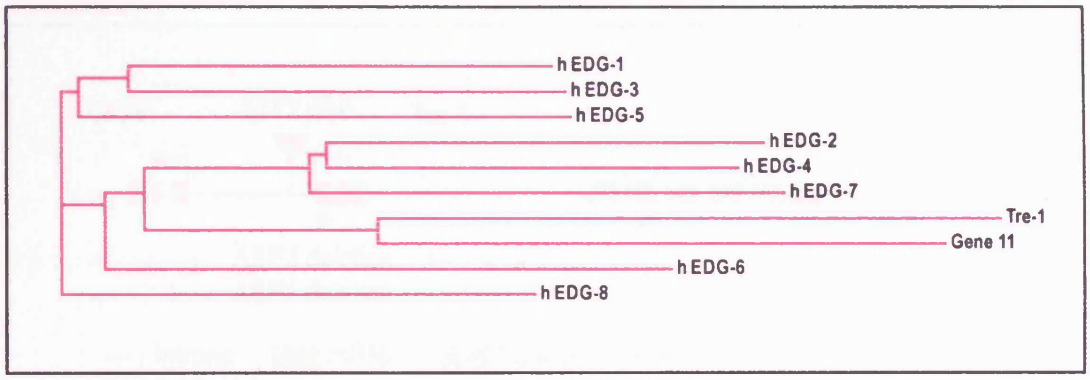

Fig.33. Phylogenetic tree. *The phylogenetic tree was constructed using ClustalW, and sequences with the following accession numbers: human Edg1 to Edg8 =* ***NM001400, NM057159, NM005226, NM004720, NM004230, NM003775, NM012152, NM030760.*** *Tre-1 =* ***NM080053****, Gene 11 =* ***NM130614.***

The phylogenetic tree indicated that Tre-1 is closer to the LPA receptors (Edgs2, 4 and 7) than the S1P receptors. Consequently *tre-1* appeared to be a candidate locus for *sctt,* and thus a candidate receptor involved in the regulation of both PGC migration and PGC death.

4.22) Phenotypic analyses

4.22a) tre-1, Gr5a *and Tre-1*$^{\Delta EP3}$

tre-1 was originally identified as encoding a taste receptor to the sugar trehalose (Ishimoto et al., 2000). Further analyses of the region, however, identified the neighbouring gene *Gr5a*, and not *tre-1*, to be responsible for trehalose sensitivity, leaving Tre-1 with an unknown function (Dahanukar et al., 2001; Ueno et al., 2001). The *Gr5a* phenotype was uncovered through imprecise excisions of the EP element EP(x)496, located approximately one hundred base pairs upstream of the *tre-1* transcription start site and seven hundred base pairs upstream of *Gr5a*. Mobilisation

of EP(X)496 resulted in various deletions of the Tre locus, including *tre-1*$^{\Delta EP3}$ (ΔEP3) and the slightly larger *tre-1*$^{\Delta EP5}$ (ΔEP5). ΔEP3 deletes 2.1kpb, uncovering 1.4kbp toward *tre-1*, and removing the promoter, exon 1 and part of the first intron. ΔEP3 also removes 0.7kbp towards *Gr5a*, deleting the promoter (Fig.34).

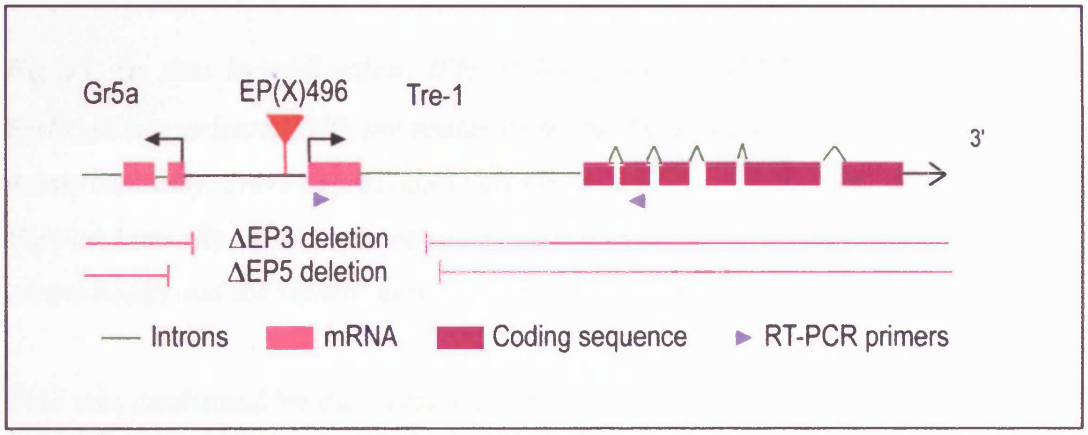

Fig.34. The* tre-1 *genomic region. *The diagram illustrates the* tre-1 *coding sequence in PURPLE, the introns in GREEN as well as the EP insertion EP(X)496 used to create the deletions* ***ΔEP3*** *and* ***ΔEP5****. Part of the neighbouring gene,* Gr5a, *is also represented to the left of the figure.*

4.22b) In situ *hybridisation*

The RE07751 cDNA was obtained from Invitrogen in the pFLC1 vector. This was used to produce labelled probes for use in ISH. ISH in wild-type W^{1118} embryos revealed transcripts in a variety of embryonic tissues, including the proventriculus and ventral nerve cord (Fig.35).

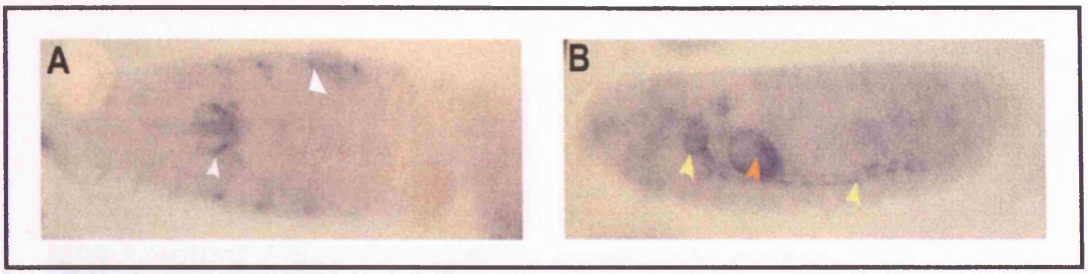

Fig.35.* In situ *hybridisation. *ISH of Tre-1 probe (RE07751) to W^{118} embryos. Embryos are oriented with the posterior to the right at around stage 16.* ***A)*** *Viewed dorso-ventrally. Tre-1 expression is observed in various tissues (WHITE arrow-heads).* ***B)*** *Viewed laterally. Tre-1 expression is observed in the proventriculus (ORANGE arrow-head) and the ventral nerve cord (YELLOW arrow-heads).*

This was confirmed by data available on the Berkeley *Drosophila* Genome Project (BDGP) gene expression page (http://www.fruitfly.org/cgi-bin/ex/insitu.pl) which reports that *tre-1* has a dynamic expression profile beginning in the maternal pole plasm and found in various tissues throughout embryogenesis. Most significantly for this work, however, *tre-1* is also expressed in the PGCs at stages 7-8 and 13-16 (Tomancak et al., 2002).

4.22c) *ΔEP3 and PGC migration*

The ΔEP3 deletion was obtained as a kind gift from Kunio Isono, as a homozygous viable purified stock extracted over an X chromosome FM7 balancer (personal communication). The germ cell phenotype in ΔEP3 flies was examined and compared to wild-type, by staining embryos with the anti-Vasa antibody and counting the number of PGCs left ectopic to the gonads by stage 13. Results clearly indicated that 47% of the PGC population showed a severe disruption in migration, without a single germ cell managing to coalesce with the gonad by stage 13. Although this phenotype displayed variable penetrance, 87% of the total population examined demonstrated perturbed migration (Fig. 36 and Fig.37).

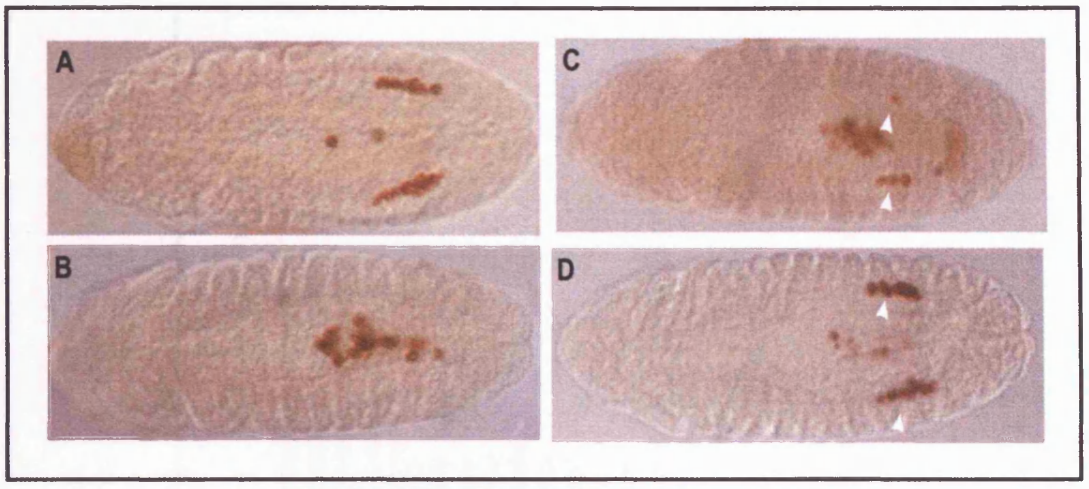

Fig.36. Phenotypic analysis of ΔEP3. *All embryos are viewed dorso-ventrally with the posterior pole oriented to the right. PGCs are stained with anti-Vasa antibody and are visualised in brown.* ***A)*** *Wild-type.* ***B-D)*** *ΔEP3 embryos demonstrating the variable phenotype. In* ***B****, no PGCs have associated with the gonads, whereas in* ***C*** *a few have made it (indicated by the white arrow-heads), and in* ***D*** *there are two definite gonads (indicated by the white arrow-heads), whilst a number of PGCs still remain in the main body of the embryo.*

4.22d) ***Genomic rescue of the PGC migration defect***

The question remained whether the observed phenotype was due to a deletion in *tre-1* or the neighbouring gene *Gr5a*. To determine this, Kunio Isono kindly sent Tre-$1^{\Delta EP3}$:m10f, a stock containing a third chromosomal insertion of a 6 Kb CG3171 genomic fragment in pCaSpeR-4 vector. Phenotypic analysis of these flies demonstrated that this addition of *tre-1* was sufficient to rescue the PGC migration defect in the ΔEP3 flies, indicating that it is the deletion in *tre-1* and not *Gr5a* that is responsible (Fig. 37).

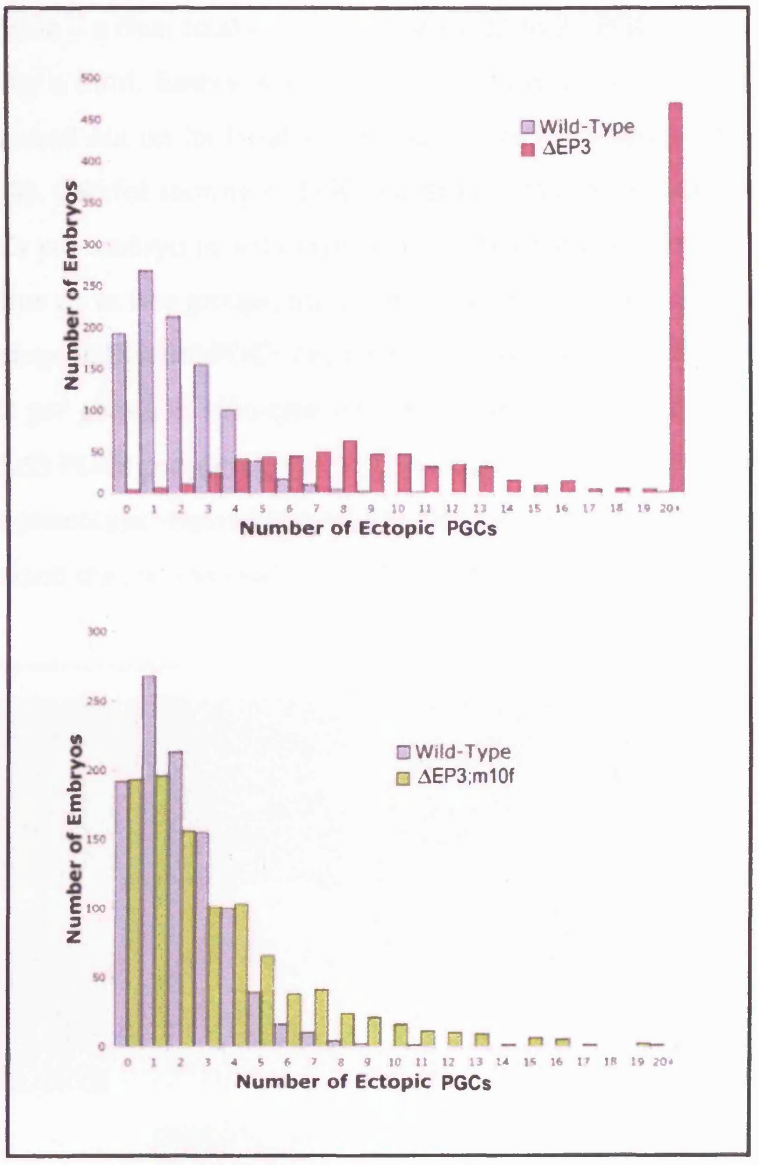

Fig.37. Tre-1 rescue. *Embryos were fixed and stained at stages 12 onwards. All PGCs ectopic to the gonads were counted. Where no PGCs at all managed to locate the gonads, numbers were scored as 20+.*

4.22e) ***PGC cell death phenotype***

The variable spread of numbers of PGCs left ectopic to the gonads in the ΔEP3 mutation indicated a heterogeneous population. However, closer analyses of these embryos revealed a second distinct phenotype. During wild-type embryogenesis, embryos start off with a complement of around 36 PGCs. By the time that they have divided into two bilateral groups and associated with the somatic gonadal precursors at around stage 12, however, there is on average only 10 to 11 PGCs per gonad, with

2 to 3 left outside – a final total of approximately 22 to 25 PGCs, and a reduction in total number by a third. Embryos were scored at stage 11, when the PGCs exit the midgut and spread out on its basal surface just prior to dividing into two bilateral groups (Fig.38). Careful scoring of PGC numbers at this stage indicated an average of 35.26 PGCs per embryo in wild-type. PGC number was scored again at stage 12 as the PGCs line up in two groups, just prior to coalescence with the gonadal tissue – again at this stage individual PGCs can be easily visualised. In contrast to an average of 10.4 PGCs per gonad in wild-type embryos at this stage, ΔEP3 embryos had an average of 15.63 PGCs per gonad with 5.47 ectopic, giving a total of 36.44 PGCs per embryo. This phenotype was scored only for those embryos in which a proportion of the PGCs escaped the gut and made it to the gonads (Fig.38).

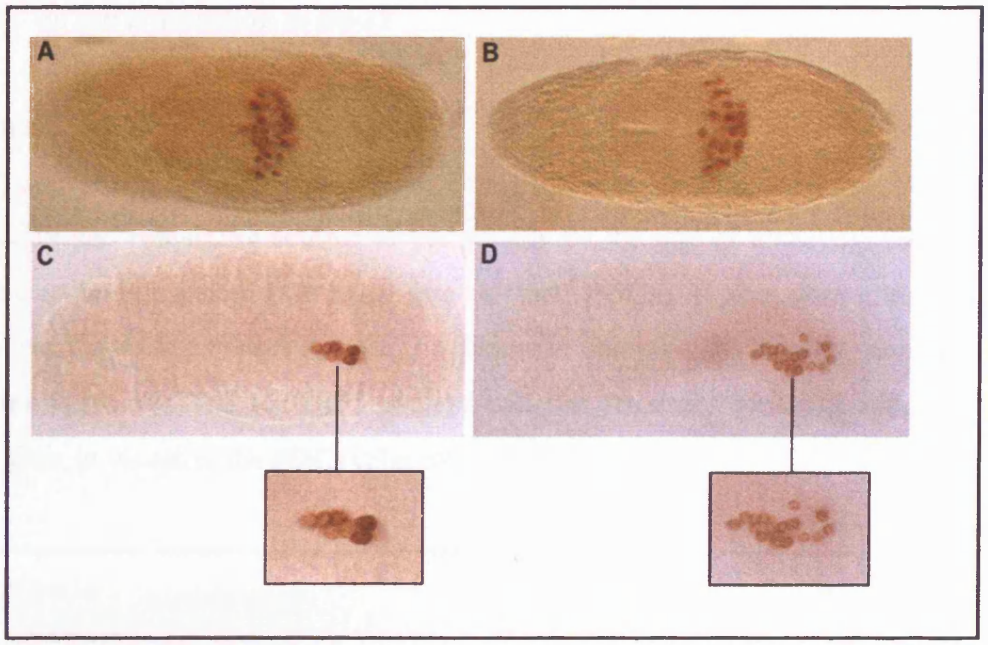

Fig.38. Cell death phenotype. *All embryos are stained with anti-Vasa.* ***A*** *and* ***B*** *are viewed dorso-ventrally,* ***C*** *and* ***D*** *are viewed laterally.* ***A)*** *Wild-type at stage 11 showing PGCs post-exit from the mid-gut, spreading out over the basal surface.* ***B)*** *ΔEP3 stage 11. There is no difference in PGC numbers as counted at this stage for wild-type and ΔEP3.* ***C)*** *Stage 12 embryo showing a wild-type gonad.* ***D)*** *ΔEP3 embryo at the same stage, showing a gonad with an increased number of associated PGCs.*

These results indicate that in those embryos that have a less severe PGC migration defect, where the vast majority of the PGCs exit the gut and correctly locate the gonads, the normal reduction in PGC number observed during wild-type embryogenesis does not occur, resulting in gonads that are over-populated by up to fifty percent. Those that do not reach the gonad continue to express Vasa, and fail to be eliminated. Furthermore, this phenotype is strikingly similar to that observed for *sctt*. In *sctt* flies, paternal rescue results in correct migration to the gonads but again the embryos retain the full complement of PGCs with no reduction in number. The difference here, however, is that in *sctt* the numbers of PGCs scored in each gonad under these conditions are wild-type, with the rest remaining ectopic but failing to be eliminated.

4.23) Is *sctt* a mutation in *tre-1*?

4.23a) *Complementation*

Both *sctt* and *tre-1* produce similar phenotypes, with PGCs failing to migrate correctly and remaining ectopic to the gonads by the end of embryogenesis whilst failing to be eliminated (the usual fate of 'lost' PGCs). If *sctt* were a mutation in *tre-1* we would not expect the ΔEP3 deletion to complement the *sctt* mutation. *sctt* virgins were crossed to ΔEP3 males, and the resultant embryos stained with anti-Vasa to visualise the PGCs (Fig. 39).

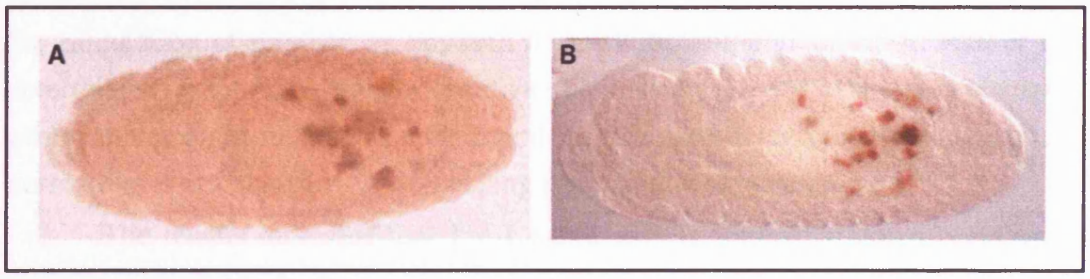

Fig.39. Complementation. *A)* sctt *embryo. B)* sctt *x ΔEP3 embryo. Both demonstrate highly perturbed PGC migration, with very few PGCs successfully locating the gonads.*

These embryos still showed perturbed PGC migration, indicating that *sctt* and *tre-1* do not complement each other.

4.23b) ***RT-PCR and real-time PCR***

If *sctt* were a mutation in *tre-1*, we would expect Tre-1 expression to be down-regulated in *sctt* mutant embryos. To test this, Clark Coffman collected embryos from *sctt* homozygous flies and the original parental stock Faf-LacZ, at specific developmental intervals: 0-3 hours, 3-6 hours, 6-9 hours and 9-12 hours. These were sent to us on dry ice. Upon arrival, RNA was extracted from each sample and subsequently converted to cDNA by reverse transcription. An aliquot of each cDNA was put through a standard polymerase chain reaction (PCR) amplification before running on an agarose gel to confirm the reaction had worked. Primers were designed to amplify the sequence between the first (Tre289Exon1) and third (Tre548Exon3) exons of *tre-1*. Control primers were also designed to amplify the house-keeping gene Actin (Actin42 and Actin361).

Quantitative real-time PCR allows more accurate quantification of RNA. To perform this, aliquots of each cDNA were added to DyNAmo SYBR® Green reagent (MJ Research) plus the relevant volume of primer mix, mixed gently and aliquoted into three wells of a 96-well plate. Samples were run with either Tre289Exon1 plus Tre548Exon3, or Actin42 plus Actin361, under parameters that had been previously optimized, in an MJ Research DNA Opticon ® 2 real-time thermal cycler. The entire run was repeated three times, using the exact same cDNA samples, before analysis by the $2^{-\Delta\Delta C}{}_T$ method (Livak and Schmittgen, 2001) (Table 8). This method relies on the calculation of relative, as opposed to absolute, amounts of RNA. Rather than determining exact copy number, relative quantification looks at the fold change in gene expression in relation to a treatment (in this case developmental staging), and normalizes it to a standard house-keeping gene, in this case Actin.

The results indicated that Tre-1 expression is somewhat down-regulated in *sctt* embryos (Table 8). Taken alongside the complementation data, it would appear that *tre-1* might be a hypomorphic allele of *sctt*. This is currently under further investigation by the Coffman lab.

	Genotype	Tre-1 C_T	Actin C_T	ΔC_T	$\Delta\Delta C_T$	$2^{-\Delta\Delta C_T}$
RUN 1	Faf 0-3	26.08	21.82	4.26		
	Sctt 0-3	27.18	25.80	1.37	-2.90	7.41
RUN 2	Faf 0-3	25.53	21.68	3.85		
	Sctt 0-3	27.42	23.65	3.76	-0.09	1.07
RUN 3	Faf 0-3	25.83	21.92	3.91		
	Sctt 0-3	28.22	23.61	4.62	0.71	0.61
RUN 1	Faf 3-6	25.57	22.40	3.18		
	Sctt 3-6	28.64	24.13	4.51	1.33	0.40
RUN 2	Faf 3-6	25.23	22.69	2.54		
	Sctt 3-6	26.65	23.45	4.19	1.66	0.32
RUN 3	Faf 3-6	24.91	22.42	2.49		
	Sctt 3-6	28.38	23.36	5.02	2.54	0.17
RUN 1	Faf 6-9	26.62	23.14	3.47		
	Sctt 6-9	27.20	22.94	4.26	0.78	0.58
RUN 2	Faf 6-9	25.66	23.07	2.60		
	Sctt 6-9	25.48	22.57	2.90	0.31	0.81
RUN 3	Faf 6-9	26.20	22.45	3.73		
	Sctt 6-9	26.50	21.91	4.59	0.87	0.55
RUN 1	Faf 9-12	25.70	23.98	1.73		
	Sctt 9-12	27.89	23.31	4.58	2.85	0.14
RUN 2	Faf 9-12	25.32	22.57	2.71		
	Sctt 9-12	26.53	21.30	5.23	2.51	0.18
RUN 3	Faf 9-12	26.06	22.31	3.74		
	Sctt 9-12	26.91	21.87	5.04	1.29	0.41

Table 8. Quantitative real-time PCR analyses of Tre-1 expression in* sctt *embryos. *The results are values from three replica runs. Values were read in an MJ Research DNA Opticon® 2 real-time thermal cycler, using SYBR Green® reagent (MJ Research) and are represented by the C_T value. C_T is the 'threshold cycle', the PCR cycle number at which the measured fluorescence for each sample exceeds the*

background. The first value of 7.41 in RUN 1 appears to be a PCR anomaly and should be discounted.

4.24) Tre-1 and Wunen

It appears from the phenotypic analyses that Tre-1 may regulate PGC survival. Over-expression of Wunen in the mesoderm results in PGC death, presumably by depletion of an extracellular factor required for PGC survival. Could Tre-1 be the receptor for the signal that Wunen mediates? If it were, one would expect over-expression of Wunen in a ΔEP3 background to have no affect on PGC number. In order to investigate this, it was first necessary to cross the twist-GAL4 mesodermal driver, and those flies carrying WunGFP, into the ΔEP3 background. The original mis-expression study utilised a twist-GAL4 inserted on the X chromosome. Since ΔEP3 is also on the X chromosome, this driver was unsuitable, and 24B-GAL4 (Brand and Perrimon, 1993) was employed instead. This stock carries a mesodermal driver on the III chromosome. Males of ΔEP3;24B-GAL4 (1:3) were crossed to virgins of ΔEP3, WunGFP (2) and ΔEP3;WunGFP (1:3). Embryos were stained with both anti-Vasa and anti-GFP antibodies, and the numbers of PGCs left by stage 13 were counted in those embryos where PGCs had clearly exited the mid-gut at stage 10.

Initial results appeared encouraging, with populated gonads clearly visible in the ΔEP3;WunGFP sample, and no significant reduction in PGC number. However, analyses of the WunGFP sample revealed that unlike the original twist-GAL4 driver, PGC loss was not nearly as significant, and the GFP staining appeared weaker. Again, gonads were visible in some of the embryos (Fig.40). This raised doubts as to the efficacy of this driver for these purposes, and the experiment was repeated with two alternatives, twist-GAL4 on the II chromosome (a kind gift from Marcel van den Heuvel) and a twist-GAL4 linked to a GFP balancer on the III chromosome (Halfon et al., 2002).

Ectopic expression in the mesoderm using either of these two drivers resulted in large numbers of 'dead' or severely degenerated embryos, making analysis of the phenotype difficult. This was not due to the fixing process, since alternative genotypes fixed and stained at the same time were normal. Observation of the

surviving embryos indicated that both drivers effectively reduced PGC number in the WunGFP embryos to virtually zero. In the ΔEP3;WunGFP embryos, many PGCs remained. Closer examination, however, indicated that it was only those PGCs that failed to exit the gut at stage 10, and so remained inside throughout embryogenesis, that survived (Fig.40). Expressing WunGFP in the mesoderm in a *huckebein* (*hkb*) mutant background also failed to result in PGC death (Fig. 40). In *hkb* embryos, PGCs enter the gut, but due to a failure in gut development, remain trapped inside (Jaglarz and Howard, 1994; Weigel et al., 1990). This would indicate that the PGCs that remain in the ΔEP3;WunGFP embryos survive because they are protected from the Wunen signal by remaining inside the gut.

These results may indicate that Tre-1 is not the receptor for the Wunen-mediated signal, however, due to the nature of the drivers used, the subsequent quality of the embryos, and the variability of the ΔEP3 phenotype, this possibility cannot be conclusively ruled out.

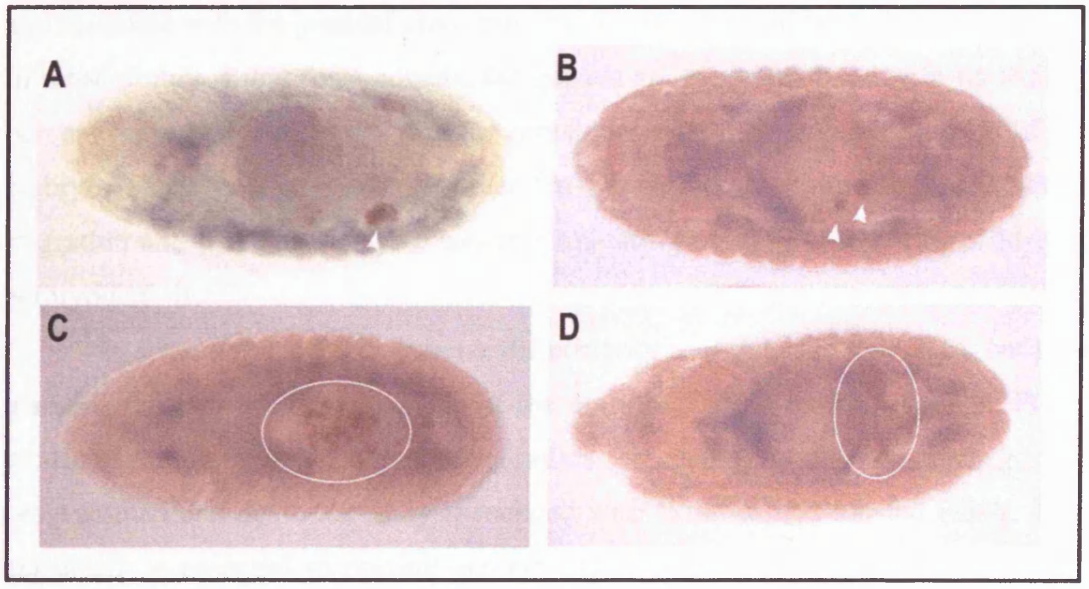

Fig.40. Ectopic expression of WunGFP in the ΔEP3 background. *All embryos are viewed dorso-ventrally with their posterior poles to the right. PGCs are stained with anti-Vasa and are visualised in brown. GFP expression is visualised in blue.* ***A)*** *ΔEP3;WunGFP x ΔEP3;24B-GAL4. Many embryos formed gonads, as indicated by the white arrow-head.* ***B)*** *WunGFP x either of the alternative twist-GAL4 drivers (the same result is observed for both). Only a couple of PGCs remain (white*

arrow-heads). Overall, most embryos within a sample were severely degenerated. C) ΔEP3;WunGFP x either alternative twist-GAL4 driver. PGCs survive, but remain trapped inside the gut, as circled. Few if any PGCs are observed outside, or having reached the somatic gonadal precursors. D) WunGFP in an hkb *background. PGCs are unaffected by overexpression of WunGFP, but also remain trapped inside the gut.*

4.3) Summary

The work presented here identifies a novel GPCR member of the rhodopsin superfamily localised to the pole plasm and expressed in PGCs at stages 7 to 8, and 13 to 16. Deletions in this gene result in perturbed PGC migration, with the ΔEP3 deletion presenting a variable phenotype. In a proportion of embryos, no PGCs contact the gonadal precursors and no gonads form, whereas in others, many reach and associate with the gonadal precursors, with a variable number remaining ectopic. In those embryos that form gonads, the gonads are over-populated with up to fifty percent more PGCs per side, with the remainder spread through the interior of the embryo. This would suggest, then, that Tre-1 function is required for correct PGC migration and that Tre-1 plays a role in eliminating excess PGCs during wild-type embryogenesis.

In *sctt* embryos, PGCs traverse the posterior mid-gut as in wild-type, but then disperse through the posterior half of the embryo, failing to form gonads. PGCs continue to express PGC markers, indicating that they fail to undergo the programmed cell death normally associated with 'lost' or mis-located PGCs. This cell-death is essential to prevent ectopic PGCs potentially forming teratomas or metastases. Full characterisation of this process has yet to be completed, however, therefore it cannot be stated categorically that ectopic PGCs are eliminated through programmed cell death, or 'apoptosis'. Interestingly, zygotic rescue of *sctt* results in normal numbers of PGCs migrating to the gonads, but again, failure of ectopic PGCs to be eliminated. This indicates that the zygotic and maternal components of *sctt* can be uncoupled – the recessive maternal component is required for correct PGC migration, whereas the zygotic component is required for cell death.

In contrast to *sctt*, the phenotype observed for ΔEP3 embryos as described above, is highly variable. ΔEP3 is not a simple deletion of *tre-1* since it removes the promoter region but leaves the coding sequence intact. Preliminary quantitative real-time PCR analysis of the ΔEP3 embryos from over-night lays indicates that Tre-1 expression is severely reduced but not completely absent in these embryos (data not shown). This may indicate that ΔEP3 is a regulatory allele, and this may account for the variability in phenotypes observed. Further work is required to fully characterise the genetic and molecular properties of this deletion.

Considering their relative map positions and the similarities in phenotype, the question remains, is *tre-1 sctt*? Analyses presented here, although somewhat inconclusive, appear to indicate that *tre-1* may be a hypomorphic allele of *sctt*. More recent research may yet substantiate this, as it is now believed that *sctt* may be a splice variant and may undergo alternative splicing. This is currently under further investigation (Clark Coffman, personal communication).

Originally called *tre-1* because of its supposed role as a trehalose receptor, *tre-1* has recently been renamed '*trapped in endoderm-1*', due to findings with the ΔEP5 deletion by the Lehmann lab. They extracted this deletion over an X chromosome FM7 balancer and observed a fully penetrant phenotype, in which PGCs were unable to cross the posterior mid-gut epithelium at stage 10, and instead remained trapped inside the gut, as seen in the most severe cases reported for ΔEP3 (Fig.36B) (Kunwar et al., 2003). They reported that Tre-1 is inherited maternally, and that ΔEP5 removes both the maternal and early zygotic components. They observed that embryos lacking just the zygotic component were effectively wild-type, concluding that it is only maternal Tre-1 that is required for correct PGC migration. They further reported that paternal rescue resulted in an increased number of PGCs traversing the gut and successfully making it to the gonads. This is similar to observations for *sctt*, in which paternal rescue resulted in a wild-type number of PGCs locating the gonad, although those left outside failed to be eliminated, demonstrating a failure in programmed cell death. Isogenisation of Kunio Isono's ΔEP3 stock by extraction of individual chromosomes over an FM7 balancer, gave similar results to the Lehmann lab's isogenised ΔEP5, with almost all embryos demonstrating a 'trapped in gut' phenotype, as opposed to the variability observed with the original stock. Unfortunately, the nature of this phenotype makes it very

difficult to accurately count numbers of PGCs, since many are tightly clustered or stacked 'on top' of each other. However, it was reported that PGC numbers appear wild-type in the ΔEP5 deletion, something that is contrary to observations on the original ΔEP3 (Kunwar et al., 2003). This may indicate that as with *sctt*, *tre-1* regulates both PGC migration and survival, by means of a complex genetic interaction that is lost upon isolation and purification of the deletion.

The Lehmann lab also investigated the relationship of *tre-1* to *sctt*. Having sequenced the area and found no significant changes, they too concluded that *tre-1* is a hypomorphic allele of *sctt*.

The question remains as to whether or not *tre-1* encodes a receptor for the Wunen-mediated guidance and survival signal. It appears that PGCs inside the gut are protected from Wunen activity, regardless of genetic background, but data as to what befalls those PGCs that successfully cross the midgut in ΔEP3 embryos, during ectopic expression of WunGFP in the mesoderm, is inconclusive. It must also be remembered that ectopic expression of WunGFP results in unnaturally high levels of this protein in tissues where it is not normally found. This may over-ride wild-type mechanisms, resulting in loss of PGCs through alternative pathways that would not normally be employed. Whether a genetic interaction exists between *wunen* and *tre-1* is an interesting and important question, and will continue to be investigated in greater detail.

Tre-1 demonstrates a variable and dynamic expression pattern. Among other tissues, it is found in the ventral nerve cord, ventral midline and central nervous system of *Drosophila* embryos, and was pulled out in a gain-of-function screen for genes involved in neural development (Norga et al., 2003). Further provisional analyses of the ΔEP3 mutants indicate that there are deficiencies in hemocyte formation (Nathalie Franc, personal communication), and it is interesting to note that Tre-1 expression is also reported in the embryonic and larval circulatory system (Tomancak et al., 2002). Although implicated in the regulation of PGC migration and survival, it seems likely, that in the future, Tre-1 will prove to function in a number of alternative and significant roles during development.

5) DISCUSSION

5.1) Summary

Primordial germ cells (PGCs) are the embryonic stem cell precursors of the adult gametes, and as such, carry the genetic information from generation to generation. They are capable of generating not only an entirely new individual, but also the future germline of that individual. In many organisms, including *Drosophila*, the PGCs are set aside as a distinct sub-set of cells early on in embryogenesis, in a location both temporally and spatially removed from their target tissue, the somatic gonad. During their migration to the developing somatic gonad, the PGCs display motile, proliferative and invasive behaviours, and come under the influence of a variety of guidance, survival and cell death signals. In studying PGC migration and survival in *Drosophila*, therefore, we hope to gain insights into the processes that regulate and control both cell migration and stem cell survival in general.

The work presented here reports novel findings for the lipid phosphate phosphatases (LPPs) Wunen and Wunen-2, both of which are involved in the regulation of PGC migration and survival in *Drosophila*. This work demonstrates that *Drosophila* Wunen displays a far narrower substrate range *in vitro* than previously reported for the mammalian LPPs, and that *in vivo*, human LPP-3 can recognise and regulate the same endogenous PGC-specific factor as Wunen, whilst mouse LPP-1 cannot. Importantly, these findings establish that the effect of Wunen on PGC migration and survival is due to the phosphatase activity of the protein, and not to an alternative function as yet determined. Furthermore, this work proves that, as previously believed but not shown, the LPPs are capable of forming oligomeric complexes, that these interactions are dependent on the C-terminus and an intact catalytic site, but that oligomerisation is not required for activity either *in vitro*, or *in vivo* within the assays presented here. Finally, this work identifies a novel GPCR expressed on the surface of PGCs that also regulates both PGC migration and survival. One of the key questions within this field, is what is the PGC survival factor that the LPPs regulate? It is hoped that this research will help to identify this elusive substrate.

5.2) Models for Wunen/Wunen-2 function

Two main models have been suggested for Wunen and Wunen-2 function in *Drosophila*. The first is that Wunen and Wunen-2 act redundantly in the posterior mid-gut to degrade an attractive guidance signal that acts as a PGC survival factor. The second is that their activities result in the production of a repellent factor, that at high levels of exposure kills PGCs. Recent data, simultaneously published by two independent groups, adds significantly to our current understanding of these two proteins. Combined with the discovery of Tre-1 as a potential receptor within this system, these data lead us to consider alternative and more complex models for LPP function within *Drosophila*.

The recently published results demonstrated that Wunen-2 is in fact inherited maternally, is expressed ubiquitously in early cleavage embryos, and is consequently localised to the PGCs themselves. The first zygotic expression of Wunen-2 was observed in a posterior stripe beginning at stage 5 (Hanyu-Nakamura et al., 2004; Renault et al., 2004). Loss of maternal Wunen-2 resulted in a dramatic reduction in PGC number, a phenotype similar to that observed for ectopic expression of Wunen, Wunen-2 or hLPP-3 in the mesoderm. This PGC loss could be rescued by driving expression of any one of these proteins using a PGC-specific driver. Whilst PGCs formed normally, entered the posterior mid-gut and traversed to the other side in mutant embryos, by stage 11, when they began to associate with the mesoderm, they demonstrated a dramatic reduction in number, and 80% of the resultant germline Wunen-2 null females were agametic. If zygotic Wunen and Wunen-2 expression was removed alongside germline Wunen-2 expression, this PGC loss was rescued. Conversely, simultaneous over-expression of both Wunen and Wunen-2 in the mesoderm and Wunen-2 in the PGCs partially rescued this loss, although PGCs still mis-migrated to the gonads (Hanyu-Nakamura et al., 2004; Renault et al., 2004). It was clearly demonstrated that the distributions of various pole plasm components such as *nanos*, *germ cell-less* and Nanos were wild-type, that transcriptional repression was not altered, and that the control of zygotic gene expression was normal within the Wunen-2 null PGCs (Hanyu-Nakamura et al., 2004). Furthermore, both groups demonstrated that this requirement for Wunen-2 in the PGCs was dependent on the phosphatase activity of the protein. Significantly, it was shown through the use of a photoactivatable lineage tracer (caged flourescein), combined

with an anti-Vasa antibody that PGC loss in these embryos occurred in a caspase 3-independent manner. This is contrary to observations for 'lost' PGCs in wild-type embryos, that were seen to die in a caspase-3-dependent manner (Hanyu-Nakamura et al., 2004). This suggests that although conventional apoptotic pathways are employed in the normal elimination of 'lost' or ectopic PGCs, the loss of PGCs that lack maternal Wunen-2 expression occurs by an alternative, as yet undiscovered, mechanism.

Both groups propose the same model: germline Wunen-2 competes with Wunen and Wunen-2 activities in the soma, for uptake (via dephosphorylation and subsequent internalisation) of a common lipid phosphate substrate required for PGC survival. Local depletion of this substrate by somatic Wunen and Wunen-2 results in a gradient that guides the PGCs towards the gonads. If maternal Wunen-2 is absent, PGCs are incapable of competing for this substrate, cannot make the survival signal, and die, through an as yet undetermined mechanism. If somatic Wunen and Wunen-2 are absent, PGCs survive, but are unable to locate the gonad due to a failure to form a gradient of lipid phosphate. If Wunen or Wunen-2 are over-expressed in the soma, the resultant widespread depletion of the substrate makes it unavailable to the PGCs, again resulting in their death. If Wunen-2 is simultaneously over-expressed in the PGCs, however, they can now compete for the substrate, and thereby survive. This model is supported by biochemical data which indicate that membrane fractions from Hi5 cells expressing Wunen-2 are capable of dephosphorylating both PA and LPA, and that Wunen-2 promotes the rapid internalisation, and cytoplasmic localisation, of flourescein labelled PA analogs into intact cells (Renault et al., 2004). One potential caveat to this model is that PGCs survive in the absence of both maternal and zygotic Wunen and Wunen-2. This could be explained by three possibilities – firstly, other, as yet uncharacterised *Drosophila* LPPs may act redundantly in the absence of germline Wunen-2 (there are 8 known *Drosophila* LPPs in the database). Secondly, trace amounts of maternally inherited Wunen-2 remain which may be sufficient for dephosphorylation and internalisation of the substrate. Thirdly, alternative mechanisms may exist that work in parallel to promote PGC survival (Hanyu-Nakamura et al., 2004; Renault et al., 2004).

How would Tre-1 fit into this model? Results presented here indicate that a decrease in Tre-1 expression results in a loss of the reduction in PGC number observed post stage 10-11 in wild-type embryos. This would indicate that Tre-1

plays a role in the elimination of excess PGCs, reducing their number from around 36 to a final average of around 23. We know that Wunen and Wunen-2 are expressed in the posterior mid-gut at the time of PGC exit, and that loss of both proteins in the double mutant 10201/k (Starz-Gaiano et al., 2001; Zhang et al., 1997) results in PGCs exiting the midgut normally, but then failing to orient toward the mesoderm or undergo guided migration. Closer phenotypic analyses of these embryos, however, reveals that in those embryos where both somatic Wunen and Wunen-2 are absent, PGCs also fail to undergo any sort of elimination, and are found in similar final numbers as in ΔEP3, with an average of 37 PGCs by the end of embryogenesis (data not shown). These data were not reported in the original or subsequent papers on these mutants. Furthermore, analysis of PGC numbers in *hkb* embryos also reveals no reduction in PGC number, with an average of 40 PGCs trapped inside the gut (data not shown). This may indicate that in wild-type embryos, somatic Wunen and Wunen-2 function to eliminate a 'swathe' of central PGCs after they exit the mid-gut at around stages 10-11. This could occur by local dephosphorylation of the PGC-specific lipid phosphate substrate, and would serve two functions – elimination of central PGCs and the division of the remainder into two distinct bilateral groups, and formation of a gradient of the substrate, which would provide directional cues for correct migration of PGCs to the mesoderm. A reduction in Tre-1 expression gives similar results to loss of somatic Wunen and Wunen-2, with no reduction in PGC number. In this model, Wunen/Wunen-2 and Tre-1 *must* interact genetically, otherwise in the ΔEP3 mutants, PGCs would still be exposed to the reduction in signal by Wunen upon exiting the midgut, and would still undergo elimination by a Tre-1-independent Wunen/Wunen-2-mediated mechanism. This model suggests separate roles for Wunen-2 and Tre-1 in PGCs – whilst Wunen-2 acts to dephosphorylate the lipid phosphate, internalise the lipid moiety and protect PGCs from cell death, Tre-1 acts to detect the localised reduction in this same signal and so eliminate the central 'superfluous' PGCs.

In this model, loss of zygotic Wunen/Wunen-2, as in the 10201/k stock (maternal supply of Wunen-2 in the PGCs is provided by the balancer chromosome) would result in an abundance of lipid phosphate substrate and a failure to form a gradient. Tre-1 would not be activated, whilst Wunen-2 would continue to dephosphorylate the substrate leading to its internalisation and subsequent PGC

survival. Thus we would expect loss of directional migration, and the preservation of the full complement of PGCs - both conditions are observed in these embryos. Loss of Wunen-2 in the PGCs would result in an inability to dephosphorylate and internalise the lipid phosphate substrate, resulting in PGC death, as seen. Over-expression of the somatic Wunens would result in global depletion of the substrate. Tre-1 would be activated in a greater proportion of PGCs, initiating cell death. At the same time, less substrate would be available to Wunen-2, and failure to internalise the dephosphorylated lipid would again result in PGC death, through a Tre-1-independent mechanism. Concurrent over-expression of germline Wunen-2 would enable PGCs to compete for, and internalise, more of the substrate before its depletion, increasing PGC survival, whereas loss of Tre-1 would simply mean that PGCs would not detect the localised depletion in signal and would survive, leading to increased final numbers of PGCs, as observed in ΔEP3 embryos.The incorporation of Tre-1 into this model may explain the discrepancies observed between PGC death in germline Wunen-2 null embryos, and elimination of ectopic PGCs in wild-type embryos (Hanyu-Nakamura et al., 2004). Authors observed that caspase 3-mediated cell death occurred in ectopic PGCs in wild-type embryos, but that this did not account for the dramatic loss of PGCs in Wunen-2 null embryos. In the model proposed here, PGC elimination in wild-type embryos would occur through a Tre-1-mediated mechanism, potentially leading to activation of classic apoptotic pathways. Germline Wunen-2 would act to promote PGC survival through uptake and internalisation of the lipid phosphate substrate. Loss of germline Wunen-2 would mean that PGCs could no longer internalise this substrate, and so would die through a *Tre-1-independent* pathway not seen in wild-type embryos.

In this model one would expect that those PGCs trapped in the gut in *hkb* embryos, which are not exposed to this survival factor, to also die. This does not appear to be the case. It may simply be that the survival signal is present within the interior of the gut lumen and is only depleted on the exterior, or it may be that PGCs only require this signal post-exit, when they enter a different environment, become more motile and require directional cues. It is interesting to note that PGC numbers in *hkb* embryos are slightly greater than in ΔEP3 embryos – ΔEP3, however, is not a total depletion in Tre-1 and there may be a very low level of expression sufficient to result in loss of a few PGCs. It should also be noted that isogenisation of the ΔEP3

stock results in a failure of PGCs to exit the mid-gut, suggesting a further role of Tre-1 in transepithelial migration.

It is also possible that germline Wunen-2 acts at the cell-surface as a novel type of transmembrane receptor. Rather than dephosphorylating and internalising a substrate that is then used to promote PGC survival, dephosphorylation of the lipid phosphate substrate would result in a conformational change in Wunen-2. This change would then signal to the PGCs directly, or would result in the recruitment of an associating protein to promote PGC survival. This model is consistent with a local pool of substrate that somatic Wunen/Wunen-2 and germline Wunen-2 compete for.

Are there further models that fit with the current data and incorporate the information on Tre-1, but which have not yet been fully proposed or explored within the literature?

It is possible that somatic Wunen/Wunen-2 activity produces a species that kills PGCs upon exposure, rather than depleting a factor required for their survival. This species would be produced locally in the specific region of somatic Wunen/Wunen-2 expression resulting in a repellent gradient, and PGCs would be exposed to it immediately post-exit from the gut. Central PGCs, exiting within the region of highest Wunen/Wunen-2 expression, would receive critical levels of this signal via Tre-1, and be eliminated, whilst those remaining on either side, now in two groups and in regions of lower or negligible expression, would survive and move away from this area towards the mesoderm. It may be that once in the mesoderm PGCs are protected, and alternative guidance mechanisms take over. Prior to entry into the mesoderm, however, PGCs may be protected from further exposure to this cell 'death' signal, by the action of germline Wunen-2. It would follow in this model that the role of germline Wunen-2 would be to recognise this 'death' signal, and further dephosphorylate it to an inactive form. Rather than dephosphorylating and internalising a signal used to promote cell survival then, Wunen-2 would instead protect PGCs from cell death, by modifying and attenuating the presence of a repellent, lethal, receptor-active signal. The loss of somatic Wunen/Wunen-2 would result in a loss in the production of this death signal, resulting in a full complement of PGCs at the end of embryogenesis, as seen in 10201/k. Loss of Tre-1 would result in a failure of the central PGCs to receive this signal in the area of highest somatic Wunen/Wunen-2 expression, resulting in excessive numbers. PGCs trapped in the gut would also fail to receive this signal, and would not be eliminated. Loss of

germline Wunen-2 would mean that the signal would no longer be modified/inactivated in the peripheral PGCs, and PGC death would increase. Loss of somatic Wunen and Wunen-2, together with the loss of germline Wunen-2, however, would mean that the signal would no longer be produced, negating the need for a protective role of germline Wunen-2, and PGCs would survive. Over-expression of Wunen/Wunen-2 in the soma would produce more of the death signal, over-whelming the PGC-specific Wunen-2, whilst concomitant over-expression of Wunen-2 in the PGCs would somewhat compensate for this, and increase the conversion to the inactive/secondary form, leading to a partial rescue (Tre-1 would still eliminate central PGCs, further decreasing the observed rescue affect).

This model suggests that Tre-1 and Wunen-2 act simultaneously within the PGCs, but at different thresholds of signal – in the regions of highest somatic Wunen/Wunen-2 expression, Tre-1 activation would eclipse Wunen-2 dephosphorylation of the lipid phosphate, resulting in PGC elimination. At the outer limits of the gradient, where Wunen/Wunen-2 activities would be weaker or even absent, Wunen-2 would over-ride Tre-1 activation, or Tre-1 expression would be down-regulated (Fig.41).

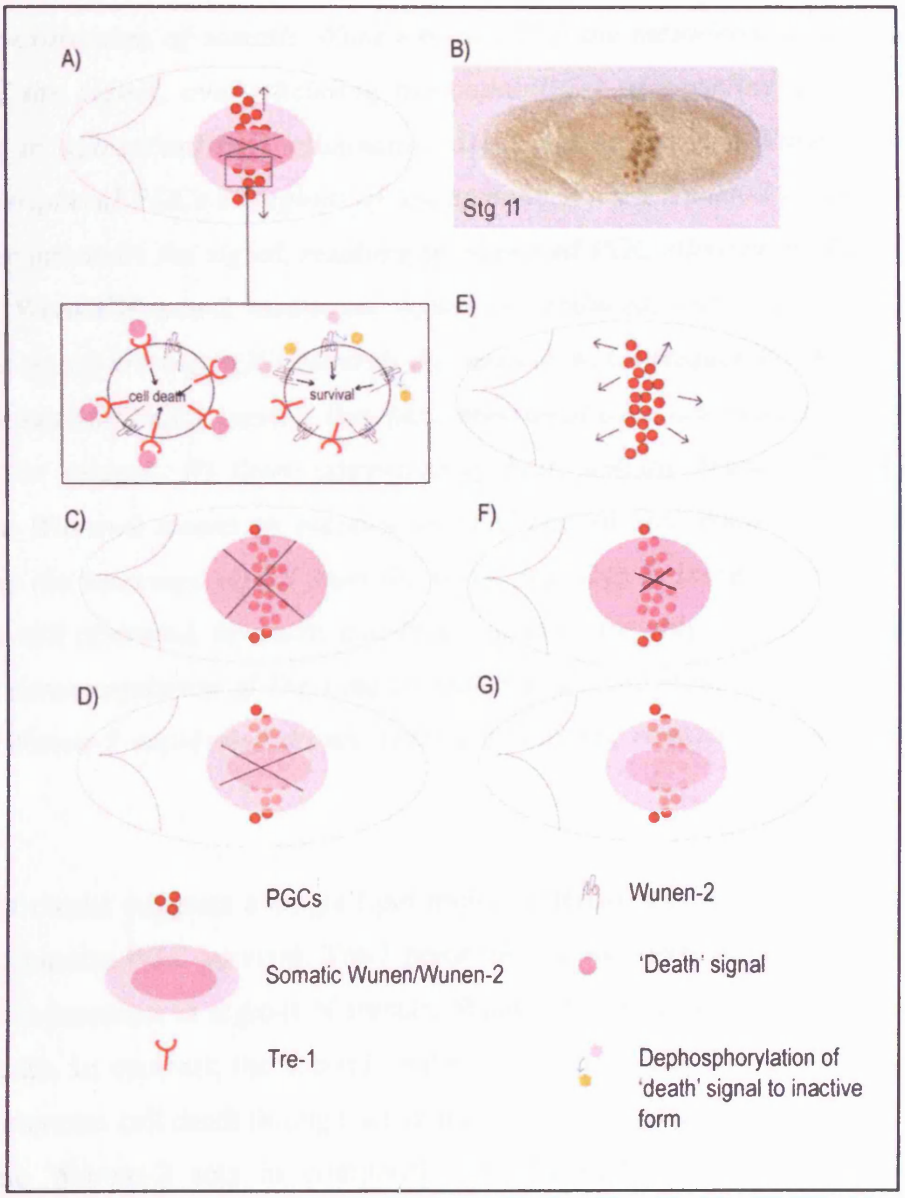

Fig.41. Proposed model for Wunen/Wunen-2/Tre-1 function.

A) *Proposed action of the somatic Wunens, germline Wunen-2 and Tre-1 in a wild-type embryo. Embryos are represented dorso-ventrally at stage 11 as the PGCs exit the posterior midgut and spread out on its surface, and can be compared to a wild-type embryo stained for anti-Vasa at stage 11 in* ***B****. The central dark pink region shows the highest level of somatic Wunen/Wunen-2 expression, and PGCs within this region are eliminated, as demonstrated by the black cross. Central PGCs receive the 'death' signal via the Tre-1 receptor expressed on their surface. Peripheral PGCs in regions of lower expression, as indicated by the pale pink area, attenuate the signal through action of germline-specific Wunen-2 at the cell surface.*

C) Over-expression of somatic Wunen/Wunen-2 in the mesoderm results in high levels of the signal, over-whelming the capabilities of germline Wunen-2 and resulting in widespread PGC elimination. D) A loss of germline Wunen-2 activity means peripheral PGCs in regions of low somatic Wunen/Wunen-2 expression can no longer attenuate the signal, resulting in increased PGC elimination. E) A loss of somatic Wunen/Wunen-2 means no signal is produced, but neither is there a repellent signal driving PGCs towards the mesoderm. Consequently whilst Tre-1 is not activated and PGCs survive, they lack directional cues, and scatter widely upon exiting the midgut. F) Over-expression of both somatic Wunen/Wunen-2 and germline Wunen-2 means an increase in PGC cell-surface Wunen-2 available to attenuate the increased signal from the soma, resulting in increased cell survival. Tre-1 is still activated, however, and PGC numbers are only partially rescued. G) Loss or down-regulation of Tre-1 means that PGCs in the highest region of somatic Wunen/Wunen-2 expression do not receive the signal, resulting in survival of all PGCs.

The first model suggests a single lipid moiety internalised by germline Wunen-2, which promotes PGC survival. Tre-1 perceives the localised reduction in the lipid phosphate precursor in regions of somatic Wunen/Wunen-2 expression, and initiates PGC death. In contrast, the second model proposes a lipid species that at critical levels promotes cell death through activation of PGC-specific Tre-1. In this scenario, germline Wunen-2 acts in competition at the cell-surface, to attenuate the receptor-active signal, reducing its availability to Tre-1. The dephosphorylation or attenuation of receptor-active substrates is an already recognised function of the plasma membrane-bound mammalian LPPs (Le Stunff et al., 2002; Brindley, 2004). This model, however, suggests that PGC death occurs through a single pathway, activation of Tre-1, and this does not explain the observation that PGCs in the Wunen-2 null embryos died in a manner independent of that seen for ectopic PGCs in wild-type embryos (Hanyu-Nakamura et al., 2004).

It remains a possibility that Tre-1 and the Wunens are not epistatic. It may also be that due to the nature of both Tre-1 activation and the ΔEP3 deletion, epistasis between Tre-1 and Wunen/Wunen-2 will be impossible to prove conclusively. Ectopic expression of Wunen and Wunen-2 in the mesoderm results in

extremely high levels of protein, which might activate alternative pathways independent of Tre-1 receptor activation. Moreover, it appears that ΔEP3 is not a total deletion in Tre-1. It may be that residual low level Tre-1 expression is insufficient to initiate PGC loss when Wunen/Wunen-2 expression is wild-type in the ΔEP3 background. Over-expression of Wunen/Wunen-2, however, results in far more signal, which may be sufficient for Tre-1 activation. That ΔEP3 is not a Tre-1 null is a significant point, since the phenotypic consequences of Tre-1 loss-of-function are currently unknown. Isogenisation of either deletion (ΔEP3 or ΔEP5) results in late stage embryonic lethality, but these too are not true loss-of-function. Determination of this phenotype is an important step that may give more insight into the role of Tre-1 during *Drosophila* embryogenesis.

5.3) LPA and S1P as potential substrates for the *Drosophila* LPPs

It has previously been shown that mammalian LPPs are capable of dephosphorylating a number of phospholipid substrates, specifically LPA, PA, S1P, C1P, and DGPP, in an apparently non-specific manner (Dillon et al., 1997; Jasinska et al., 1999; Kai et al., 1997; Roberts et al., 1998; Waggoner et al., 1996). The work presented here demonstrates that *Drosophila* Wunen can dephosphorylate LPA *in vitro*, but has little activity on PA or C1P. Its activity on S1P remains unconfirmed. Exogenous application of S1P has been shown to promote mammalian oocyte survival in culture, whereas *in vivo* application of S1P prevented oocyte loss due to irradiation (Morita et al., 2000). Furthermore, over-expression of LPP-1 results in severely disrupted spermatogenesis and atrophic testes in mice, although females appear grossly unaffected (Yue et al., 2004). Both LPA and S1P exert their affects through a number of cell-surface GPCRs ($Edgs_{1-8}$), which can associate with different G proteins, dependent on the cell type involved. The receptors have been shown to influence a wide range of down-stream effectors including Ras, Rac, RhoA, phospholipase C and adenylate cyclase. The resultant range of receptor/effector/G protein combinations means that S1P and LPA can influence a huge variety of cellular responses including migration, proliferation, cell survival or apoptosis (for a comprehensive review, see (Saba, 2004)). It would seem possible that either S1P or LPA could be the cell survival/migration/apoptotic factor that Wunen and Wunen-2 recognise. How would this theory fit with the current models?

LPPs act to dephosphorylate LPA to biologically inactive monoacylglycerol (MAG). According to the first model, LPA would exist as a local pool of attractant, promoting cell survival through dephosphorylation and subsequent internalisation by germline Wunen-2. Somatic Wunen/Wunen-2 activity would deplete this reservoir. Both somatic and germline Wunen/Wunen-2 activity, however, would result in the production and internalisation of biologically inactive MAG, perhaps ruling LPA out. LPA would not fit comfortably as a substrate in the second model, which proposes that Wunen/Wunen-2 activity results in a repellent factor that induces cell death at high concentrations. Although LPA could be this factor, Wunen/Wunen-2 activity would most likely convert it to an *inactive* form.

The action of LPPs on S1P results in its dephosphorylation to sphingosine. Although both S1P and sphingosine are able to induce a range of cell responses, in general S1P promotes cell survival, whereas sphingosine promotes apoptosis (for comprehensive reviews see (Pyne, 2002; Pyne and Pyne, 2000)). Sphingosine can be rapidly internalised by a range of cell-types and metabolised intracellularly to produce a variety of sphingolipids, including S1P (Pushkareva et al.,). In the first model, S1P would act as an attractive survival factor. Dephosphorylation by either somatic or germline Wunen/Wunen-2 would result in sphingosine, which would be internalised and used to promote PGC survival, perhaps by intracellular phosphorylation back to S1P. Tre-1 would act to detect the extracellular depletion in S1P, and initiate PGC death. In the second model, however, although dephosphorylation of S1P would result in apoptotic levels of sphingosine in regions of somatic Wunen/Wunen-2 expression, germline Wunen-2 would be unable to attenuate sphingosine by further dephosphorylation. As an alternative Wunen-2 could promote the dephosphorylation and uptake of sphingosine, and intracellular conversion to a cell-survival factor. This model suggests two distinct pathways regulating PGC survival through one substrate. In regions of somatic Wunen/Wunen-2 expression, critical levels of sphingosine would activate Tre-1 and initiate PGC death. PGCs would move up the gradient of S1P towards the mesoderm. Wunen-2 would then dephosphorylate S1P to sphingosine within a microenvironment at the cell-surface, maintaining Tre-1 in an inactive state. Sphingosine internalised through Wunen-2 would then be used to promote cell survival.

Until the lipid phosphate in question is identified, the mechanism of LPP action within *Drosophila* will remain uncertain.

5.4) Vertebrate systems

Are any of these models paralleled in vertebrate systems, or can knowledge of PGC migration in vertebrates give us insights into possible substrates for the LPPs? The route of PGC migration in mice mimics that of *Drosophila*, and a number of proteins have been identified that regulate individual steps along the way. PGC determination in mice differs from that in flies in that mice do not possess germ plasm, and instead PGCs arise during gastrulation through cell-cell signalling events. As in many other organisms including *Drosophila*, mouse PGCs first appear in a location remote from their target tissue the developing gonad, and actively migrate through the embryonic tissues. The PGCs arise in the embryonic ectoderm (epiblast) and move through the posterior primitive streak during gastrulation. From here they move into the definitive endoderm and are incorporated into the developing hind-gut. As with entry of PGCs into the posterior midgut in *Drosophila*, it is unclear whether this is an active or passive incorporation. As the hindgut extends to form a tube, the PGCs remain inside, before beginning an active migration around the cells of the hindgut epithelium, to emerge from the dorsal side, where they divide into two streams and begin their migration towards the two genital ridges. PGCs that are retarded fragment and die (McLaren, 2003; Molyneaux and Wylie, 2004; Molyneaux et al., 2001; Wylie, 1999).

Whilst a variety of growth factors have been shown to influence mouse PGC survival and migration *in vitro*, *in vivo* two main signalling systems that guide the PGCs to the genital ridge have been characterised. The first involves the receptor tyrosine kinase c-kit, encoded by *W*, and its ligand Steel Factor, encoded by *Steel*. Steel Factor is expressed as a membrane-bound growth factor that can undergo proteolysis to a soluble form, and is found along the migratory route of the PGCs as well as in the urogenital ridges. The receptor, c-kit, is expressed on the surface of migrating PGCs. Mutations in either the receptor or its ligand result in a severe decrease in PGC number, and a failure to migrate through the hind-gut wall; whilst the majority of PGCs remain as clumps inside the hind-gut, those that do exit migrate into ectopic locations and die. In these mutants, PGCs are determined normally and begin to increase in number, before proliferation ceases (McLaren, 2003; Molyneaux

and Wylie, 2004). This regulation of migration and proliferation bears similarities to the co-activation of the STAT92E/Ras signalling pathway activated by the receptor tyrosine kinase Torso in *Drosophila*, whereby inactivation of this signalling system results in a failure in PGC proliferation and guided migration (Li et al., 2003).

The second system in mice involves the chemokine SDF-1 (stromal-derived factor 1) and its receptor CXCR4. SDF-1, the only known ligand for CXCR4, is known to act as a guidance cue for a range of cell types, including PGCs. SDF-1 is expressed throughout the dorsal body wall, and is especially enriched in the genital ridges. Addition of soluble SDF-1 to cultured embryo slices disrupts PGC migration by decreasing their motility, whereas the addition of SDF-1 coated beads is sufficient to attract PGCs over short distances (Molyneaux et al., 2003). In SDF-1 null mice, PGCs are retarded and reduced numbers reach the genital ridges. Once associated with the genital ridges, however, proliferation occurs normally (Ara et al., 2003). CXCR4 is expressed on the surface of migrating PGCs. In embryos deficient in CXCR4, the number of PGCs that successfully colonize the genital ridge is greatly reduced. Once in the gonad, however, PGCs continue to proliferate normally. Thus the SDF-1/CXCR4 interaction is required in mice for PGC survival and migration (Molyneaux et al., 2003).

Zebrafish PGC migration differs somewhat from mice, but also employs SDF-1 and CXCR4. PGCs arise as 4 distinct clusters, distributed in any one of 3 separate orientations towards the dorso-ventral axes. As gastrulation proceeds, these clusters move dorsally and align with the head and trunk mesoderm. Two of the clusters on each side move and join up with each other, and the resulting two clusters migrate posteriorly towards the somatic gonadal tissue (Molyneaux and Wylie, 2004; Santos and Lehmann, 2004a; Weidinger et al., 1999). Whilst CXCR4b is expressed in the PGCs, SDF-1a is expressed along their migratory route. The use of morpholino antisense oligonucleotides to knock-out either, results in PGCs scattering randomly and demonstrating irregular and non-directional movements. Conversely, over-expression of SDF-1a in the PGCs has the same effect, whereas ectopic expression of SDF-1a is sufficient to attract PGCs to those areas (Doitsidou et al., 2002; Knaut et al., 2003).

Recent data indicates that zebrafish PGC migration is dependent on the prenylation of proteins by geranylgeranyl transferase (GGT1), and that HMGCoAR is required to supply the necessary lipid precursors. Investigators found that

inhibition of HMGCoAR with statins results in severe PGC migration defects, rescued by the addition of mevalonate, the downstream product of HMGCoAR activity. Squalene, a downstream product in the cholesterol branch of the pathway fails to rescue, whereas injection of compounds from the isoprenoid branch of the pathway does result in rescue. Addition of GGT1 inhibitors, but not farnesyl transferase inhibitors, perturbs PGC migration, leading authors to conclude that protein prenylation by GGT1 is required for correct PGC migration in zebrafish, and that this pathway is independent of the SDF-1a/CXCR4 pathway (Thorpe et al., 2004). These results parallel findings in *Drosophila*, which also demonstrate the importance of isoprenoid synthesis in the regulation of PGC migration (Santos and Lehmann, 2004b).

Despite extensive computational analyses, no homologue for SDF-1 has been found within the *Drosophila* genome, and over-expression of zebrafish SDF-1a (a kind gift from Holgaer Knaut) did not result in any obvious defects. Thus, preliminary results indicate that the SDF-1/CXCR4 system is unlikely to regulate PGC migration or survival in *Drosophila*. Both the c-kit/Steel and HMGCoAR/isoprenoid pathways, however, do appear to be conserved in flies. Neither of these pathways, however, point towards, or appear to involve, substrates for Wunen/Wunen-2 or the LPPs in general, and so far the LPPs have not been shown to influence PGC migration or survival in vertebrates. Data on the physiological functions of the vertebrate LPPs *in vivo*, however, has been decidedly sparse until recently. As work in this area continues to gain pace, new roles for the LPPs will undoubtedly be exposed.

Indeed, recent findings on PRG-1 suggest a role for LPA as a physiological substrate. In this study, LPA was found to act as a repellent, inducing axonal collapse (Brauer et al., 2003). LPA is still a candidate for an Wunen/Wunen-2 substrate, but it is more likely to act as an attractive survival factor in this scenario, rather than a repellent.

5.5) Substrate specificity of the LPP isoforms

Most of the work to date on LPPs has concentrated on the 5 main phospholipid substrates already mentioned. Considering the potent bioactivity of these molecules, it is surprising that the LPPs should act non-specifically when presented to them *in vitro*. It may well be that substrate specificity varies dependent on which LPP

isoform is expressed in which tissue, for whichever function. Thus in tissue A, S1P may be the substrate for LPP-3, whilst in tissue B, it may act on C1P. This would certainly account for the non-specificity seen in biochemical assays, where endogenous controls are absent. It may also account for the discrepancy in results reported by different groups using slightly different assay conditions or cell types. As we have seen with the M3 tag, however, biochemical activity *in vitro* is not always a true reflection of biological activity *in vivo*. Whilst these 5 substrates are certainly very good candidates for the physiological substrates of the LPPs, investigators should perhaps be wary of restricting their studies to these 5 alone. As more and more physiological functions of the LPPs are revealed, it may be worth considering alternative substrates related to these alternative functions, as possible candidates. It is particularly noteworthy that VCIP (hLPP-3) can interact with a variety of integrins (Humtsoe et al., 2003), and that recent findings demonstrate a function of LPP-3 in mouse development that is independent of its phosphatase activity (Escalante-Alcalde et al., 2003). Conversely, it is clearly demonstrated here that the influence of LPP-3 on PGC migration and survival in *Drosophila is* dependent on its phosphatase activity.

5.6) Conclusion

In conclusion, the work presented here demonstrates novel results for the *Drosophila* LPPs Wunen and Wunen-2, and identifies a GPCR expressed on the surface of PGCs that is involved in PGC migration and survival. Whatever the substrate for the LPPs (and it seems increasingly likely that there will be more than one), it is hoped that this work will contribute to further understanding of this important and interesting family of enzymes.

6) Further Work

6.1) Alternative functions of oligomerisation

It is intriguing that the LPPs oligomerise in a highly specific manner, yet there is currently no discernable function either biochemically, or biologically, for the interactions observed. It may be that oligomerisation regulates functions in *Drosophila* that are unrelated to PGC migration and survival. VCIP (hLPP-3) appears to function in capillary morphology and cell-cell interactions via its integrin-binding RGD domain. Like Wunen and Wunen-2, mLPP-3 lacks an RGD domain but it also has a critical role in vasculogenesis and capillary formation. It would be interesting to see whether *Drosophila* Wunen can influence cell-cell interactions/aggregation *in vitro*, and whether this function is abolished in the monomeric WunD2 truncation. This could be approached relatively simply, by over-expressing each GFP-tagged construct in *Drosophila* S2 cells alongside a GFP control, seeding the cells sparsely into tissue culture dishes, and observing cell behaviour with time-lapse fluorescence imaging. If S2 cells proved inappropriate, full-length Wunen and WunD2 could be cloned into a suitable vector and expressed in HEK293 cells, as used in the original study.

6.2) Characterisation of ΔEP3

6.21) *Molecular characterisation of the deletion*

The original ΔEP3 stock displays significant phenotypic variability, whereas isogenisation over FM7 is far more penetrant. This may indicate a complicated genetic interaction that is lost upon isogenisation of the chromosome, or it may indicate another 'floating' copy of *tre-1* that is responsible for variability in protein expression. This is an important question that must be addressed. Previous work involving these stocks centred on the deletion of the neighbouring gene *Gr5a* as a potential trehalose receptor, and consequently neither the ΔEP3, nor the ΔEP5, deletions have been properly sequenced. This is a priority, and will be performed after Southern analyses have been completed for both the isogenised and non-isogenised stocks.

6.22) *Genetics*

It is reported for the ΔEP5 deletion that paternal rescue results in an increased number of PGCs crossing the midgut wall. What is not reported, however, is that embryos from ΔEP5 homozygous mothers crossed to ΔEP5 males (and the same for the isogenised ΔEP3) die during the late stages of embryogenesis, and that the stock is in fact sterile. It will be important to determine whether this late stage embryonic death is due to the deletion in *tre-1* or to a deletion/mutation elsewhere. If embryonic death is due to a deficiency in Tre-1, this should be followed up and reported, as it would indicate a vital role for Tre-1 during embryogenesis, one that is not so simply restricted to PGC migration and survival. Preliminary experiments using a hemocyte driver to overexpress Tre-1, showed extreme degeneration of the embryos, similar to that observed with the twist-GAL4 drivers and Wun-GFP. It would appear that Tre-1 is expressed in the hemocytes (BDGP gene expression data) and preliminary analyses of hemocytes in the ΔEP3 stock indicate perturbation in their development. These data are extremely provisional, but interesting, and will require detailed further study.

6.23) *Mis-expression studies*

The Lehmann lab reported that expression of Tre-1 in the PGCs themselves, using the insertion EP(X)496, results in rescue of the ΔEP5 migration defect. Since Tre-1 appears to regulate PGC migration, it would be interesting to see whether mis-expression in alternative tissues could redirect migrating PGCs. One way of doing this would be to clone Tre-1 into the pUAST vector and cross these flies to a number of different tissue-specific drivers. This work is underway, but initial results using nervous system and mesoderm-specific drivers have been disappointing. This construct, however, failed to reproduce the rescue reported for ΔEP5 when expressed in the PGCs of ΔEP3 embryos. This pUAST-Tre1 construct has been completely sequenced through its coding sequence, but it may be that the particular insertion site in question blocks effective expression. This work should be repeated using alternative insertions alongside EP(X)496 as a rescue control. Although ISH could be used to look for up-regulation of the protein in the appropriate tissues, it would be more beneficial to GFP tag the receptor, and follow its expression that way. The

caveat here, however, is that there is no way of knowing whether the GFP-tag (either N- or C-terminal) will compromise biological activity.

6.24) *Epistasis between Tre-1, Wunen and Wunen-2*

Initial studies into the possible interaction between Tre-1 and the Wunen-mediated signal were somewhat inconclusive. It is important that this relationship is fully characterised, as one goal of this research is to determine what the PGC guidance and survival signal is. If Tre-1 is the receptor for this signal, it is an important piece in the puzzle, and may provide novel methods for searching for the signal in the future. Furthermore, analyses of the ΔEP3 phenotype in the non-isogenised stock indicate a role for the receptor in the regulation of PGC survival. It is extremely important that this phenotype be carefully and accurately characterised, so that the function of Tre-1 in this process can be established. The first approach would be to repeat the mis-expression studies, using further alternative mesoderm-specific drivers. It has been reported that expression of Wunen in tissues other than the mesoderm, for example the nervous-system, also result in PGC loss (Starz-Gaiano et al., 2001). The mis-expression of WunGFP in the ΔEP3 background could be repeated using drivers specific to a range of tissues other than the mesoderm.

It is important to determine the effect of the combined loss of Wunen, Wunen-2 and Tre-1. This would involve crossing flies carrying a double deletion of Wunen and Wunen-2 into the ΔEP3 background, and then staining embryos to observe the PGC migration phenotype. This work is currently underway. Perhaps more pertinent will be to study the effect of loss of germline Wunen-2 and Tre-1. If the model proposed here that suggests that Tre-1 detects local depletion in a substrate required for PGC survival is accurate, one might expect to see PGCs exit the gut with those in the centre of the group at stage 11 surviving, whilst those on the outer flanks are eliminated. The Wunen-2 maternal deletions are now available, and work is underway to cross them into the ΔEP3 background.

6.3) Microarray analyses

Microarray analyses of both ΔEP3 stocks and the ΔEP5 stock would reveal what genes are up- or down-regulated along with the down-regulation of Tre-1. This may begin to elucidate what signalling pathways Tre-1 activates or suppresses.

6.4) Tre-1 receptor activation

It is possible that Tre-1 and Wunen/Wunen-2 are epistatic, but that Tre-1 and germline Wunen-2 respond to separate extracellular factors. Either way, Tre-1 plays an important part in PGC migration and survival, and as such, determining its ligand(s) is a primary goal for the future, which might eventually reveal the true substrate for the *Drosophila* LPPs. Desensitisation of the majority of GPCRs occurs through a common mechanism involving β-arrestins. β-arrestins bind to agonist-activated receptors, terminating signal transduction. This interaction has been employed to help identify the ligands for a number of orphan GPCRs, including several neuropeptide receptors in *Drosophila* (Barak et al., 1997; Johnson et al., 2003). This technique involves the use of GFP-tagged β-arrestin2. Initially distributed throughout the cytosol and excluded from the nucleus, β-arrestin2-GFP translocates to the plasma membrane upon receptor activation. One benefit of this technique is that the receptor remains untagged. To investigate possible agonists for Tre-1, cells would be co-transfected with both β-arrestin2-GFP and Tre-1 before the addition of a range of potential agonists. Translocation of the GFP signal would be followed by real-time GFP imaging. The β-arrestin2-GFP construct is already available and work will begin with sphingosine and S2 cells. If S2 cells prove to be too small for this purpose, then HEK293 or Cos-7 cells will be employed instead.

7) MATERIALS AND METHODS

7.1) Chapter One

2.21a) *Sequence analysis of Wunen and the mammalian LPPs*

To investigate conservation between the genes and draw up a phylogenetic tree, ClustalW was employed: http://www.ebi.ac.uk/clustalw/.

To determine the transmembrane domains, TMPRED was employed: http://www.ch.embnet.org/software/TMPRED_form.html.

Genbank accession numbers were obtained from PubMed: http://www.ncbi.nlm.nih.gov/entrez/query.fcgi.

2.21c) *Transfection of S2 cells*

Drosophila S2 cells (Invitrogen) were maintained in HyQCCM3 media (Perbio Science) plus penicillin and streptomycin at 25°C. All DNA was prepared by Cesium Chloride density gradient centrifugation and resuspended in Millipledge double distilled water, before concentrations were ascertained in a spectrophotometer. Cells were transfected using Effectene Transfection Reagent (Qiagen) according to the manufacturer's protocol. 48 hrs post transfection, cells were washed in phosphate buffered saline (PBS), spun at 3000rpm and lysed on ice in cell lysis buffer (50mM HEPES, 0.1M sodium chloride, 10mM sodium fluoride, 5mM EDTA, 0.5mM sodium orthovanadate, 0.1% triton X-100, Complete protease inhibitors (Roche)).

Western blots were performed using standard techniques, utilizing the NuPAGE® Novex Bis-Tris and XCell *SureLock*™ Mini-Cell system (Invitrogen). Blots were incubated with a mouse monoclonal anti-body to GFP (Roche) at 1:500 in PBS plus 0.1% tween (PT) plus 3% BSA, for 1 hour at room temperature, washed extensively in PT and incubated with HRP-conjugated anti-mouse (Jackson ImmunoResearch Laboratories) at 1:40,000 in PT plus 5% powdered milk, for 1 hour at room temperature. After extensive washes in PBS, blots were visualized with ECL Plus™ Western Blotting Detection Reagent (Amersham Biosciences).

2.22a) *Immunocapture of GFP-tagged proteins*

S2 cells were transfected and lysed in cell lysis buffer as before, and an equal volume of lysate added to an aliquot of Fusion Aid GFP resin (Vector laboratories). The

resin was washed several times prior to addition of the lysate in cell lysis buffer. After incubation for two hours at 4°C, the resin was washed extensively to remove extraneous unbound protein and resuspended in 5 x volume cell lysis buffer prior to Western analyses as above.

2.22b) ***Inorganic phosphate release assay***

The Molecular Probes PiPer® phosphate release assay (Cambridge Bioscience) was specifically adapted for this assay. In the presence of inorganic phosphate, maltose phosphorylase converts maltose to glucose-1-phosphate and glucose. Gluconolactone and hydrogen peroxide (H2O2) are then formed by the action of glucose oxidase. Using horseradish peroxidase as a catalyst, the H2O2 reacts with the Amplex™ Red reagent to produce the fluorescent product resorufin. The increase in detectable fluorescence/absorbance is therefore proportional to the amount of phosphate present.

Each reaction was performed in triplicate, using 50 µl of the anti-GFP resin containing the immunocaptured proteins. Assays were performed at 37°C and the resulting fluorescence read in a SPECTRAmax™ GEMINI XS Dual Scanning Microplate Spectrafluorometer in a final volume of 100µl at up to 7 time points during the assay period. Each substrate control gave a small but constant value, which was subtracted from each of the samples. LPA (Sigma) in 50% ethanol and C1P (Affiniti) in 100% ethanol were used at a final concentration of 500µM. PA (Sigma) in 100% ethanol was used at a final concentration of 70µM in the supplied buffer plus 0.01% phosphate free triton X-100 (Sigma) plus 1mg/ ml fatty acid free BSA (Sigma). In order to test the linearity of the detection system, a range of phosphate standards were simultaneously run in triplicate. Activity was examined at an arbitrary time point that appeared to fall within the linear range for the enzymes for each assay. The phosphate standards were converted to nMoles phosphate at this time, and used to produce a standard curve. This was linear in each case, indicating that the detection system displays first order kinetics in the presence of up to 4 nMole phosphate. A line of best fit was used to calculate the amount of phosphate released from each protein sample. Each sample was Western blotted and densitometry performed using Bio-Rad Quantity One software to compare relative protein amounts in each, on the same blot.

Lipid substrates were prepared as follows:

LPA – A stock solution of 5mg/ml in 50% ethanol was prepared and stored at -20°C. When required, this was warmed to room temperature before bath sonicating at 65°C for 20 minutes. 100µl was then added to 900µl of the supplied reaction buffer plus 0.01% phosphate free triton X-100 (Sigma) plus 1mg/ ml fatty acid free BSA (Sigma) and this solution bath sonicated for a further 10 minutes at 65°C. The resin was resuspended in this solution before assaying.

PA – A stock solution of 1mg/ml was prepared in 100% ethanol and stored at -20°C. When required this stock was warmed to room temperature before bath sonicating at 37°C for 10 minutes. 100µl of this was then added to 900µl of the supplied reaction buffer plus BSA plus triton as above.

C1P – A stock solution of 5mg/ml was prepared in 100% ethanol and stored at -20°C. When required, this was warmed to room temperature before bath sonicating at 65°C for 20 minutes. 100µl was then added to 900µl of the supplied reaction buffer plus BSA plus triton as above.

Densitometry was performed by scanning Western blots into a Bio-Rad GS-710 Calibrated Imaging Densitometer, and employing BioRad Quantity One software.

2.23a) ***Ectopic expression in the mesoderm***

Fly husbandry – all flies were maintained on standard agar/yeast/molasses/malt extract and fed with live baker's yeast. Flies were raised, and all experiments performed, at 25°C.

Microinjection - All constructs were prepared by Cesium Chloride density gradient centrifugation and resuspended in Millipledge double distilled water, before microinjection into White[118] embryos alongside the helper plasmid pUAST-Turbo (a kind gift from Michael Levine) in a 3:1 ratio. Transformants were recovered and mapped using standard techniques (Rubin and Spradling, 1982).

Unless otherwise stated, all other stocks were obtained from the Bloomington *Drosophila* Stock Center at Indiana University.

Expression in the mesoderm – four to ten day old adult males carrying a homozygous viable GFP-tagged insert on an autosome were crossed *en masse* to twist-Gal4 virgins carrying the mesoderm-specific twist driver on the X chromosome. The twist-GAL4 stock was obtained as a kind gift from Gerry Rubin.

Embryo collection – fly crosses were set up and allowed to mate for 24 hours at 25°C before being transferred to a laying 'cage'. Flies were allowed to lay on fresh agar plates containing 25 % apple juice, 2.25% agar and 2.5% brown sugar and seeded with live baker's yeast paste.

Embryo fixation - when ready, embryos were washed off the plates onto nylon mesh in a 12-place Millipore Filtration manifold, with distilled water plus 0.01% triton X-100. After washing 3-4 times in distilled water, embryos were dechorionated by incubation for 2 minutes in 50% bleach solution, before extensive washing with distilled water. Embryos were transferred into the interface of 2.25mls PBS plus 0.75mls 16% w/v formaldehyde (TAAB), and 3mls heptane, where they were agitated for 20 minutes at room temperature before the bottom phase was removed and 3mls of methanol added. The test-tube was shaken and de-vitellinised embryos allowed to fall to the bottom before removal into a fresh test-tube. Embryos were then dehydrated through several changes of 100% methanol until storage at -20°C.

Embryo staining – embryos were rehydrated through several changes of PT, before incubation with the primary antibody in PT plus 4% BSA over-night at 4°C. Embryos were then washed several times before incubation with the secondary antibody in PT for two hours at room temperature. For biotinylated secondary antibodies, embryos were further incubated for 30 minutes with VECTASTAIN® ABC reagents (Vector Laboratories) before further washing and visualization with a standard DAB reaction, and quenching in PT plus 0.01% sodium azide. Where alkaline-phosphatase conjugated secondary antibodies were used, the signal was visualized by incubation in NBT/BCIP solution (NBT/BCIP Ready-to-Use Tablets, Roche) before washing in PT.

A mouse monoclonal primary antibody to GFP (Roche) at 1:500, followed by alkaline phosphatase conjugated anti-mouse secondary antibody (Jackson

ImmunoResearch Laboratories) at 1:500 was used to visualize the GFP-tagged proteins in the mesoderm.

A chicken anti-Vasa primary antibody (Ken Howard) at 1:10,000, followed by biotin-conjugated anti-chicken antibody (Jackson ImmunoResearch Laboratories) at 1:500 was used to visualize the PGCs.

Mounting – Embryos were dehydrated through 100% ethanol, cleared in methyl salicylate and mounted in Canadian balsam (Polysciences Inc.). Slides were then heated at 60°C for 2 days.

Microscopy – Embryos were observed with a Zeiss Axiophot combined with an Optronics © MicroFire digital camera (Indigo Scientific). Images were recorded with Pictureframe 0.9 software (Indigo Scientific).

2.24a) ***Confocal microscopy***

Flies carrying an autosomal viable GFP-tagged insert were crossed to twist-GAL4 virgins. Embryos were fixed in 4% formaldehyde and observed under glycerol with a BioRad MRC1024 upright Confocal microscope.

2.24b) ***Cell-surface biotinylation***

S2 cells expressing the protein of interest were washed twice in PBS and counted. 25 x 10^6 cells in 1ml PBS were incubated with Pierce No-Weigh™ Premeasured NHS-PE04 Biotin (Perbio Science) according to the manufacturer's protocol for 45 minutes at room temperature. The reaction was quenched with 100 mM ammonium chloride for 10 minutes. Cells were washed twice in PBS to remove extraneous unbound biotin, lysed on ice in 1.5 ml cell lysis buffer (1% triton X-100) and spun for 5 minutes at 13000rpm, 4°C. The supernatant was applied to a Pierce Immunopure Monomeric Avidin column (Perbio Science) according to the manufacturer's instructions. Fractions were analyzed by Western blot using antibodies to the specific tag as before.

7.2) Chapter Two

3.22a) ***Confirmation of protein expression in S2 cells***

S2 cells were transfected with both GFP and M3-tagged constructs alongside the Actin-5C-GAL4 driver, lysed and analysed by Western blot according to the protocol above (**2.21c**). Two gels were run for each sample. The M3 tag was detected with a mouse monoclonal 9e10 anti-myc primary antibody (Laboratory for Molecular Cell Biology stock) at 1:500, plus HRP conjugated anti-mouse (Jackson ImmunoResearch Laboratories) at 1:500. The GFP tag was detected with a mouse monoclonal anti-body to GFP (Roche) at 1:500, followed by HRP conjugated anti-mouse (Jackson ImmunoResearch Laboratories) also at 1:500.

3.22b) ***Immunoprecipitation assays: formation of homo-oligomers***

S2 cells were transiently co-transfected with GFP and M3 tagged constructs alongside the Actin-5C-GAL4 driver, and allowed to express for 2-3 days. Cells were spun down, washed and lysed in cell lysis buffer as before, and an equal volume of lysate added to an aliquot of Anti-c-Myc Agarose Affinity Gel (Sigma). The resin was washed several times prior to addition of the lysate in cell lysis buffer plus protease inhibitors. After incubation for two hours at 4°C, the resin was washed extensively to remove extraneous unbound protein and resuspended in 10 x volume cell lysis buffer prior to Western analyses with antibodies as before.

3.22c) ***Immunoprecipitation assays: formation of hetero-oligomers***

The same protocol was followed as for **3.22b**.

3.22d) ***Immunoprecipitation assays: prevention of oligomerisation***

The same protocol was followed as for **3.22b**.

3.22e) ***Immunoprecipitation assays: repeat with NEM***

The same protocol was followed as for **3.22b**, but 2mM NEM was included in the cell lysis buffer.

3.22f) ***Immunoprecipitation assays: Wunen and Wunen-2***

The same protocol was followed as for **3.22b.**

3.22g) ***Immunoprecipitation assays: 1% triton X-100***

The same protocol was followed as for **3.22b**, but 1% triton X-100 was added to the cell lysis buffer rather than 0.1%. The resin was washed several times in this buffer prior to addition of the cell lysate.

3.22h) ***Immunoprecipitation assays: post-transfection***

S2 cells were singly transfected with each construct, allowed to express protein for 2-3 days, spun down, washed and lysed in 0.1% triton X-100 cell lysis buffer as before. 25µl of each was then combined in an eppendorf and left on ice for 30 minutes. These lysates were then immunocaptured on Anti-c-Myc Agarose Affinity Gel (Sigma) for 2 hours. This was repeated with either incubation on ice for 60 minutes, or at 25 °C. 1mM zinc chloride was added to the lysis buffer in half of the samples. Captures were then Western blotted as before.

3.23a) Para formaldehyde cross-linking

Cells expressing each tagged protein were incubated at room temperature with 3% or 12% para formaldehyde (PFA) for 30 or 60 minutes in PBS, quenched with 100 mM ammonium chloride for 10 minutes at room temperature, washed in PBS plus ammonium chloride followed by just PBS, lysed on ice in 0.1% triton X-100 cell lysis buffer and snap frozen in liquid nitrogen, before running on a gel and analysing by Western blot.

3.24a) ***Biochemical activities of the multimer and monomer***

This followed the same protocol as **2.22b**. Each reaction was performed in triplicate, using 50 µl of the anti-c-Myc resin containing the immunocaptured proteins. The LPA control gave a small but constant value, which was subtracted from each of the samples. LPA (Sigma) in 50% ethanol was used at a final concentration of 500µM in the supplied buffer plus 0.01% phosphate free triton X-100 (Sigma) plus 1mg/ ml fatty acid free BSA (Sigma). Each sample was Western blotted and densitometry performed using Bio-Rad Quantity One software to compare relative protein amounts in each, on the same blot.

3.24b) ***Biological activities of the multimer and monomer***

This followed the same protocol as **2.23a** using the same antibodies for protein and PGC visualization.

3.25a) ***Biotinylation of cell-surface proteins***

This followed the same protocol as **2.24b**. S2 cells expressing WunM3 plus the cell surface marker CD2 were biotinylated and analysed by Western blot. Blots were probed with monoclonal anti-myc (Laboratory for Molecular Cell Biology stock), anti-CD2 (Serotec) or anti-tubulin (Sigma), before addition of HRP-conjugated anti-mouse at 1:40,000.

7.3) Chapter Three

4.21b) ***Identification of*** **tre-1**

Identification of *tre-1* utilised the Genome Annotation Database of *Drosophila* (GadFly) and the Berkeley Fly BLAST services, which have subsequently been retired. Equivalent services can be found at: http://flybase.net/annot/.

4.22b) In situ ***hybridisation probe synthesis***

A standard restriction digest was set up on 500ng of RE07751 in pFLC1, with either EcoR1 or Eco01091, incubated for 4 hours and heat-killed. Four reactions were set up to synthesise a probe, a control anti-probe and two negative controls, using a standard transcription reaction and T3 or T7 polymerase. Products were precipitated by the addition of 10M lithium chloride and ethanol at -20°C for 2 hours. The probe and anti-probe were then spun for 20 minutes at 13,000rpm, and the pellets resuspended in 50µl double distilled water. An incorporation assay with alkaline phosphatase conjugated anti-DIG (Roche) antibody and NBT/BCIP confirmed that the reaction was successful.

In situ ***hybridisation protocol*** – Embryos were rehydrated through 70% then 30% ethanol before rinsing 3 times for 2 minutes each in DEPC (Diethyl pyrocarboante, Sigma) treated PBS plus 0.1% tween (PTD). Embryos were incubated for 3 minutes in PTD plus a 1:400 dilution of proteinase k (Boehringer Manneheim) before rinsing 2 x 30 seconds in 2mg/ml glycine (Sigma) in PTD to stop the digestion. Embryos

were then washed twice in PTD and fixed for 5 minutes in 4% formaldehyde in PTD. Embryos were washed a further 5 times in PTD and then once in 1:1 PTD:hybridisation buffer (hybridisation buffer - deionised formamide (Sigma) (5.0ml), 20 x SSC (Sigma) (2.5ml), tRNA (Sigma)(10mg/ml) (100µl), heparin (100mg/ml) (5µl), tween 20 (10µl), DEPC treated dH2O to 10ml. The samples were pre-hybridised in hybridisation buffer at 55 °C for several hours before addition of the probe at a dilution of 1:2000 in hybridisation buffer. These were left to hybridise overnight. In the meantime, the anti-DIG antibody (Boehringer Manneheim) was allowed to pre-absorb for as long as possible with spare embryos at a dilution of 1:400 in PTD plus a 1:1000 dilution of ribonucleoside vanadyl complex (RVC, New England Biolabs).

Post-hybridisation, the probe was washed off the embryos with hybridisation buffer for 20 minutes at 55°C before a further wash in 1:1 hybridisation buffer:PTD (plus 1:1000 RVC (PTDvc)). Embryos were then washed extensively in PTDvc before hybridisation with α-DIG 1:400 in PTDvc for one hour at room temperature. Embryos were again washed extensively in PTDvc before the signal was visualised by incubation in BCIP/NBT solution (Boehringer Mannheim). Washing the embryos in PTD plus 10mM EDTA without RVC stopped the reaction.

4.22c) ***ΔEP3 and PGC migration***

Flies were maintained, and embryos fixed and stained, as in **2.23a**, using only chicken anti-Vasa primary antibody (Ken Howard) at 1:10,000, followed by biotin-conjugated anti-chicken antibody (Jackson ImmunoResearch Laboratories) at 1:500. Flies were allowed to lay for 2 hours, the plates were removed, and the embryos aged for a further 9 hours, to ensure embryos were between stages 12 and 14.

4.22d) ***Genomic rescue of the PGC migration defect***

Embryos were collected and stained as in **4.22c**.

4.22e) ***PGC cell death phenotype***

ΔEP3 flies were allowed to lay on apple juice plates at 25°c for 2 hours before plates were removed, and aged for either 5 hours to stages 10-11, or 7 hours to stages 11-12. Embryos were collected and fixed as before, and stained with chicken anti-Vasa primary antibody (Ken Howard), followed by biotin-conjugated anti-chicken antibody (Jackson ImmunoResearch Laboratories).

4.23a) ***Complementation***

Embryos were collected and stained as in **4.22c**.

4.23b) ***RT-PCR and real-time PCR***

Embryos from Clark Coffman were received on dry ice. Total RNA was extracted using the RNeasy Mini Kit (Qiagen) and quantified in a spectrophotometer.

500ng of each RNA sample was then converted to cDNA using the Superscript™ First-Strand Synthesis System for RT-PCR (Invitrogen). 1μl of each sample was put through a standard PCR reaction on '3-step', in a MJ Research Inc. PTC-100™ Programmable Thermal Controller, with either Tre289Exon1 plus Tre548Exon3, or Actin 42 plus Actin 361 (see primer and PCR details below), before running on a 1% agarose gel to confirm the presence of DNA.

3μl of each cDNA was added to 42μl of double distilled H20 and mixed gently. 18.75μl of DyNAmo SYBR® Green reagent (MJ Research) and primers (Actin 42 plus Actin 361 or Tre289Exon1 plus Tre548Exon3 – see primer details below) were added and the mixture dispensed into three wells of a standard 96-well plate, before transferral to the DNA Opticon-2.

PRIMER	SEQUENCE 5' – 3'
Tre289Exon1	GAAAACAGTGAAACGGGTTCGAG
Tre548Exon3	CGAAATGACGAAGGCGGTTG
Actin 42	TCAGCCAGCAGTCGTCTAATCC
Actin 361	ACCGTGCTCAATGGGGTACTTC

Table 9. Primer sequences for RT-PCR and quantitative real-time PCR.

PCR Runs:

3-Step:

1. 94°C	60 seconds
2. 92°C	40 seconds
3. 60°C	40seconds
4. 75°C	90 seconds
5. GOTO step 2 29 times	
6. 75°C	5 minutes
7. 4°C	hold

Opticon-2:

1. 95°C	10 minutes
2. 94°C	10 seconds
3. 60°C	20 seconds
4. 72°C	20 seconds
5. 81°C	20 seconds
6. Plate read	
7. GOTO step 2 35 times	
8. 72°C	5 minutes

9. Melting curve 75-95°C every 0.5 seconds, hold 1 second
10. End.

4.24) Tre-1 and Wunen

To place each mesoderm driver into the ΔEP3 background, the following crosses were performed:

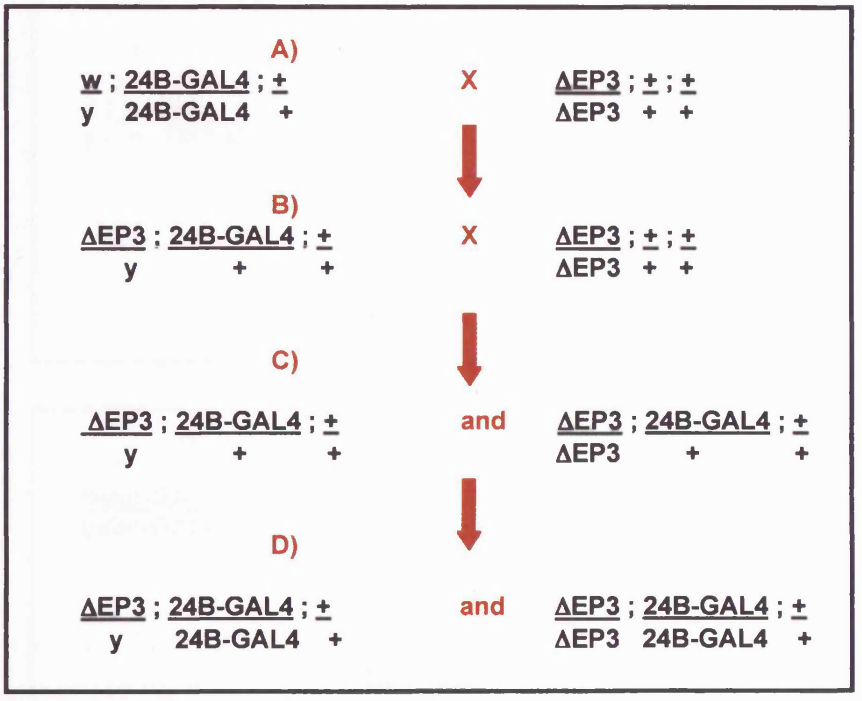

Fig.42. Fly crosses to place the mesoderm driver in the ΔEP3 background.

The 24B-GAL4 carries a w+ marker giving red-eyed flies. ΔEP3 flies have white-eyes.

A) Males carrying the 24B-GAL4 driver on the second chromosome were crossed to ΔEP3 virgins.

B) Resulting F1 males were selected and crossed again to ΔEP3 virgins.

C) Red-eyed males were selected in the next generation alongside red-eyed virgins and these were inter-crossed.

D) Males and virgins were selected from the resulting progeny that had the darkest red eyes, and so were presumed to be homozygous for the driver. These were selfed and maintained for 3 generations to ensure that this was the case.

This scheme was repeated for both the alternative mesoderm drivers, and for WunGFP on the second chromosome, to make it homozygous in the ΔEP3 background.

In order to express WunGFP in an *hkb* background driven by twist-GAL4, the following crosses were performed:

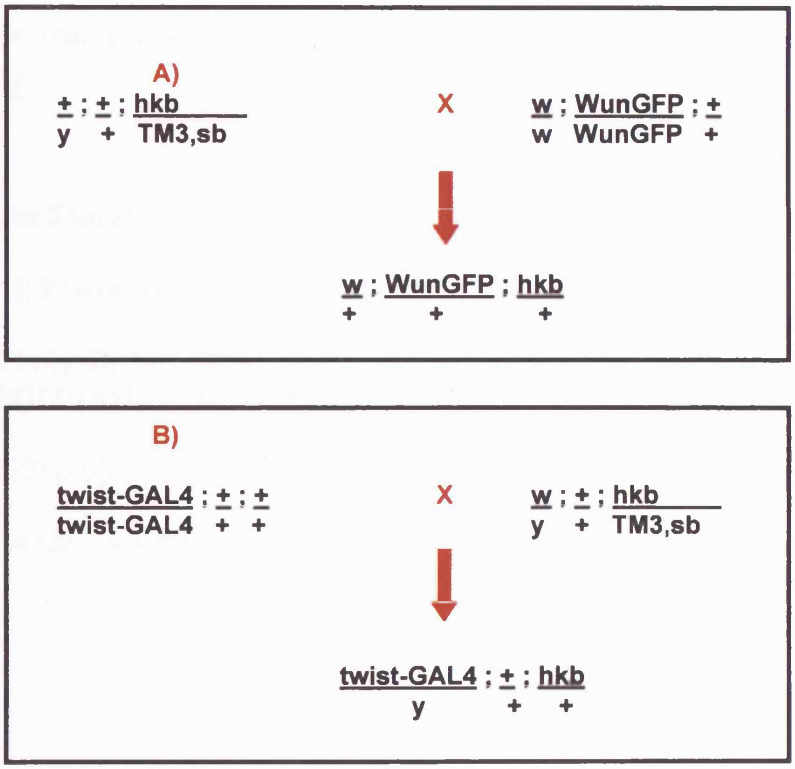

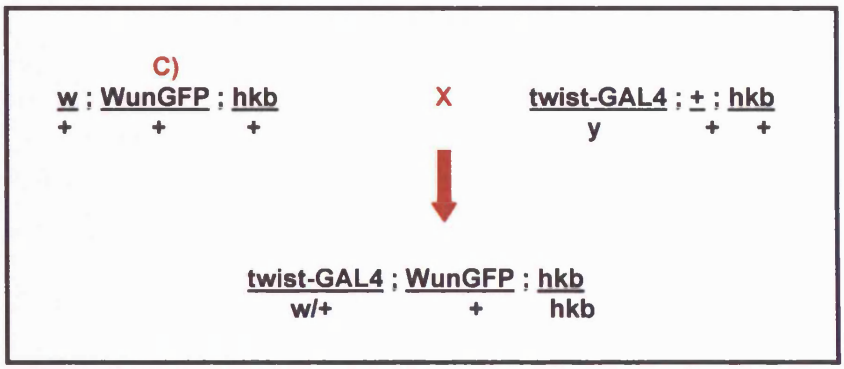

Fig.43. Fly crosses to place WunGFP in an* hkb *background with twist-GAL4.

A) *Males heterozygous for* hkb *on the third chromosome were crossed to virgins carrying WunGFP as a homozygous insert on the second chromosome. Virgins were selected in the next generation that lack the TM3,sb balancer.*

B) *Simultaneously, virgins homozygous for twist-GAL4 on the X chromosome were crossed to males heterozygous for* hkb *on the third. Males were selected in the next generation that lack the TM3,sb balancer.*

C) *The selected virgins were crossed to the selected males. The result is a proportion of embryos that express WunGFP in the mesoderm in an* hkb *homozygous background.*

Bloomington Stocks:

- w[*]; P{w[+mW.hs]=GawB}how[24B] = **24B-GAL4 (1;3)**
- w[1118]; Dr[Mio]/TM3, P{w[+mC]=GAL4-twi.G}2.3, P{UAS-2xEGFP}AH2.3, Sb[1] Ser[1] **= twist-GAL4 (1;3)**
- hkb[2] p[p]/TM3, p[+] Sb[1]

twist-GAL4 (2) - a gift from Marcel van den Heuvel

8) Citation Index

Citation Index for:

- **Burnett, C. and Howard, K.** (2003). Fly and mammalian lipid phosphate phosphatase isoforms differ in activity both *in vitro* and *in vivo*. *EMBO Rep* **4**, 793-9.

Brauer, A. U., Savaskan, N. E., Kuhn, H., Prehn, S., Ninnemann, O. and Nitsch, R. (2004). Reply to 'Is PRG-1 a new lipid phosphatase?' *Nat Neurosci* **7**, 789-90.

Brindley, D. N. (2004). Lipid phosphate phosphatases and related proteins: Signalling functions in development, cell division, and cancer. *J Cell Biochem* **92**, 900-12.

Hanyu-Nakamura, K., Kobayashi, S. and Nakamura, A. (2004). Germ cell-autonomous Wunen2 is required for germline development in *Drosophila* embryos. *Development* **131**, 4545-53.

Kunwar, P. S., Starz-Gaiano, M., Bainton, R. J., Heberlein, U. and Lehmann, R. (2003). Tre1, a g protein-coupled receptor, directs transepithelial migration of *Drosophila* germ cells. *PLoS Biol* **1**, E80.

Oskouian, B. and Saba, J. D. (2004). Death and taxis: what non-mammalian models tell us about sphingosine-1-phosphate. *Semin Cell Dev Biol* **15**, 529-40.

Pyne, S., Kong, K. C. and Darroch, P. I. (2004). Lysophosphatidic acid and sphingosine 1-phosphate biology: the role of lipid phosphate phosphatases. *Semin Cell Dev Biol* **15**, 491-501.

Renault, A. D., Sigal, Y. J., Morris, A. J. and Lehmann, R. (2004). Soma-germ line competition for lipid phosphate uptake regulates germ cell migration and survival. *Science* **305**, 1963-6.

Saba, J. D. (2004). Lysophospholipids in development: Miles apart and edging in. *J Cell Biochem* **92**, 967-92.

Santos, A. C. and Lehmann, R. (2004). Germ Cell Specification and Migration in *Drosophila* and beyond. *Curr Biol* **14**, R578-R589.

Zhao, Y., Usatyuk, P. V., Cummings, R., Saatian, B., He, D., Watkins, T., Morris, A., Spannhake, E. W., Brindley, D. N. and Natarajan, V. (2004). Lipid phosphate phosphatase-1 regulates lysophosphatidic acid-induced calcium release, NF-kappaB activation and IL-8 secretion in human bronchial epithelial cells. *Biochem J.*

Citation Index for:

- **Burnett, C., Makridou, P., Hewlett, L. and Howard, K.** (2004). Lipid phosphate phosphatases dimerise, but this interaction is not required for *in vivo* activity. *BMC Biochem* **5**, 2.

Brindley, D. N. (2004). Lipid phosphate phosphatases and related proteins: Signalling functions in development, cell division, and cancer. *J Cell Biochem* **92**, 900-12.

Pyne, S., Kong, K. C. and Darroch, P. I. (2004). Lysophosphatidic acid and sphingosine 1-phosphate biology: the role of lipid phosphate phosphatases. *Semin Cell Dev Biol* **15**, 491-501.

9) REFERENCES

(2003). The FlyBase database of the Drosophila genome projects and community literature. *Nucleic Acids Res* **31**, 172-5.

A.M.Hayden. (2000). Molecular cloning and functional characterisation of Drosophila Tunen, a homolog of the germ cell guidance factor Wunen. In *MRC Laboratory for Molecular Cell Biology*, (ed., pp. 129. London: University College London.

Affolter, M. and Shilo, B. Z. (2000). Genetic control of branching morphogenesis during Drosophila tracheal development. *Curr Opin Cell Biol* **12**, 731-5.

Alderton, F., Darroch, P., Sambi, B., McKie, A., Ahmed, I. S., Pyne, N. and Pyne, S. (2001). G-protein-coupled receptor stimulation of the p42/p44 mitogen-activated protein kinase pathway is attenuated by lipid phosphate phosphatases 1, 1a, and 2 in human embryonic kidney 293 cells. *J Biol Chem* **276**, 13452-60.

Andrake, M. D. and Skalka, A. M. (1995). Multimerization determinants reside in both the catalytic core and C terminus of avian sarcoma virus integrase. *J Biol Chem* **270**, 29299-306.

Ara, T., Nakamura, Y., Egawa, T., Sugiyama, T., Abe, K., Kishimoto, T., Matsui, Y. and Nagasawa, T. (2003). Impaired colonization of the gonads by primordial germ cells in mice lacking a chemokine, stromal cell-derived factor-1 (SDF-1). *Proc Natl Acad Sci U S A* **100**, 5319-23.

Asaoka-Taguchi, M., Yamada, M., Nakamura, A., Hanyu, K. and Kobayashi, S. (1999). Maternal Pumilio acts together with Nanos in germline development in Drosophila embryos. *Nat Cell Biol* **1**, 431-7.

Balazs, L., Okolicany, J., Ferrebee, M., Tolley, B. and Tigyi, G. (2001). Topical application of the phospholipid growth factor lysophosphatidic acid promotes wound healing in vivo. *Am J Physiol Regul Integr Comp Physiol* **280**, R466-72.

Barak, L. S., Ferguson, S. S., Zhang, J. and Caron, M. G. (1997). A beta-arrestin/green fluorescent protein biosensor for detecting G protein-coupled receptor activation. *J Biol Chem* **272**, 27497-500.

Barber, S. C., Mellor, H., Gampel, A. and Scolding, N. J. (2004). S1P and LPA trigger Schwann cell actin changes and migration. *Eur J Neurosci* **19**, 3142-50.

Barila, D., Murgia, C., Nobili, F., Gaetani, S. and Perozzi, G. (1994). Subtractive hybridization cloning of novel genes differentially expressed during intestinal development. *Eur J Biochem* **223**, 701-9.

Barila, D., Plateroti, M., Nobili, F., Muda, A. O., Xie, Y., Morimoto, T. and Perozzi, G. (1996). The Dri 42 gene, whose expression is up-regulated during epithelial differentiation, encodes a novel endoplasmic reticulum resident transmembrane protein. *J Biol Chem* **271**, 29928-36.

Bate, M. a. M. A., A. (1993). The Development of Drosophila melanogaster: Cold Spring Harbor Laboratory Press.

Beccari, S., Teixeira, L. and Rorth, P. (2002). The JAK/STAT pathway is required for border cell migration during Drosophila oogenesis. *Mech Dev* **111**, 115-23.

Bian, D., Su, S., Mahanivong, C., Cheng, R. K., Han, Q., Pan, Z. K., Sun, P. and Huang, S. (2004). Lysophosphatidic Acid Stimulates Ovarian Cancer Cell Migration via a Ras-MEK Kinase 1 Pathway. *Cancer Res* **64**, 4209-17.

Binari, R. and Perrimon, N. (1994). Stripe-specific regulation of pair-rule genes by hopscotch, a putative Jak family tyrosine kinase in Drosophila. *Genes Dev* **8**, 300-12.

Bouvier, M. (2001). Oligomerization of G-protein-coupled transmitter receptors. *Nat Rev Neurosci* **2**, 274-86.

Brand, A. H. and Perrimon, N. (1993). Targeted gene expression as a means of altering cell fates and generating dominant phenotypes. *Development* **118**, 401-15.

Brauer, A. U., Savaskan, N. E., Kuhn, H., Prehn, S., Ninnemann, O. and Nitsch, R. (2003). A new phospholipid phosphatase, PRG-1, is involved in axon growth and regenerative sprouting. *Nat Neurosci* **6**, 572-8.

Brauer, A. U., Savaskan, N. E., Kuhn, H., Prehn, S., Ninnemann, O. and Nitsch, R. (2004). Reply to 'Is PRG-1 a new lipid phosphatase?' *Nat Neurosci* **7**, 789-90.

Brindley, D. N. (2004). Lipid phosphate phosphatases and related proteins: Signalling functions in development, cell division, and cancer. *J Cell Biochem* **92**, 900-12.

Brown, S., Hu, N. and Hombria, J. C. (2001). Identification of the first invertebrate interleukin JAK/STAT receptor, the Drosophila gene domeless. *Curr Biol* **11**, 1700-5.

Burnett, C. and Howard, K. (2003). Fly and mammalian lipid phosphate phosphatase isoforms differ in activity both in vitro and in vivo. *EMBO Rep* **4**, 793-9.

Burnett, C., Makridou, P., Hewlett, L. and Howard, K. (2004). Lipid phosphate phosphatases dimerise, but this interaction is not required for in vivo activity. *BMC Biochem* **5**, 2.

Callaini, G., Riparbelli, M. G. and Dallai, R. (1995). Pole cell migration through the gut wall of the Drosophila embryo: analysis of cell interactions. *Dev Biol* **170**, 365-75.

Campus-Ortega, J. A. a. H., V. (1985). Stages of Drosophila embryogenesis. In The Embryonic Development of Drosophila melanogaster. Berlin: Springer-Verlag.

Chan, W. M., Siu, W. Y., Lau, A. and Poon, R. Y. (2004). How many mutant p53 molecules are needed to inactivate a tetramer? *Mol Cell Biol* **24**, 3536-51.

Cho, N. K., Keyes, L., Johnson, E., Heller, J., Ryner, L., Karim, F. and Krasnow, M. A. (2002). Developmental control of blood cell migration by the Drosophila VEGF pathway. *Cell* **108**, 865-76.

Coffman, C. R., Strohm, R. C., Oakley, F. D., Yamada, Y., Przychodzin, D. and Boswell, R. E. (2002). Identification of X-linked genes required for migration and programmed cell death of Drosophila melanogaster germ cells. *Genetics* **162**, 273-84.

Dahanukar, A., Foster, K., van der Goes van Naters, W. M. and Carlson, J. R. (2001). A Gr receptor is required for response to the sugar trehalose in taste neurons of Drosophila. *Nat Neurosci* **4**, 1182-6.

Dekker, N., Tommassen, J., Lustig, A., Rosenbusch, J. P. and Verheij, H. M. (1997). Dimerization regulates the enzymatic activity of Escherichia coli outer membrane phospholipase A. *J Biol Chem* **272**, 3179-84.

Deshpande, G., Swanhart, L., Chiang, P. and Schedl, P. (2001). Hedgehog signalling in germ cell migration. *Cell* **106**, 759-69.

Dillon, D. A., Chen, X., Zeimetz, G. M., Wu, W. I., Waggoner, D. W., Dewald, J., Brindley, D. N. and Carman, G. M. (1997). Mammalian Mg2+-independent phosphatidate phosphatase (PAP2) displays diacylglycerol pyrophosphate phosphatase activity. *J Biol Chem* **272**, 10361-6.

Dillon, D. A., Wu, W. I., Riedel, B., Wissing, J. B., Dowhan, W. and Carman, G. M. (1996). The Escherichia coli pgpB gene encodes for a diacylglycerol pyrophosphate phosphatase activity. *J Biol Chem* **271**, 30548-53.

Doitsidou, M., Reichman-Fried, M., Stebler, J., Koprunner, M., Dorries, J., Meyer, D., Esguerra, C. V., Leung, T. and Raz, E. (2002). Guidance of primordial germ cell migration by the chemokine SDF-1. *Cell* **111**, 647-59.

Duchek, P. and Rorth, P. (2001). Guidance of cell migration by EGF receptor signalling during Drosophila oogenesis. *Science* **291**, 131-3.

Duchek, P., Somogyi, K., Jekely, G., Beccari, S. and Rorth, P. (2001). Guidance of cell migration by the Drosophila PDGF/VEGF receptor. *Cell* **107**, 17-26.

Duffy, J. B. (2002). GAL4 system in Drosophila: a fly geneticist's Swiss army knife. *Genesis* **34**, 1-15.

Dunin-Borkowski, O. M. and Brown, N. H. (1995). Mammalian CD2 is an effective heterologous marker of the cell surface in Drosophila. *Dev Biol* **168**, 689-93.

Escalante-Alcalde, D., Hernandez, L., Le Stunff, H., Maeda, R., Lee, H. S., Jr Gang, C., Sciorra, V. A., Daar, I., Spiegel, S., Morris, A. J. et al. (2003). The lipid phosphatase LPP3 regulates extra-embryonic vasculogenesis and axis patterning. *Development* **130**, 4623-37.

Fang, X., Gaudette, D., Furui, T., Mao, M., Estrella, V., Eder, A., Pustilnik, T., Sasagawa, T., Lapushin, R., Yu, S. et al. (2000). Lysophospholipid growth factors in the initiation, progression, metastases, and management of ovarian cancer. *Ann N Y Acad Sci* **905**, 188-208.

Foe, V. E. and Alberts, B. M. (1983). Studies of nuclear and cytoplasmic behaviour during the five mitotic cycles that precede gastrulation in Drosophila embryogenesis. *J Cell Sci* **61**, 31-70.

Forbes, A. and Lehmann, R. (1998). Nanos and Pumilio have critical roles in the development and function of Drosophila germline stem cells. *Development* **125**, 679-90.

Furneisen, J. M. and Carman, G. M. (2000). Enzymological properties of the LPP1-encoded lipid phosphatase from Saccharomyces cerevisiae. *Biochim Biophys Acta* **1484**, 71-82.

Gertler, F. B., Chiu, C. Y., Richter-Mann, L. and Chin, D. J. (1988). Developmental and metabolic regulation of the Drosophila melanogaster 3-hydroxy-3-methylglutaryl coenzyme A reductase. *Mol Cell Biol* **8**, 2713-21.

Gether, U. (2000). Uncovering molecular mechanisms involved in activation of G protein-coupled receptors. *Endocr Rev* **21**, 90-113.

Golic, K. G. and Lindquist, S. (1989). The FLP recombinase of yeast catalyzes site-specific recombination in the Drosophila genome. *Cell* **59**, 499-509.

Greig, S. and Akam, M. (1993). Homeotic genes autonomously specify one aspect of pattern in the Drosophila mesoderm. *Nature* **362**, 630-2.

Halfon, M. S., Gisselbrecht, S., Lu, J., Estrada, B., Keshishian, H. and Michelson, A. M. (2002). New fluorescent protein reporters for use with the Drosophila Gal4 expression system and for vital detection of balancer chromosomes. *Genesis* **34**, 135-8.

Hanyu-Nakamura, K., Kobayashi, S. and Nakamura, A. (2004). Germ cell-autonomous Wunen2 is required for germline development in Drosophila embryos. *Development* **131**, 4545-53.

Harrison, D. A., McCoon, P. E., Binari, R., Gilman, M. and Perrimon, N. (1998). Drosophila unpaired encodes a secreted protein that activates the JAK signalling pathway. *Genes Dev* **12**, 3252-63.

Hayashi, Y., Hayashi, M. and Kobayashi, S. (2004). Nanos suppresses somatic cell fate in Drosophila germ line. *Proc Natl Acad Sci U S A* **101**, 10338-42.

Hemrika, W., Renirie, R., Dekker, H. L., Barnett, P. and Wever, R. (1997). From phosphatases to vanadium peroxidases: a similar architecture of the active site. *Proc Natl Acad Sci U S A* **94**, 2145-9.

Hofmann, K. a. S., W. (1993). TMbase – a database of membrane spanning proteins segments. *Biol. Chem. Hoppe Seyler* **374**.

Hofseth, L. J., Hussain, S. P. and Harris, C. C. (2004). p53: 25 years after its discovery. *Trends Pharmacol Sci* **25**, 177-81.

Hombria, J. C. and Brown, S. (2002). The fertile field of Drosophila Jak/STAT signalling. *Curr Biol* **12**, R569-75.

Hooks, S. B., Ragan, S. P. and Lynch, K. R. (1998). Identification of a novel human phosphatidic acid phosphatase type 2 isoform. *FEBS Lett* **427**, 188-92.

Hou, X. S., Melnick, M. B. and Perrimon, N. (1996). Marelle acts downstream of the Drosophila HOP/JAK kinase and encodes a protein similar to the mammalian STATs. *Cell* **84**, 411-9.

Humtsoe, J. O., Feng, S., Thakker, G. D., Yang, J., Hong, J. and Wary, K. K. (2003). Regulation of cell-cell interactions by phosphatidic acid phosphatase 2b/VCIP. *Embo J* **22**, 1539-54.

Illmensee, K. and Mahowald, A. P. (1974). Transplantation of posterior polar plasm in Drosophila. Induction of germ cells at the anterior pole of the egg. *Proc Natl Acad Sci U S A* **71**, 1016-20.

Ingham, P. W. and McMahon, A. P. (2001). Hedgehog signalling in animal development: paradigms and principles. *Genes Dev* **15**, 3059-87.

Ishikawa, T., Kai, M., Wada, I. and Kanoh, H. (2000). Cell surface activities of the human type 2b phosphatidic acid phosphatase. *J Biochem (Tokyo)* **127**, 645-51.

Ishimoto, H., Matsumoto, A. and Tanimura, T. (2000). Molecular identification of a taste receptor gene for trehalose in Drosophila. *Science* **289**, 116-9.

Jaglarz, M. K. and Howard, K. R. (1994). Primordial germ cell migration in Drosophila melanogaster is controlled by somatic tissue. *Development* **120**, 83-9.

Jaglarz, M. K. and Howard, K. R. (1995). The active migration of Drosophila primordial germ cells. *Development* **121**, 3495-503.

Jamal, Z., Martin, A., Gomez-Munoz, A. and Brindley, D. N. (1991). Plasma membrane fractions from rat liver contain a phosphatidate phosphohydrolase distinct from that in the endoplasmic reticulum and cytosol. *J Biol Chem* **266**, 2988-96.

Jasinska, R., Zhang, Q. X., Pilquil, C., Singh, I., Xu, J., Dewald, J., Dillon, D. A., Berthiaume, L. G., Carman, G. M., Waggoner, D. W. et al. (1999). Lipid phosphate phosphohydrolase-1 degrades exogenous glycerolipid and sphingolipid phosphate esters. *Biochem J* **340 (Pt 3)**, 677-86.

Jia, Y. J., Kai, M., Wada, I., Sakane, F. and Kanoh, H. (2003). Differential localisation of lipid phosphate phosphatases 1 and 3 to cell surface subdomains in polarized MDCK cells. *FEBS Lett* **552**, 240-6.

Jiang, G., den Hertog, J. and Hunter, T. (2000). Receptor-like protein tyrosine phosphatase alpha homodimerizes on the cell surface. *Mol Cell Biol* **20**, 5917-29.

Johnson, E. C., Bohn, L. M., Barak, L. S., Birse, R. T., Nassel, D. R., Caron, M. G.

and Taghert, P. H. (2003). Identification of Drosophila neuropeptide receptors by G protein-coupled receptors-beta-arrestin2 interactions. *J Biol Chem* **278**, 52172-8.

Kai, M., Wada, I., Imai, S., Sakane, F. and Kanoh, H. (1996). Identification and cDNA cloning of 35-kDa phosphatidic acid phosphatase (type 2) bound to plasma membranes. Polymerase chain reaction amplification of mouse H2O2-inducible hic53 clone yielded the cDNA encoding phosphatidic acid phosphatase. *J Biol Chem* **271**, 18931-8.

Kai, M., Wada, I., Imai, S., Sakane, F. and Kanoh, H. (1997). Cloning and characterization of two human isozymes of Mg2+-independent phosphatidic acid phosphatase. *J Biol Chem* **272**, 24572-8.

Kanoh, H., Imai, S., Yamada, K. and Sakane, F. (1992). Purification and properties of phosphatidic acid phosphatase from porcine thymus membranes. *J Biol Chem* **267**, 25309-14.

Kobayashi, S., Yamada, M., Asaoka, M. and Kitamura, T. (1996). Essential role of the posterior morphogen nanos for germline development in Drosophila. *Nature* **380**, 708-11.

Kopczynski, C. C., Noordermeer, J. N., Serano, T. L., Chen, W. Y., Pendleton, J. D., Lewis, S., Goodman, C. S. and Rubin, G. M. (1998). A high throughput screen to identify secreted and transmembrane proteins involved in Drosophila embryogenesis. *Proc Natl Acad Sci U S A* **95**, 9973-8.

Knaut, H., Werz, C., Geisler, R. and Nusslein-Volhard, C. (2003). A zebrafish homologue of the chemokine receptor Cxcr4 is a germ-cell guidance receptor. *Nature* **421**, 279-82.

Kraut, R., Menon, K. and Zinn, K. (2001). A gain-of-function screen for genes controlling motor axon guidance and synaptogenesis in Drosophila. *Curr Biol* **11**, 417-30.

Kunwar, P. S., Starz-Gaiano, M., Bainton, R. J., Heberlein, U. and Lehmann, R. (2003). Tre1, a g protein-coupled receptor, directs transepithelial migration of Drosophila germ cells. *PLoS Biol* **1**, E80.

Kupperman, E., An, S., Osborne, N., Waldron, S. and Stainier, D. Y. (2000). A sphingosine-1-phosphate receptor regulates cell migration during vertebrate heart development. *Nature* **406**, 192-5.

Lee, H., Goetzl, E. J. and An, S. (2000). Lysophosphatidic acid and sphingosine 1-phosphate stimulate endothelial cell wound healing. *Am J Physiol Cell Physiol* **278**, C612-8.

Leptin, M. (1991). twist and snail as positive and negative regulators during Drosophila mesoderm development. *Genes Dev* **5**, 1568-76.

Leung, D. W., Tompkins, C. K. and White, T. (1998). Molecular cloning of two alternatively spliced forms of human phosphatidic acid phosphatase cDNAs that are differentially expressed in normal and tumor cells. *DNA Cell Biol* **17**, 377-85.

Li, J., Xia, F. and Li, W. X. (2003). Coactivation of STAT and Ras is required for germ cell proliferation and invasive migration in Drosophila. *Dev Cell* **5**, 787-98.

Ligoxygakis, P., Strigini, M. and Averof, M. (2001). Specification of left-right asymmetry in the embryonic gut of Drosophila. *Development* **128**, 1171-4.

Livak, K. J. and Schmittgen, T. D. (2001). Analysis of relative gene expression data using real-time quantitative PCR and the 2(-Delta Delta C(T)) Method. *Methods* **25**, 402-8.

Majeti, R., Bilwes, A. M., Noel, J. P., Hunter, T. and Weiss, A. (1998). Dimerization-induced inhibition of receptor protein tyrosine phosphatase function through an inhibitory wedge. *Science* **279**, 88-91.

Makridou, P., Burnett, C., Landy, T. and Howard, K. (2003). Hygromycin B-selected cell lines from GAL4-regulated pUAST constructs. *Genesis* **36**, 83-7.

Martinez-Arias, A. and Lawrence, P. A. (1985). Parasegments and compartments in the Drosophila embryo. *Nature* **313**, 639-42.

McDermott, M. I., Sigal, Y. J., Sciorra, V. A. and Morris, A. J. (2004). Is PRG-1 a new lipid phosphatase? *Nat Neurosci* **7**, 789.

McLaren, A. (2003). Primordial germ cells in the mouse. *Dev Biol* **262**, 1-15.

Messerschmidt, A. and Wever, R. (1996). X-ray structure of a vanadium-containing enzyme: chloroperoxidase from the fungus Curvularia inaequalis. *Proc Natl Acad Sci U S A* **93**, 392-6.

Mills, G. B., Eder, A., Fang, X., Hasegawa, Y., Mao, M., Lu, Y., Tanyi, J., Tabassam, F. H., Wiener, J., Lapushin, R. et al. (2002). Critical role of lysophospholipids in the pathophysiology, diagnosis, and management of ovarian cancer. *Cancer Treat Res* **107**, 259-83.

Molyneaux, K. and Wylie, C. (2004). Primordial germ cell migration. *Int J Dev Biol* **48**, 537-44.

Molyneaux, K. A., Stallock, J., Schaible, K. and Wylie, C. (2001). Time-lapse analysis of living mouse germ cell migration. *Dev Biol* **240**, 488-98.

Molyneaux, K. A., Zinszner, H., Kunwar, P. S., Schaible, K., Stebler, J., Sunshine, M. J., O'Brien, W., Raz, E., Littman, D., Wylie, C. et al. (2003). The chemokine SDF1/CXCL12 and its receptor CXCR4 regulate mouse germ cell migration and survival. *Development* **130**, 4279-86.

Montell, D. J. (2003). Border-cell migration: the race is on. *Nat Rev Mol Cell Biol* **4**, 13-24.

Moolenaar, W. H. (1999). Bioactive lysophospholipids and their G protein-coupled receptors. *Exp Cell Res* **253**, 230-8.

Moore, L. A., Broihier, H. T., Van Doren, M., Lunsford, L. B. and Lehmann, R. (1998). Identification of genes controlling germ cell migration and embryonic gonad formation in Drosophila. *Development* **125**, 667-78.

Morita, Y., Perez, G. I., Paris, F., Miranda, S. R., Ehleiter, D., Haimovitz-Friedman, A., Fuks, Z., Xie, Z., Reed, J. C., Schuchman, E. H. et al. (2000). Oocyte apoptosis is suppressed by disruption of the acid sphingomyelinase gene or by sphingosine-1-phosphate therapy. *Nat Med* **6**, 1109-14.

Nanjundan, M. and Possmayer, F. (2001a). Molecular cloning and expression of pulmonary lipid phosphate phosphohydrolases. *Am J Physiol Lung Cell Mol Physiol* **281**, L1484-93.

Nanjundan, M. and Possmayer, F. (2001b). Pulmonary lipid phosphate phosphohydrolase in plasma membrane signalling platforms. *Biochem J* **358**, 637-46.

Neuwald, A. F. (1997). An unexpected structural relationship between integral membrane phosphatases and soluble haloperoxidases. *Protein Sci* **6**, 1764-7.

Norga, K. K., Gurganus, M. C., Dilda, C. L., Yamamoto, A., Lyman, R. F., Patel, P. H., Rubin, G. M., Hoskins, R. A., Mackay, T. F. and Bellen, H. J. (2003). Quantitative analysis of bristle number in Drosophila mutants identifies genes involved in neural development. *Curr Biol* **13**, 1388-96.

Nusse, R. (2003). Wnts and Hedgehogs: lipid-modified proteins and similarities in signalling mechanisms at the cell surface. *Development* **130**, 5297-305.

Nusslein-Volhard, C. and Wieschaus, E. (1980). Mutations affecting segment number and polarity in Drosophila. *Nature* **287**, 795-801.

Pierrugues, O., Brutesco, C., Oshiro, J., Gouy, M., Deveaux, Y., Carman, G. M., Thuriaux, P. and Kazmaier, M. (2001). Lipid phosphate phosphatases in Arabidopsis. Regulation of the AtLPP1 gene in response to stress. *J Biol Chem* **276**, 20300-8.

Pushkareva, M., Chao, R., Bielawska, A., Merrill, A. H., Jr., Crane, H. M., Lagu, B., Liotta, D. and Hannun, Y. A. (1995). Stereoselectivity of induction of the retinoblastoma gene product (pRb) dephosphorylation by D-erythro-sphingosine supports a role for pRb in growth suppression by sphingosine. *Biochemistry* **34**, 1885-92.

Pyne, S. (2002). Cellular signalling by sphingosine and sphingosine 1-phosphate. Their opposing roles in apoptosis. *Subcell Biochem* **36**, 245-68.

Pyne, S. and Pyne, N. J. (2000). Sphingosine 1-phosphate signalling in mammalian cells. *Biochem J* **349**, 385-402.

Pyne, S., Kong, K. C. and Darroch, P. I. (2004). Lysophosphatidic acid and sphingosine 1-phosphate biology: the role of lipid phosphate phosphatases. *Semin Cell Dev Biol* **15**, 491-501.

Raisman, G. (2000). Sniffing out new approaches to spinal cord repair. *Nat Med* **6**, 382-3.

Raisman, G. (2003). A promising therapeutic approach to spinal cord repair. *J R Soc Med* **96**, 259-61.

Renault, A. D., Sigal, Y. J., Morris, A. J. and Lehmann, R. (2004). Soma-germ line competition for lipid phosphate uptake regulates germ cell migration and survival. *Science* **305**, 1963-6.

Ribeiro, C., Petit, V. and Affolter, M. (2003). Signalling systems, guided cell migration, and organogenesis: insights from genetic studies in Drosophila. *Dev Biol* **260**, 1-8.

Riboni, L., Bassi, R., Prinetti, A., Viani, P. and Tettamanti, G. (1999). Predominance of the acylation route in the metabolic processing of exogenous sphingosine in neural and extraneural cells in culture. *Biochem J* **338 (Pt 1)**, 147-51.

Roberts, R., Sciorra, V. A. and Morris, A. J. (1998). Human type 2 phosphatidic acid phosphohydrolases. Substrate specificity of the type 2a, 2b, and 2c enzymes and cell surface activity of the 2a isoform. *J Biol Chem* **273**, 22059-67.

Rorth, P. (1996). A modular misexpression screen in Drosophila detecting tissue-specific phenotypes. *Proc Natl Acad Sci U S A* **93**, 12418-22.

Rorth, P. (2002). Initiating and guiding migration: lessons from border cells. *Trends Cell Biol* **12**, 325-31.

Rubin, G. M. and Spradling, A. C. (1982). Genetic transformation of Drosophila with transposable element vectors. *Science* **218**, 348-53.

Saba, J. D. (2004). Lysophospholipids in development: Miles apart and edging in. *J Cell Biochem* **92**, 967-92.

Sabio, G., Mora, A., Rangel, M. A., Quesada, A., Marcos, C. F., Alonso, J. C., Soler, G. and Centeno, F. (2001). Glu-256 is a main structural determinant for oligomerisation of human arginase I. *FEBS Lett* **501**, 161-5.

Santos, A. C. and Lehmann, R. (2004). Isoprenoids control germ cell migration downstream of HMGCoA reductase. *Dev Cell* **6**, 283-93.

Santos, A. C. and Lehmann, R. (2004). Germ Cell Specification and Migration in Drosophila and beyond. *Curr Biol* **14**, R578-R589.

Schupbach, T. and Wieschaus, E. (1989). Female sterile mutations on the second chromosome of Drosophila melanogaster. I. Maternal effect mutations. *Genetics* **121**, 101-17.

Sciorra, V. A. and Morris, A. J. (1999). Sequential actions of phospholipase D and phosphatidic acid phosphohydrolase 2b generate diglyceride in mammalian cells. *Mol Biol Cell* **10**, 3863-76.

Siess, E. A. and Hofstetter, M. M. (1996). Identification of phosphatidate phosphohydrolase purified from rat liver membranes on SDS-polyacrylamide gel electrophoresis. *FEBS Lett* **381**, 169-73.

Simon, M. A. (1994). Signal transduction during the development of the Drosophila R7 photoreceptor. *Dev Biol* **166**, 431-42.

Snijder, H. J., Ubarretxena-Belandia, I., Blaauw, M., Kalk, K. H., Verheij, H. M., Egmond, M. R., Dekker, N. and Dijkstra, B. W. (1999). Structural evidence for dimerization-regulated activation of an integral membrane phospholipase. *Nature* **401**, 717-21.

Stankiewicz, P. J., Tracey, A. S. and Crans, D. C. (1995). Inhibition of phosphate-metabolizing enzymes by oxovanadium(V) complexes. *Met Ions Biol Syst* **31**, 287-324.

Starz-Gaiano, M., Cho, N. K., Forbes, A. and Lehmann, R. (2001). Spatially restricted activity of a Drosophila lipid phosphatase guides migrating germ cells. *Development* **128**, 983-91.

Stukey, J. and Carman, G. M. (1997). Identification of a novel phosphatase sequence motif. *Protein Sci* **6**, 469-72.

Le Stunff, H., Peterson, C., Liu, H., Milstien, S. and Spiegel, S. (2002). Sphingosine-1-phosphate and lipid phosphohydrolases. *Biochim Biophys Acta* **1582**, 8-17.

Sutcliffe, J. E. and Brehm, A. (2004). Of flies and men; p53, a tumour suppressor. *FEBS Lett* **567**, 86-91.

Suzuki, R., Sakagami, H., Owada, Y., Handa, Y. and Kondo, H. (1999). Localisation of mRNA for Dri 42, subtype 2b of phosphatidic acid phosphatase, in the rat brain during development. *Brain Res Mol Brain Res* **66**, 195-9.

Takeda, A., Matsuda, A., Paul, R. M. and Yaseen, N. R. (2004). CD45-associated protein inhibits CD45 dimerization and up-regulates its protein tyrosine phosphatase activity. *Blood* **103**, 3440-7.

Takeda, A., Wu, J. J. and Maizel, A. L. (1992). Evidence for monomeric and dimeric forms of CD45 associated with a 30-kDa phosphorylated protein. *J Biol Chem* **267**, 16651-9.

Takuwa, Y., Takuwa, N. and Sugimoto, N. (2002). The Edg family G protein-coupled receptors for lysophospholipids: their signalling properties and biological activities. *J Biochem (Tokyo)* **131**, 767-71.

Tallquist, M. and Kazlauskas, A. (2004). PDGF signalling in cells and mice. *Cytokine Growth Factor Rev* **15**, 205-13.

Tepass, U., Fessler, L. I., Aziz, A. and Hartenstein, V. (1994). Embryonic origin of hemocytes and their relationship to cell death in Drosophila. *Development* **120**, 1829-37.

Thorpe, J. L., Doitsidou, M., Ho, S. Y., Raz, E. and Farber, S. A. (2004). Germ cell migration in zebrafish is dependent on HMGCoA reductase activity and prenylation. *Dev Cell* **6**, 295-302.

Toke, D. A., Bennett, W. L., Oshiro, J., Wu, W. I., Voelker, D. R. and Carman, G. M. (1998). Isolation and characterization of the Saccharomyces cerevisiae LPP1 gene encoding a Mg2+-independent phosphatidate phosphatase. *J Biol Chem* **273**, 14331-8.

Tomancak, P., Beaton, A., Weiszmann, R., Kwan, E., Shu, S., Lewis, S. E., Richards, S., Ashburner, M., Hartenstein, V., Celniker, S. E. et al. (2002). Systematic determination of patterns of gene expression during Drosophila embryogenesis. *Genome Biol* **3**, RESEARCH0088.

Ueno, K., Ohta, M., Morita, H., Mikuni, Y., Nakajima, S., Yamamoto, K. and Isono, K. (2001). Trehalose sensitivity in Drosophila correlates with mutations in and expression of the gustatory receptor gene Gr5a. *Curr Biol* **11**, 1451-5.

Uv, A., Cantera, R. and Samakovlis, C. (2003). Drosophila tracheal morphogenesis: intricate cellular solutions to basic plumbing problems. *Trends Cell Biol* **13**, 301-9.

Van Doren, M., Broihier, H. T., Moore, L. A. and Lehmann, R. (1998). HMG-CoA reductase guides migrating primordial germ cells. *Nature* **396**, 466-9.

Waggoner, D. W., Gomez-Munoz, A., Dewald, J. and Brindley, D. N. (1996). Phosphatidate phosphohydrolase catalyzes the hydrolysis of ceramide 1-phosphate, lysophosphatidate, and sphingosine 1-phosphate. *J Biol Chem* **271**, 16506-9.

Waggoner, D. W., Xu, J., Singh, I., Jasinska, R., Zhang, Q. X. and Brindley, D. N. (1999). Structural organization of mammalian lipid phosphate phosphatases: implications for signal transduction. *Biochim Biophys Acta* **1439**, 299-316.

Wang, F., Van Brocklyn, J. R., Hobson, J. P., Movafagh, S., Zukowska-Grojec, Z., Milstien, S. and Spiegel, S. (1999). Sphingosine 1-phosphate stimulates cell migration through a G(i)-coupled cell surface receptor. Potential involvement in angiogenesis. *J Biol Chem* **274**, 35343-50.

Warrior, R. (1994). Primordial germ cell migration and the assembly of the Drosophila embryonic gonad. *Dev Biol* **166**, 180-94.

Weaver, C. and Kimelman, D. (2004). Move it or lose it: axis specification in Xenopus. *Development* **131**, 3491-9.

Weidinger, G., Wolke, U., Koprunner, M., Klinger, M. and Raz, E. (1999). Identification of tissues and patterning events required for distinct steps in early migration of zebrafish primordial germ cells. *Development* **126**, 5295-307.

Weigel, D., Jurgens, G., Klingler, M. and Jackle, H. (1990). Two gap genes mediate maternal terminal pattern information in Drosophila. *Science* **248**, 495-8.

Wylie, C. (1999). Germ cells. *Cell* **96**, 165-74.

Xu, T. and Rubin, G. M. (1993). Analysis of genetic mosaics in developing and adult Drosophila tissues. *Development* **117**, 1223-37.

Xu, Y., Fang, X. J., Casey, G. and Mills, G. B. (1995a). Lysophospholipids activate ovarian and breast cancer cells. *Biochem J* **309 (Pt 3)**, 933-40.

Xu, Y., Gaudette, D. C., Boynton, J. D., Frankel, A., Fang, X. J., Sharma, A., Hurteau, J., Casey, G., Goodbody, A., Mellors, A. et al. (1995b). Characterization of an ovarian cancer activating factor in ascites from ovarian cancer patients. *Clin Cancer Res* **1**, 1223-32.

Xu, Y., Shen, Z., Wiper, D. W., Wu, M., Morton, R. E., Elson, P., Kennedy, A. W., Belinson, J., Markman, M. and Casey, G. (1998). Lysophosphatidic acid as a potential biomarker for ovarian and other gynecologic cancers. *Jama* **280**, 719-23.

Yan, H., Lu, D. and Rivkees, S. A. (2003). Lysophosphatidic acid regulates the proliferation and migration of olfactory ensheathing cells in vitro. *Glia* **44**, 26-36.

Yan, R., Small, S., Desplan, C., Dearolf, C. R. and Darnell, J. E., Jr. (1996). Identification of a Stat gene that functions in Drosophila development. *Cell* **84**, 421-30.

Yue, J., Yokoyama, K., Balazs, L., Baker, D. L., Smalley, D., Pilquil, C., Brindley, D. N. and Tigyi, G. (2004). Mice with transgenic overexpression of lipid phosphate

phosphatase-1 display multiple organotypic deficits without alteration in circulating lysophosphatidate level. *Cell Signal* **16**, 385-99.

Zhang, N., Sundberg, J. P. and Gridley, T. (2000a). Mice mutant for Ppap2c, a homolog of the germ cell migration regulator wunen, are viable and fertile. *Genesis* **27**, 137-40.

Zhang, N., Zhang, J., Cheng, Y. and Howard, K. (1996). Identification and genetic analysis of wunen, a gene guiding Drosophila melanogaster germ cell migration. *Genetics* **143**, 1231-41.

Zhang, N., Zhang, J., Purcell, K. J., Cheng, Y. and Howard, K. (1997). The Drosophila protein Wunen repels migrating germ cells. *Nature* **385**, 64-7.

Zhang, Q. X., Pilquil, C. S., Dewald, J., Berthiaume, L. G. and Brindley, D. N. (2000b). Identification of structurally important domains of lipid phosphate phosphatase-1: implications for its sites of action. *Biochem J* **345 Pt 2**, 181-4.